Modeling intercellular interactions in the peripheral immune system

by

Christina Elizabeth Warrender

B.S., Physics, Massachusetts Institute of Technology, 1984
M.S., Computer Science, University of Colorado, 1997

DISSERTATION

Submitted in Partial Fulfillment of the
Requirements for the Degree of

Doctor of Philosophy
Computer Science

The University of New Mexico

Albuquerque, New Mexico

December 2004

Acknowledgments

I would like to thank my dissertation committee: Ed Angel, Rob Miller, Cris Moore, Lee Segel, and particularly my advisor, Stephanie Forrest. Lee gets special recognition for getting me started on this track. Special thanks also go to Fred Koster, who put a lot of his time into helping me with the tuberculosis model. I also had many fruitful contacts with both biologists and modelers through the Center for the Spatiotemporal Modeling of Cell Signaling Networks, thanks in particular to Jan Oliver.

My officemates were invaluable; Dennis Chao helped with just about everything, and both he and Gabriela Barrantes managed to give useful critiques of very rough drafts. Many thanks also to the rest of Steph's research group, past and present. I also greatly appreciated Vladimir Vuksan and the other members of the support group who made it possible to keep the simulations running.

Lastly, but most important, thanks to my husband Charles and my children Scott and Diane for putting up with this long and disruptive process.

This work was partially supported by grants from the National Institutes of Health (P20 GM066283), the National Science Foundation (ANIR-9986555), the Defense Advanced Research Projects Agency (grants AGR F30602-00-2-0584), and the Office of Naval Research (N00014-99-1-0417).

Modeling intercellular interactions in the peripheral immune system

by

Christina Elizabeth Warrender

ABSTRACT OF DISSERTATION

Submitted in Partial Fulfillment of the

Requirements for the Degree of

Doctor of Philosophy

Computer Science

The University of New Mexico

Albuquerque, New Mexico

December 2004

Modeling intercellular interactions in the peripheral immune system

by

Christina Elizabeth Warrender

B.S., Physics, Massachusetts Institute of Technology, 1984
M.S., Computer Science, University of Colorado, 1997

Ph.D., Computer Science, University of New Mexico, 2004

Abstract

Peripheral tissue microenvironments play an important role in determining responses to infection, but these small-scale interactions are usually not included in immune system models. An immune response to a pathogen involves numerous cells of several different types, each with a limited ability to sense its environment and to act. These cells produce many kinds of signalling molecules called cytokines that act locally to affect cell behavior. The dynamical interactions among this heterogeneous collection of cells and molecules are extremely complex. To begin to understand such a system, we need modeling approaches that can relate population-level dynamics to individual cell interactions and responses to cytokines. This thesis describes a spatially explicit simulator that tracks individual cell responses to local molecular signals, and the use of that simulator to study models of peripheral tissue dynamics in normal and disease conditions.

The simulator implements a hybrid framework combining discrete representation of individual cells and continuous representation of molecular concentrations. Cell behaviors

consist of sensing, intracellular processing, and action functions that can be combined in various ways to accommodate a variety of models. Connecting extracellular signals to individual cell actions is difficult because intracellular signalling itself is complex and incompletely understood. Many of the processes involved occur on different timescales and stochastic effects may be important. The approach presented here abstracts away much of this intracellular signalling complexity, while capturing the aspects most likely to affect intercellular dynamics. Separation of sensing and processing allows the kind of pleiotropy seen in intercellular systems—each cytokine may affect multiple cell actions, and multiple cytokines may affect a single action.

The goal of this work is to relate individual cell actions and intercellular interactions to observed population-level dynamics. For concreteness, this study focuses on alveolar lung tissue and the response to *Mycobacterium tuberculosis*. In the absence of infection, a dynamic population of peripheral immune system effector cells provides a sentinel function. In an effective response to pathogenic challenge, this population expands and changes function to either eliminate the pathogen, or—as in many cases of tuberculosis—isolate it and minimize the effects on surrounding tissues. This requires recruitment and spatial organization of the right kinds of cells and appropriate regulation of their effector functions. The models presented here explore the relative importance of various regulatory mechanisms in effectively controlling a local population of immune cells.

Contents

List of Figures

List of Tables

Chapter 1

Introduction

Infectious agents enter the body through its most accessible tissues in the skin, lungs, and gut. Some of these microorganisms are eliminated without causing symptoms, some establish a local infection, and some spread to cause systemic disease. The development of disease or immunity often depends on the initial interactions between the pathogen and immune system cells in the peripheral tissues.

Cells called macrophages are key components of peripheral defense; they are often the first immune systems cells to encounter pathogens. Macrophages engulf and digest many kinds of microbes. They also interact directly with other cells of the immune system, notably T cells, to enhance immune activity. In addition to these contact-dependent interactions, macrophages also produce and respond to a vast array of extracellular molecular mediators. A class of molecules known as cytokines are particularly important in maintaining homeostasis and in initiating, regulating, and resolving responses to infection.

Most efforts at modeling the effects of cytokine signaling in the immune system have focused either at the systemic level, or the intracellular level. Systemic models describe the major feedback loops between activating and inhibiting effects of cytokines in circulation. These models do not account for the characteristics of peripheral tissues, spatial effects,

or the contributions of individual cells. At the other extreme, intracellular models try to capture the detailed molecular interactions within a single cell. These intracellular interactions can affect the way individual cells respond to different stimuli. Differences between individual cell responses due to cellular and spatial heterogeneity in turn affect the overall population dynamics. I believe that it is important to develop methods for investigating interactions on this intermediate scale.

In order to investigate intercellular interactions within localized microenvionments, I developed a hybrid simulator that models the interactions of individual cells with each other and with a continuous molecular environment. This simulator is called CyCells and is described in Chapter 3. CyCells abstracts much of the complexity of intracellular signal transduction in order to capture the cell behaviors most likely to affect intercellular dynamics. Cell behaviors are defined within a general model framework that gives the simulator the flexibility to accommodate many different models of multicellular behavior. I used CyCells to explore intercellular interactions in several different contexts; in turn, the individual models helped refine the modeling approach.

Although studies of cytokine signaling often focus on their role in disease, these signals are important in maintaining homeostasis as well. In the immune system, this includes maintenance of an appropriate sentinel population that can rapidly detect and respond to infection. The regulatory signals that allow maintenance of a steady-state population are of interest in their own right, and are also somewhat simpler than those induced by infection. Therefore, the first simulation experiments study the baseline system in the absence of infection. These are described in Chapter 4. Models in Chapter 5 explore the effects of this homeostatic regulation on the response to foreign organisms.

Chapter 5 models the initial interactions between macrophages and pathogens. Simulations are used to evaluate factors that affect the ability of macrophages to locate pathogens and either destroy them or limit their growth. A key factor in the initial response to a pathogen is the development of an inflammatory response that recruits more immune

system cells to the site of infection. Chapter 5 looks at the effect of this inflammatory response under different assumptions about macrophage effectiveness, particularly focusing on pathogens capable of surviving within macrophages.

Building on the earlier models, the simulation experiments in Chapter 6 consider the initial response to the pathogen that causes pulmonary tuberculosis. Infection with *Mycobacterium tuberculosis* is characterized by localized, roughly spherical lesions known as granulomas. An effective response requires recruitment and spatial organization of the right kinds of cells and appropriate regulation of their effector functions, while minimizing damage done by growth of the granuloma [Kaufmann, 1999]. A detailed model was developed using data from multiple experiments documenting the role of individual cell and molecule types. The simulations are used to evaluate the ability of this integrated model to explain characteristics of the initial response to infection.

There is a great deal to be learned about the importance of intercellular interactions in the immune system. The contributions of this thesis are primarily in 1) providing a tool with which to study the system at a level that captures both individual cell behaviors and intercellular interactions, and 2) developing models that capture important aspects of macrophage-pathogen dynamics in peripheral tissues. These models illustrate the ability of simulations to integrate data from multiple experiments and test the relative importance of different mechanisms. They also highlight areas in which both biological understanding and the modeling approach can be improved.

Chapter 2

Background

Observable immune system behavior is the result of individual cell actions and regulatory interactions between them. This chapter reviews some of the relevant biology and the modeling approaches that have been used to understand various aspects of intercellular dynamics. Observations both from the experimental literature and the modeling community motivate the choice of modeling approach described in the next chapter.

2.1 Intercellular Signaling

Immune system activity must be tightly regulated because antimicrobial products can damage host tissues as well as the target pathogen. Regulation is accomplished through controlled interactions between individual cells. Cell interactions are mediated by a large variety of molecular signals present on cell surfaces or secreted into the extracellular environment. Cells have numerous receptors on their surfaces that can bind to these molecules or *ligands*. Receptor binding of an appropriate ligand triggers one or more intracellular signalling pathways that ultimately change gene expression and cell behavior [Kishimoto et al., 1994, Weiss and Littman, 1994]. This molecular recognition mecha-

nism is important for detecting pathogens, for cell-cell interactions, and for sensing the local molecular environment.

Macrophages play a central role in detecting many pathogens and initiating immune responses. They are distributed throughout the body, particularly in tissues likely to be exposed to pathogens [Gordon, 1998]. There are also related cell types in circulation that can migrate to peripheral tissues and carry out similar functions or differentiate into macrophages. For the most part, I will ignore the distinctions between the various phagocyte subsets. Macrophage literally translates to "big eater"; these cells ingest, or *phagocytose* cell debris, foreign particles, and microbes. The initial step in phagocytosis is binding between phagocytic receptors on the surface of the macrophage and molecules on the surface of the target. Macrophages and other phagocytes express a wide variety of receptors that are involved in molecular recognition and phagocytosis [Underhill and Ozinsky, 2002]. Some of these receptors bind to molecular components shared by large classes of infectious agents [Medzhitov and Janeway, 1997].

Macrophages can produce a number of antimicrobial substances to destroy phagocytosed pathogens, but must be *activated* to exercise this effector function to its fullest extent [Ma et al., 2003]. Full macrophage activation requires interactions with T cells. Initiation of T cell responses begins with transport of pathogen components or products to lymphoid organs, usually by dendritic cells [Jenkins et al., 2001]. T cell recognition of these *antigens* together with the appropriate costimulatory signals induces T cell activation and proliferation[Weiss and Littman, 1994]. Proliferation in the lymphoid organs produces an expanded population of antigen-specific T cells capable of migrating to infected tissues [Jenkins et al., 2001]. Recognition of the same antigens on the surface of macrophages in the infected tissues stimulates recruited T cells to produce a number of molecular signals that activate macrophages and regulate their effector functions [Ma et al., 2003].

Phagocytosis and antigen presentation require contact between the cells involved. Binding between molecules on the surface of each cell allows the prolonged contact

necessary and also induces the changes in cell behavior associated with phagocytosis [Underhill and Ozinsky, 2002] and T cell activation [Weiss and Littman, 1994]. Direct contact between T cells and macrophages can also enhance macrophage activation [Ma et al., 2003]. However, a number of secreted *cytokines* are also very important in regulating these functions.

Cytokines affect all aspects of cell behavior, including phagocytosis and activation. They are produced by and affect all cells, although different cell types produce and respond to different kinds of cytokines. Cytokines can have stimulatory or inhibitory effects on cell division, death, migration, effector functions, and production of other cytokines [Thomson, 1998]. Some cytokines known as chemokines affect cell movement; cells tend to move in the direction of a chemokine gradient if one exists. Cytokine effects are pleiotropic—a single type of cytokine may have multiple effects on one type of cell, and may affect different cell types in different ways [Moqattash and Lutton, 1998, Woo, 1997]. Different cytokines may have cooperative or antagonistic effects on each cell type.

Cells produce cytokines in response to molecular stimuli. This is particularly true for macrophages; phagocytosis involves numerous binding events that trigger production of a large variety of cytokines. Different phagocytic receptors induce different cytokine secretion patterns; for example, while phagocytosis of pathogens often induces an inflammatory response, phagocytosis of apoptotic bodies (debris resulting from normal cell death) is believed to induce anti-inflammatory signals [Aderem, 2003]. Also, while there are some common cytokine subsets secreted in response to all pathogens, there are also some pathogen-specific patterns [Nau et al., 2002, 2003]. Segel proposed that cytokines represent a 'diffuse informational network' [Segel, 2000, 2001b,a,c], in which combinations of cytokine concentrations provide information to cells about the current state of the system. This view emphasizes the association of cytokine production with current conditions, rather than with a desired future result. He has also demonstrated the usefulness of cells adapting their behavior in response to changes in this information, particularly by consid-

ering multiple cytokines simultaneously [Segel and Bar-Or, 1999, Warrender et al., 2001]. However, there is a great deal still to learn about what information cytokines represent and how different cells respond to it. Segel himself points out [Segel, 2001a] that it is difficult to consider the information cytokines may represent separately from the effect they have on cells.

Patters of cytokine secretion are often determined by measuring concentrations in serum, but Nickerson et al. [1997] point out that cytokine concentrations within peripheral tissues are likely to be very different from those in serum. Since many cytokines act locally, the cytokines in localized tissue microenvironments have the most significant effect on the developing response [Lee and Lee, 1999]. Each cell only senses cytokines in its immediate neighborhood, so the distance at which cytokines can act is limited by the distance they can travel and the rates at which they are broken down or removed.

A source of further complexity in this already complicated system of interacting cells and molecules is that cells are also individually complex. Detection of neighboring cells and soluble molecules are both mediated by receptors on a cell's surface. Binding of these receptors to the appropriate ligand molecule triggers numerous signal transduction cascades that ultimately affect gene expression and cell behavior [Kishimoto et al., 1994, Weiss and Littman, 1994]. Different intracellular pathways may be independent, amplify each other, or inhibit each other to various degrees [Moqattash and Lutton, 1998]. The time between signal detection and response ranges from seconds to days, depending on the type of response. Changes in cell behavior may be transient or sustained. For example, a signal may trigger immediate release of pre-synthesized stored molecules, or induce cell differentiation requiring a large number of internal changes that take many hours or even days. There are numerous feedback loops involved in intracellular signalling; the same signal may have different effects at different times, depending on the internal cell state. Finally, there are indications that gene expression is inherently stochastic [Kelso, 1995, Hume, 2000]. This, in addition to differences in each cell's local environment, contributes

to significant heterogeneity in cell responses.

2.2 Modeling Approaches

A wide variety of mathematical and computational models have been used to try to understand the behavior of the immune system and its various components. Most common are differential equation models, for which a large array of analysis tools are available. However, researchers have identified a number of deficiencies with differential equation models of multicellular systems and have consequently proposed a number of alternatives. This section describes the types of approaches that have been used to model immune system dynamics and the behavior of other multicellular systems that use similar kinds of intercellular signalling.

The cellular and molecular processes that drive immune system dynamics are generally nonlinear. These nonlinear interactions can lead to unexpected behavior that is difficult to predict from an understanding of individual components of the system. Dynamical systems analysis using differential equation models can provide some insights into different behavioral regimes. Differential equation models have been used to study various aspects of disease dynamics [Asachenkov et al., 1994, Marchuk, 1997, Antia and Koella, 1994, Antia et al., 1996, Head et al., 1996, Nowak and May, 2000] and the contribution of the cytokine network [Fishman and Perelson, 1994, 1999, Callard et al., 1999, Segel and Bar-Or, 1999, Yates et al., 2000, Warrender et al., 2001, Bergmann et al., 2002]. These models attempt to determine which properties of the system affect the type and magnitude of the immune response and resolution or progression of disease. By determining which parameters most strongly affect the system dynamics, they may also identify system components most amenable to treatment.

The majority of these models focus on the systemic response; models

of the local response at the site of infection are relatively rare. Some notable exceptions are Lauffenburger's models of general tissue inflammation [Lauffenburger, 1980, Lauffenburger and Kennedy, 1981] and bacterial clearance from the lungs [Fisher et al., 1988, Fisher and Lauffenburger, 1990], and models of influenza [Bocharov and Romanyukha, 1994, Asachenkov et al., 1994], and tuberculosis [Wigginton and Kirschner, 2001, Gammack et al., 2004, Marino and Kirschner, 2004]. Several of these models use partial differential equations to capture spatial distributions of cells. However, the models that include cytokine interactions are primarily ordinary differential equations.

Although differential equation models can aid understanding of the complexities of immune system dynamics, Louzoun et al. [2003] claim that they are fundamentally flawed for representing many biological systems. They point out that partial differential equations are useful for systems with the following characteristics:

- a large density of interacting particles;
- a diffusion rate high enough to smooth local fluctuations;
- an immediate result of each interaction.

Cellular systems generally do not meet these restrictions. Although the immune system certainly has large numbers of cells and molecules, the number of local interactions may be relatively small, especially in the early stages of an infection. The primary point that Louzoun et al. make is that encounter rates in differential equations are typically proportional to the product of the concentrations of the entities involved, which is valid only when those concentrations are independent. In their example, one species promoted proliferation of another, inducing correlations between their concentrations. Such correlations could also arise due to chemotactic movement of cells, as is common in immune responses. As described in section 2.1, key aspects of immune responses involve cell-cell

contact. Representing these encounters accurately requires the use of discrete cells, explicit representation of the spatial environment, and incorporation of state information to account for delays between interactions and their results.

There are a number of reasons for representing the immune system as a discrete population of cells rather than with the continuous variables used in differential equations. In individual-based models, each individual has its own state which is updated according to certain rules governing interactions with other individuals or the environment. Model properties are therefore more closely related to the properties of components of the modelled system than is true in differential equations. Discrete models can also explicitly represent the large degree of heterogeneity that exists in multicellular systems. They have primarily been used in models incorporating the effect of diversity in antigen recognition on immune response efficacy [Seiden and Celada, 1992, Smith et al., 1999, Chao et al., 2004]. However, as noted in section 2.1, there are numerous sources of heterogeneity in intercellular signaling. Some of this heterogeneity is due to inherently stochastic processes, which can be represented in individual-based models by stochastic interaction rules. At the start of an immune response, when small numbers of cells are involved, random events may have a significant effect on the eventual outcome. Incorporating stochastic dynamics allows the models to explore a distribution of system behaviors, rather than just the average behavior that would be described by a deterministic model.

When those events are encounters between cells, spatial relationships are extremely important. A variety of spatial representations have been used in models of intercellular interactions. Drawing an analogy with fluid dynamics models, Dallon [2000] points out that there are essentially two views of model spatial coordinates: Eulerian approaches use fixed spatial coordinates; in Lagrangian approaches, the spatial coordinates move with the fluid. Most biological modeling is Eulerian. Partial differential equations for inherently continuous problems are discretized to a regular grid for numerical analysis purposes. In other models, an inherently discrete spatial structure motivates the use of a spatial lat-

tice. Models of this type include various kinds of cellular automata; some relevant examples are given in [Lee et al., 1995, Strain et al., 2002, Edelstein-Keshet and Spiros, 2002, Alber et al., 2003]. In models that include both cellular and molecular dynamics, the same spatial lattice is often used for both.

In contrast, a number of physics models use some combination of Lagrangian and Eulerian approaches to combine unrestricted particle movement with a fixed grid that defines field properties. Dallon [2000] used this approach to model local interactions between discrete cells in a chemical environment represented as a continuum. In his models of wound healing and slime mold aggregation, cell movement is significantly influenced by the local chemical environment. The resulting spatial distributions of cells would have been difficult to capture in a lattice model. Fleischer and Barr [1994] used a similar approach to model morphogenesis. This kind of hybrid spatial model seems well-suited for modeling the tissue microenvironments that develop in localized infections.

Although Dallon's models have discrete elements, they are completely deterministic. The relative merits of deterministic and stochastic representations have been debated for a long time, particularly in terms of their applicability to molecular dynamics. Chemical reactions can be numerically evaluated either with differential equations or a stochastic representation such as Gillespie's algorithm [Gillespie, 1976]. Typically the choice of which is most appropriate depends on the size of the system and on the degree of spatial homogeneity. A few simulators have the ability to switch between the two representations as appropriate [Alur et al., 2002, Takahashi et al., 2004]. These are most often used to model molecular interactions within a single cell, but the authors claim that they can be extended to multicellular systems.

However, extensions from molecular reactions to intercellular interactions are complicated by the differences in complexity and time scales between cellular and molecular systems. As mentioned above, the time for a response to an encounter between cells or to sensing of molecular ligands by cells may vary widely. Often, responses are assumed to

happen instantaneously for simplicity. However, there are a number of examples showing that explicit consideration of delays leads to different results [Bocharov and Romanyukha, 1994, Baker et al., 1998, Pilyugin and Antia, 2000]. A delay is one of the simplest ways to represent the net effect of intracellular changes that may affect a cell's interactions with other cells; as mentioned above, the molecular mechanisms behind a visible cell response are extremely complex. It is not clear how much of this internal cell state must be included in order to accurately capture the intercellular dynamics. Alur et al. [2002] combine intracellular molecular dynamics with intercellular dynamics. They point out that internal changes in cell behavior that are often described by stiff, nonlinear differential equations can be effectively modeled by discrete switches between piecewise linear functions. This type of hybrid approach allows them to construct hierarchical models that accommodate multiple scales.

One problem with individual-based models and the different kinds of hybrids described above is that they are more difficult to develop than differential equation models. Attempts to ease development of such models have had marginal success. Although there are a number of agent-based modeling frameworks that are supposed to ease program development (e.g., Swarm [Swarm], RePast [RePast], XRaptor [Bruns et al.], Charon [Charon]), a significant amount of coding is still required to create useful models. More importantly, most are not designed to handle the multiple spatial and temporal scales required to accommodate mixed cellular and molecular processes. Two simulators were developed specifically for multicellular systems with molecular interactions: the biological toolbox [Vawer and Rashbass, 1997] used a mix of unrestricted cell movement and continuous molecular concentrations similar to that in [Dallon, 2000]; SIMMUNE [Meier-Schellersheim, 2001] used a regular lattice to define cell positions and discretization of molecular concentrations. Both allowed mixed stochastic and deterministic dynamics. However, these programs are no longer available, and the source code was never released.

Chapter 3

CyCells Simulator

As described in the previous chapter, there are a number of potential advantages in using spatially explicit individual-based models to understand localized intercellular interactions. However, this approach is often used to implement a single, special-purpose model of some particular system. Modeling is a process; creation of a single model by itself is not as useful as the ability to compare multiple models within a common framework. I wanted a simulator that would allow modification of the functional form of cell behaviors in order to allow both iterative refinement of a single model and exploration of different models of intercellular interactions.

It is often necessary to build a model of a complex process incrementally. Sometimes very simple assumptions produce useful results; in other cases, additional complexity must be added to capture the behavior of interest. In biological systems, there are often competing hypotheses in the literature, and it is helpful to be able to compare them. Finally, sometimes the original conceptual model or its implementation simply fails to produce the expected dynamics. The process of iteratively trying alternatives and determining when and why they fail or succeed is instructive in itself. In addition, multiple models of the same system also lead to greater understanding. As an obvious example, biologists use

both animal models and culture experiments to try to understand cell functions. Different experimental protocols highlight different aspects of the system.

One of the great advantages of purely mathematical approaches is that they are flexible. It is very easy to change the functional form of the equations as well as the parameter values without recoding the solver. Similar flexibility should be possible in computational models. This is generally not true of agent-based models, where the implementation is often closely tied to a particular model. Given the amount of effort required to develop spatial, agent-based simulations, it does not make sense to limit them to special cases. A number of 'general-purpose' frameworks have the opposite problem; they are often too general to be of much use in a particular scientific discipline.

I developed a simulator called CyCells which is used throughout the rest of this dissertation. CyCells is not a general-purpose agent-based development framework. It was designed for studying intercellular interactions and has a number of features particularly chosen to represent intracellular infection. However, it allows significant flexibility in choosing cell behaviors and molecular properties, and thus supports incremental model development and refinement. It could also be used to model a broad variety of multicellular systems, not just the specific examples in this dissertation. Section 3.1 describes some of the general characteristics that motivated particular design decisions; more detail on the simulator itself is given in later sections.

3.1 Hybrid Modeling Approach

The approach used here combines the behaviors of individual cells with continuous dynamics of extracellular molecules, incorporating elements of agent-based and particle-system models. The numbers of cells involved in the earliest stages of infection are generally very small, and they interact within a very localized region. Continuous rep-

resentations for cell populations are not appropriate in this case. Even when larger cell populations are involved, modeling individual cells can help clarify the effects of spatial and cellular heterogeneity on the overall dynamics. Cytokines have a strong influence on what those individual cells do, so models need to incorporate the molecular environment. However, the number of molecules involved can be much greater than the number of cells, making representation of individual molecules in a multicellular system intractable.

In general, cell behavior depends both on internal state and on the local environment. In CyCells, the molecular environment and most components of cell state are represented as continuous variables updated each time step. Changes to cell state are not always continuous, however. The most obvious exceptions are discrete events such as cell death and division; cells may also differentiate, which can affect multiple aspects of cell behavior. These events may be triggered either stochastically or by a continuous variable passing a threshold. A special case of internal cell state is the representation of intracellular infection. A discrete variable tracks the number of pathogens within an infected cell, and changes to this variable may be made to reflect intracellular replication or killing of individual pathogens.

Section 3.1.1 outlines the framework for specifying cell behavior and section 3.1.2 presents a conceptual view of the tissues in which these cells are situated.

3.1.1 Sense-Process-Act

In order to allow modeling of many different kinds of cell behaviors, I made use of a common abstraction in multi-agent systems: that agent behaviors can be segregated into functions that handle sensing the external environment, those that update the internal state, and those that implement some concrete action that affects the cell or its environment or both. Simulation models are defined by describing the sense, process, and act functions appropriate for each cell type.

Cells may die, divide, differentiate, or migrate, all of which affect the composition of the local population. Cells also secrete cytokines and antimicrobial molecules. Each of these individual actions occurs with a probability that is usually not constant, but depends on the cell's history and current signals from the environment. Intracellular signalling functions determine how a cell's state and its perception of the local environment are combined to update these probabilities. Sensing functions manage the cell's interactions with neighboring cells or the local molecular environment. Sensing the molecular concentration may also modify it; cells often internalize bound receptors [Thomson, 1998], which may have important feedback effects. Separation of sensing and processing allows the kind of pleiotropy seen in intercellular systems—each cytokine may affect multiple cell actions, and multiple cytokines may affect a single action.

3.1.2 The Tissue Compartment

Each cell's environment is determined by its location within some tissue. One complicating factor in a spatially explicit model of peripheral immune responses is the influx of new cells from circulation. Conceptually, cells enter the compartment that is explicitly simulated from some other compartment (circulation) that is not explicitly simulated. A typical modeling approach is to assume new cells enter at the boundary of the simulated compartment, but any reasonably sized tissue actually has numerous blood vessels running through it that allow circulatory cells easy access to all parts of the tissue. Although the exact layout of the vasculature is not of interest here, the possibility of influx rates varying in different parts of the tissue due to local expression of cytokines and chemokines is important.

Modeling tissue inflammation requires some mechanism for allowing new cells to be added at various locations throughout the simulated space. In CyCells, this is under control of cells already in the simulated tissue. One of the actions that can be defined for a cell type

is the ability to admit new cells into the simulation. This allows cells to act as 'gateways' controlling cell migration, mimicking the action of endothelial or epithelial cells. The probability with which a 'gateway' cell admits a new cell may depend on the local cytokine environment. This implementation is not very different from that of cell division—in both cases, a new cell appears in the vicinity of an existing cell.

Inflammation may result in very irregular spatial distributions of cells, with localized regions of very high densities. In addition, multiple cell types of varying sizes may be involved. A grid-based scheme for cell positions, in which each grid space may be occupied by a single cell, does not adequately capture these spatial distributions. In CyCells, cell positions are continuous-valued coordinates and cells may overlap to some degree when cell densities are high. Cells adjust their positions to balance pressure from other cells and their own motive forces. There is therefore no explicit limit on the number of cells allowed within a simulated volume. However, various density-dependent survival schemes can be implemented within the model framework.

3.2 CyCells Overview

CyCells is a three-dimensional, discrete-time simulator for studying intercellular interactions mediated by molecular signals. Many of the features are particularly designed for modeling intracellular infections. The code is written in C++ and has been tested under Linux; the program and user manual are available at http://www.cs.unm.edu/∼christy/simcode.

There is significant flexibility in the way cell types can be defined, and a number of different cell and molecule types can be combined in any given model. As a result, a large variety of conceptual models that fit this general framework can be implemented and executed with the simulator. Running a simulation requires three steps: model definition,

model initialization, and the actual execution. These are explained in sections 3.2.1, 3.2.2, and 3.2.3; more detail is available in the user manual.

3.2.1 Model Definition

A model definition file like the one shown in Figure 3.1 specifies the behavior of each molecule and cell type used in a simulation. The file consists of a list of cell type names, followed by a block for each molecule type and a block for each cell type.

Molecule types are defined by giving them a name and specifying the appropriate decay and/or diffusion rates. Note that cells can also change the molecular concentration by secreting or binding molecules. Although there is only one molecule type in the example, multiple molecule types are allowed.

A cell type definition specifies the attributes all cells of that type have, how those attributes should be initialized, and how they should be updated or used to make decisions during each time step. The actual values of those attributes are stored for each individual cell. In the example shown in Figure 3.1, macrophages have six attributes. Some of these are initialized at specific values, while others are chosen from uniform, gaussian, or lognormal distributions. There are two initialization specifications because cells may be initialized either as new daughter cells or as cells entering the simulation in the middle of the life cycle; the macrophage attribute *S* is initialized differently for these two different situations.

The definition also includes a line for each sense, process, or action function used by each cell type, with the relevant parameter values. A few specialized functions of each type serve to cover a wide range of cell behaviors. These are explained in sections 3.4, 3.5, and 3.6.

```
cell_names { macrophage cycling tissue }

molecule_type CSF {
decay_rate 1e-4
}

cell_type macrophage {
attribute cmax lognormal 3.58 0.4 lognormal 3.58 0.4
attribute b fixed 0 fixed 0
attribute S fixed 0 uniform 0 700000
attribute sr gaussian 700000 50000 gaussian 700000 50000
attribute time fixed 0 fixed 0
attribute tc gaussian 43200 1800 gaussian 43200 1800
sense b consume-indiv CSF cmax 1.3E-13
process S update linear b 1 0
action change cycling gte_var S sr
action die calc_prob inhibiting b 1e-5 0.37
}

cell_type cycling {
attribute cmax lognormal 3.58 0.4 lognormal 3.58 0.4
attribute b fixed 0 fixed 0
attribute S fixed 0 uniform 0 700000
attribute sr gaussian 700000 50000 gaussian 700000 50000
attribute time fixed 0 uniform 0 43200
attribute tc gaussian 43200 1800 gaussian 43200 1800
sense b consume-indiv CSF cmax 1.3E-13
process time update fixed 1
action divide macrophage gte_var age tc
}

cell_type tissue {
action secrete CSF fixed 2 always
}
```

Figure 3.1: Sample model definition file. A general description is given in the text; syntax and other details are given in the user manual.

3.2.2 Initialization

An initialization file, like the one shown in Figure 3.2, specifies the simulation geometry, initial molecular concentrations, and initial numbers of each cell type. Simulation geometry is explained in section 3.3. A key component of the spatial representation is the size of the grid used to discretize molecular concentrations. Cell positions can be specified if desired; in this example, cells are positioned randomly.

```
geometry
1000x1000x1000 microns; mol_res:  0  cell_res:  0

molecule_uniform:  CSF 6E-15 0

cell_count:  tissue 1000
cell_count:  cycling 30
cell_count:  macrophage 970
```

Figure 3.2: Sample model initialization file. A general description is given in the text; syntax and other details are given in the user manual.

3.2.3 Simulation Execution

One time step of the simulation consists of the following sequence of activities:

1. Molecular diffusion and decay
2. Update of each cell according to sense, process, and act functions
3. Cell movement

In real biological systems, molecular interactions, cellular actions and interactions between cells and molecules all happen in parallel. Imposing an order on these activities for computer execution can introduce artifacts that do not reflect realistic behavior. In step 2, each cell may modify the molecular environment and thus indirectly affect cells visited later. To minimize cumulative effects of this serialization of an inherently parallel process, the cell visitation order is randomized each time step.

Order effects can also be reduced by using small time steps. However, execution time is inversely proportional to time step size, so there are practical limits on how small a time step can really be. The choice of an appropriate time step depends on characteristic rates of the modeled system, so the time step size is chosen at run time. Typical time step sizes are 1–20 seconds.

Simulation run time is directly proportional to the number of time steps T. For each time step, the molecular concentrations are updated in a time that is proportional to the number M of grid points at which molecular concentrations are stored, and cells are updated in a time that is proportional to the number of cells N. The exact time for the cell updates will depend on the number of sensing and processing actions required for each cell. Overall run time is proportional to $(T(M+N))$. Note that the number of cells may change during the course of a simulation. Spatial resolution and time step size are chosen at runtime.

3.3 Spatial Representation

CyCells is designed to accommodate spatially explicit models, although it is also possible to ignore spatial effects. There are two different ways in which cell positions may affect the overall dynamics: first, direct cell-cell interactions depend on the relative locations of the cells involved; second, concentrations of cytokines that affect cell behavior may vary in different locations. There are two components to the simulator's spatial representation to accommodate these two different effects.

Individual cell positions are represented by continuous-valued variables; these positions are not restricted to a lattice. However, the simulated volume is conceptually divided into a three-dimensional array of cubical patches. For each patch, a list of cells located in that patch is maintained to make searches for cell neighbors more efficient. Phagocytosis (described in section 3.4) and collision resolution (described in section 3.3.1) both depend on the distance between cells. These distances are calculated only for cells within the same or adjacent patches, rather than for all cells in the simulation. (Cell movement is described in section 3.3.1.) The size of each patch is specified by the *cell_res* variable in the initialization file. Generally, a patch size approximately the size of the largest cell type works best. If the simulation does not require cell movement or cell-cell contact, a value

of 0 can be used to indicate that the volume does not need to be divided in this way.

A separate three-dimensional grid is maintained for molecular concentrations, which may have a different resolution than that used for tracking cells. In the initialization file, *mol_res* determines the granularity of stored molecular concentrations; a value of 0 means that the molecular environment is assumed to be homogeneous. For nonzero *mol_res*, molecular diffusion is implemented on this grid as explained in section 3.3.2. A cell's position is used to determine which grid cell represents the local molecular environment for that cell. Any changes made to the concentration by cell sensing or secretion of molecules are applied only to the nearest grid cell.

Periodic boundary conditions are used for both cell positions and molecular diffusion.

3.3.1 Cell Movement

Cell movement in isotropic environments is described as a persistent random walk [Lauffenburger and Linderman, 1993]. Cells move at a nearly constant velocity over a short period of time, then change direction. The average time between direction changes is known as the persistence time. CyCells movement actions, described in section 3.6, govern how and when cells choose their orientation. Unimpeded cell speed is assumed to be constant in these simulations, and is the same for all cells of the same type. A cell's current orientation together with the speed for its type determine its velocity vector in the absence of collisions.

Collisions in CyCells are inelastic. Simulated cells are represented as spheres for convenience, but those spheres are allowed to overlap to account for the fact that real cells are deformable. There is an ad hoc repulsive force when cells overlap that tends to move them apart, space permitting, and that prevents cells from moving directly through each other. This is implemented by adding a velocity component from an overlapping neighbor to a moving cell's unimpeded velocity vector. The magnitude increases linearly with the

amount of overlap; the direction is from the neighbor cell center to the moving cell center. On each time step, the net velocity for each moving cell is calculated by summing its unimpeded velocity and the contributions from any overlapping neighbors, and is multiplied by the time step to get the cell's displacement. Final positions are corrected to account for periodic boundary conditions if necessary.

3.3.2 Molecular Diffusion

Changes in concentration due to diffusion are calculated using an explicit method based on concentrations from the previous time step. The change in one time step of the concentration u in a particular grid cell with indices i, j, k is given by:

$$\frac{\Delta u_{i,j,k}}{\Delta t} = D\left[\frac{(u_{i+1,j,k} + u_{i-1,j,k} + u_{i,j+1,k} + u_{i,j-1,k} + u_{i,j,k+1} + u_{i,j,k-1} - 6u_{i,j,k}}{(\Delta x)^2}\right] \quad (3.1)$$

where D is the diffusion coefficient and Δx is the width of each (cubical) grid cell. For this method to give reasonable results, the time step must meet the following constraint [Press et al., 1998]:

$$\Delta t \leq \frac{(\Delta x)^2}{6D} \quad (3.2)$$

If the simulation time step is larger than this limit, the diffusion routine takes multiple substeps on one update to ensure that this condition is met. To facilitate the above calculation with periodic boundary conditions, concentrations on each edge of the simulated volume are duplicated in extra 'guard' grid cells on the opposite edge.

This implementation of molecular diffusion does not take the presence of cells into account. This is a common simplification, but one that could misrepresent molecular concentrations and gradients in regions of high cell density.

3.4 Sensing

Cells can sense extracellular molecules or other cells. For real cells, both of these are mediated by binding of receptors on cell surfaces. In simulation, the key point is to make appropriate changes to a cell's internal state in response to the local molecular environment or contact with nearby cells.

3.4.1 Sensing Molecules: Receptor-Ligand Binding

There are two primary forms of molecular sensing used in the simulations in this dissertation. The first is simply to copy the local concentration into a cell variable; processing functions then determine how the cell uses this information. The second represents nonlinear binding and consumption of local molecules. The first requires less computation; the second accounts for cell density-dependent reduction in molecular concentrations.

Real cells are somewhat limited in their abilities to sense the local molecular environment. Sensing depends on encounters between receptors and ligands, and therefore on the relative amounts of each. As concentrations increase, the signal a cell receives will saturate at some point determined by the number of receptors that cell expresses. These effects are explicitly represented in the second, more mechanistic representation of molecular sensing. When the first approach is used, there is no limitation on the simulated cell's sensitivity, but cells can be prevented from acting on signals outside their normal range by the appropriate use of internal processing functions, which are described in section 3.5. The primary reason for using the more mechanistic model of receptor-ligand binding is to incorporate the effects on the molecular environment as well as on the cell. The remainder of this section is devoted to explaining the model of receptor-ligand binding and internalization.

Free receptors on the cell surface (R_s) bind to extracellular ligand (L)

to form receptor-ligand complexes (C_s) according to the following equations [Lauffenburger and Linderman, 1993]:

$$\frac{dR_s}{dt} = -k_f L R_s + k_r C_s - k_{eR} R_s + V_s \tag{3.3}$$

$$\frac{dC_s}{dt} = k_f L R_s - k_r C_s - k_{eC} C_s \tag{3.4}$$

where k_f and k_r are the association and dissociation rate constants. Free and bound receptors may be internalized at rates k_{eR} and k_{eC}, respectively. New receptors are synthesized at rate V_s. I assume that the signal affecting cell behavior is proportional to $k_f L R_s$.

In the presence of slowly varying ligand concentration, the system comes to a quasi-steady state ($dC_s/dt \approx 0$, $dR_s/dt \approx 0$) in which the numbers of cell-surface receptors and cell-surface complexes depend on L as follows [Lauffenburger and Linderman, 1993]:

$$R_s = \frac{(k_r + k_{eC}) C_s}{k_f L} \tag{3.5}$$

$$C_s = \frac{K_{ss} V_s L}{k_{eC}(1 + K_{ss} L)} \tag{3.6}$$

K_{ss} is a dimensionless parameter known as the apparent cellular affinity constant.

The change in ligand concentration is given by:

$$\frac{dL}{dt} = (-k_f L R_s + k_r C_s) n \tag{3.7}$$

where n is the cell density. The rate at which a single cell 'consumes' ligand is

$$c(L) = k_{eC} C_s = \frac{V_s K_{ss} L}{1 + K_{ss} L} = \frac{V_s L}{1/K_{ss} + L} \tag{3.8}$$

For growth factors, a significant amount of internalization of bound receptors always occurs [Lanza et al., 2000]. In this case, ligand binding by cells may have a significant

effect on the local concentration. It also means that the rate at which ligand is internalized is roughly equal to the rate of cell signalling, since the second term of equation (3.7) is negligible.

Equation (3.8) has the general saturating form

$$c(L) = \frac{c_{max} L}{c_{half} + L} \tag{3.9}$$

in which c_{max} represents the maximum rate at which a cell can bind and internalize ligand (in molecules cell^{-1} s^{-1}), and c_{half} represents the ligand concentration at which the consumption rate is half of the maximum. This is the form used to implement cell consumption of molecules in simulations; c_{max} and c_{half} must be specified in the model definition.

3.4.2 Sensing Cells: Direct Contact

There are two types of sensing functions that allow a cell to respond in some way to neighboring cells. The first simply detects neighbors of a certain type within a specified distance. If one is found, an associated cell variable is set to 1; otherwise it is set to 0. The second function implements phagocytosis of one cell by another, as in macrophage phagocytosis of bacteria. In order for a phagocyte to ingest a target cell, the cells must bind. Binding depends both on distance between the cells and on the relative numbers of molecules on the phagocyte and its target that can bind. There is a large variety of receptor types that mediate phagocytosis in real cells, and they vary in affinity for pathogen surface molecules and efficiency of inducing phagocytosis [Aderem, 2003]. In CyCells, phagocyte cell type definitions must include an attribute representing their phagocytic capability for a particular target type. The associated value may vary for individual cells of the same type; it is compared to a threshold to determine whether phagocytosis occurs. The distance between phagocyte and target cell must also be small. Both the maximum distance and the phagocytic threshold are specified as parameters of the phagocytosis function in the model definition. When all the conditions for phagocytosis are met, the target cell is removed

from the extracellular environment and the phagocyte's internal state is updated to reflect the number of targets ingested.

3.5 Processing - Abstraction of Intracellular Signaling

The primary purpose of process routines is to convert sensed signals and current cell state into rates or probabilities that affect cell actions. Although processing functions are roughly analogous to signal transduction in real cells, they do not represent real intracellular signalling pathways in any biochemical detail. There are also special-purpose process routines for representing intracellular pathogen dynamics.

3.5.1 Updating Internal State Variables

Most cell variables are assumed to represent continuous quantities (and all are stored as real values). CyCells provides a number of ways to manipulate these values mathematically. Processing functions can be used either to update cell variables, in which case the current value is used in determining the next value, or to replace them, in which case the current value is discarded. In either case, the new value is calculated from one or more cell state variables.

One function of intracellular processing is to implement the delays between fast receptor-ligand binding events and observable cell responses. For example, a cell needs to spend several hours exposed to growth factors before it is ready to to begin cell division. The simulator therefore needs to keep track of the total signal received. This sort of gradual state change is one scenario where incremental changes to the cell state are important.

In other cases, changes in simulated cell state may be discontinuous. This could reflect

a situation in which cell behavior changes quickly enough that we can treat the state change as if it were instantaneous. Production of some molecules can be up- or down-regulated fairly quickly, for example. It may also be used to model behavioral changes for which there is insufficient data on the timing of associated internal state changes. An internal cell variable may be recalculated each time step, if appropriate. More often, a variable associated with some cell function like secretion takes on only two values—a high and a low value, or on and off. A 'toggle' process function specifies the conditions under which a cell will switch from the low to the high value, or vice versa.

3.5.2 Intracellular Pathogen Dynamics

Pathogens that have infected a cell are not represented as encapsulated objects, but rather as one variable of the host cell's internal state. Tracking an intracellular pathogen population requires a different kind of processing than updating other cell state variables. The main difference is that the cell variable being updated represents the number of pathogens, which is a relatively small integer value. If the host cell dies in a way that can release these pathogens, this number is used to create the appropriate number of new pathogen cells.

The number of intracellular pathogens can change due to division or death of individual pathogens. The intracellular division and death rates may depend on the host cell state. However, for any given time step, I assume that the division rate g and killing rate q are constant over that time step. An intracellular population of size m should change by $(g-q)m$ during one time step. For the for the rates of bacterial growth and killing used in this dissertation, there should be no more than 1 birth or death event in a given time step Δt. Therefore, the simulator increments the intracellular population by one with probability $gm\Delta t$ and decrements it with probability $qm\Delta t$.

3.6 Cell Actions and Conditions

Most cell actions are discrete events that are triggered by some condition, so action definition actually consists of specifying a condition-action pair. There are two primary types of conditions. The first is probabilistic, in which case a random number is compared to some probability to determine whether the condition is met; the second is a threshold condition on some cell variable. The probabilities used in the first case may depend on cell state. There is also an 'always' condition, primarily used for constitutive secretion of molecules.

There are several kinds of cell actions that may be defined in CyCells models; these are listed below.

Death When the associated condition is met, the cell is removed from the simulation. Note that this may be used to represent cells leaving the simulated compartment, as well as actual death.

Differentiation A 'change' action causes a cell to change its type, as in differentiation or infection. This provides a way for a cell to keep its state information, but change the rules by which it functions.

Division When a cell divides, two new cells are created and the original is removed. The daughter cells may or may not be of the same type as the original cell; the option to create a different type is provided to allow differentiation or maturation—represented by a change in cell function—to accompany division. The two new cells are given the same position as the original with small offsets in the x coordinate.

Admit An 'admit' action implements cell influx into the simulated compartment from somewhere else. This is under the control of a cell already in the simulation, because it is assumed that endothelial and/or epithelial cells generally control entry of cells from circulation into local tissues, usually in response to their molecular

environment. So this action would be part of the definition of such a 'gateway' endothelial or epithelial cell. The new cell is positioned at the same position as the 'gateway' with a user-defined offset distance applied in a randomly chosen direction. There is also a variant in which the offset distance is applied in the direction of a molecular gradient.

Release of intracellular pathogens A similar scheme to that above is used to implement release of pathogens from a dying host cell. For a cell containing n pathogens (where n is one of the cells' internal variables), n new cells representing extracellular pathogens are created and added to the simulation. Their positions are radially distributed around the host cell's position at a user-specified distance.

Movement As explained in section 3.3, a cell's displacement depends not only on its orientation and speed, but on boundary conditions and collisions with neighboring cells; movement actions only specify how cells choose their orientation. The associated condition specifies how often a cell changes direction; typically, the condition specifies a probability inversely proportional to the persistence time. A simulated cell may move randomly or by chemotaxis. In the former case, or in the latter case if there is no detectable gradient, the cell chooses a direction at random. In chemotactic movement, the cell's orientation is chosen to match the direction of a local molecular gradient. Note that although the simulated cell aligns perfectly with the calculated gradient, the accuracy of that calculation will depend on the resolution of the molecular concentration (*mol_res* from section 3.3). Increasing the size of molecular grid cells is a crude way to represent the imperfect chemotaxis exhibited by real cells.

Secretion Cells can secrete molecules at a fixed or variable rate.

Composite Actions Finally, there is a means for specifying that two actions should triggered by the same condition; these composite actions can also be nested to allow more than two actions to be combined in the same way.

3.7 Summary

The choice of simulator implementation was greatly influenced by the models I wanted to explore. Not all capabilities are used in all models, but the applicability of each should become clear in the following chapters. Chapter 4 concentrates on the role of molecular signaling and largely ignores spatial effects, whereas Chapter 5 addresses spatial effects and cell–cell contact with less emphasis on the role of cytokines. Results from these models influenced the development of the tuberculosis model described in Chapter 6.

Chapter 4

Macrophage Homeostasis

The number of macrophages and other immune system effector cells in peripheral tissues remains fairly constant in the absence of disease, despite a large amount of turnover. Populations change through proliferation, death, and migration of individual cells. These functions are regulated by cytokines, but we are only just beginning to understand how cells interpret and respond to the information in the local molecular environment.

The regulatory signals that allow maintenance of a steady-state population are of interest in their own right, and also have an impact on the changes to that population when foreign organisms are encountered. Maintenance of an appropriate 'sentinel' population enables rapid initiation of an immune response in case of infection, and homeostatic regulation plays a role in restoring normal tissue function once the infection has been resolved.

This chapter explores simple models of peripheral effector population homeostasis, focusing on alveolar macrophages for concreteness. Alveolar macrophages provide the first line of defense against microorganisms entering through the lungs.

I first develop a model of growth factor effects on individual cell survival and proliferation. I then use this model to investigate two alternatives for population maintenance in

vivo: one in which proliferation of resident cells replenishes the macrophage population, and the other in which cells migrating from circulation are the only cells that divide. The simulations in this chapter assume a homogeneous molecular environment; spatial effects are discussed in the next chapter.

4.1 Alveolar Macrophage Dynamics

Pulmonary macrophages are classified according to where they are found. Interstitial macrophages reside within lung tissue; alveolar and airway macrophages are found along the epithelium of the alveoli and branching airways, respectively. Figure 4.1 is a sketch of macrophages in and around alveoli. Macrophages in different locations, and even within a single location, show great morphological and functional heterogeneity [Laskin et al., 2001], making the exact relationship between these various subpopulations unclear. Also, macrophages are highly mobile, capable of moving both within and between locations. As a result, there are several factors affecting the size of local populations: differentiation, migration, proliferation, and death. All of these cell behaviors are somehow kept in balance during normal conditions, but rapidly expand the population in response to infection or injury.

The origin of alveolar macrophages has not been completely resolved. Van Furth [1992] proposed that all macrophages in peripheral tissues, including the lung, are part of a mononuclear phagocyte system (MPS). This system consists of cells that derive from bone marrow precursors, which differentiate into blood monocytes that randomly leave the circulation to enter various tissues and become macrophages. The tissue macrophages were thought to be terminally differentiated and incapable of proliferating. Others, however, have argued that local proliferation is important and may even be primarily responsible for maintaining alveolar macrophage populations [Coggle and Tarling, 1984, Shellito et al., 1987]. Alveolar macrophages are capable of proliferating in vitro in the presence of the

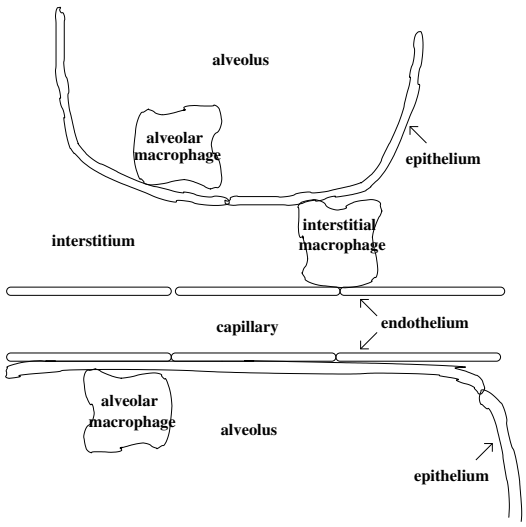

Figure 4.1: Pulmonary macrophages. Interstitial macrophages reside within pulmonary tissue; alveolar macrophages are found 'outside' the alveolar epithelium. Cells may be recruited to the alveoli from the interstitium, across the alveolar epithelium, or from circulation, across both the vascular endothelium and the alveolar epithelium.

appropriate molecular growth factors [Lin et al., 1989, Akagawa et al., 1988], in contrast to expectations for terminally differentiated cells. Also, in vivo labelling studies have shown that roughly 3% of alveolar macrophages are synthesizing DNA in preparation for cell division at any given time [Blusse van Oud Alblas et al., 1983, Coggle and Tarling, 1984, Fritsch and Masse, 1992], but the authors disagree about which cells are dividing. Several theories for the origin of alveolar macrophages have been proposed and investigated:

1. Alveolar macrophages derive from migrating blood monocytes, and are normally incapable of dividing [Blusse van Oud Alblas and van Furth, 1979];

2. Monocytes mature in lung capillaries and undergo a final maturation division in the alveoli [Fritsch and Masse, 1992];

3. Alveolar macrophages derive from interstitial macrophages through local division

and maturation [Bowden, 1984];

4. Alveolar macrophages divide *in situ* [Coggle and Tarling, 1984, Shellito et al., 1987].

There are also multiple ways in which macrophages may leave the alveoli. The most common route out of the alveoli is up the bronchi to where they can be expelled or swallowed [Perez-Arellano et al., 1990]. Trafficking of alveolar macrophages to the lymph nodes has also been reported [Corry et al., 1984, Harmsen et al., 1985], and some other routes have a minor role [Perez-Arellano et al., 1990]. Cell death is also a significant factor. It is often difficult to determine whether cell loss is due to migration or death; quantitative studies often measure a simple loss rate that does not distinguish between the various migration routes and cell death [Fritsch and Masse, 1992].

The studies referenced above attempted to quantify the rates of local proliferation, influx, death, and/or efflux, but did not address the mechanisms involved. Each of these activities depends on interactions between macrophages and the appropriate molecular signals in the environment or on other cells.

There are a number of molecular mechanisms that regulate a cell's transition from the resting state to the proliferating state and its progression through the cell cycle. In particular, the proper growth factor(s) must be present before a cell can pass a restriction point and begin DNA synthesis [Pardee, 1989] The time required between the beginning of DNA synthesis and cell division is fairly constant, but the time between one division and beginning of DNA synthesis for the next is highly variable. Increasing concentrations of growth factor can shorten this time and therefore the total cell cycle time [Metcalf, 1991]. Pardee [1989] proposed that growth factor binding drives accumulation of a rapidly decaying internal substance which must reach a critical level for the cell to begin synthesizing DNA, and Smith [1989] found that a critical number of such bindings must be reached for T cells to divide.

Macrophage-Colony Stimulating Factor (M-CSF) and Granulocyte-Macrophage-Colony Stimulating Factor (GM-CSF) have both been shown to stimulate division of murine alveolar macrophages in vitro in a dose-dependent fashion [Chen et al., 1988, Akagawa et al., 1988, Lin et al., 1989]. Injection of M-CSF has also been shown to increase alveolar macrophage numbers in vivo [Held et al., 1996].

In addition to promoting cell proliferation, growth factors are believed to promote cell survival by preventing apoptosis [Williams et al., 1990], although dose dependence has not been studied as extensively as it has been for proliferation. Tushinski et al. [1982] showed that macrophages cultured without M-CSF died, and that a low dose could maintain macrophage populations in vitro with little proliferation.

4.2 Macrophage Proliferation and Survival Model

This section develops the model of macrophage proliferation and survival. I rely on literature describing macrophage dependence on macrophage colony stimulating factor (M-CSF), first reviewing how macrophages sense M-CSF, and then the cellular response to sensed M-CSF.

4.2.1 Receptor-Ligand Binding

M-CSF is rapidly internalized and degraded by macrophages [Chen et al., 1984, Guilbert and Stanley, 1986]. This is represented in the simulations by using equation 3.9 to represent sensing and internalization of M-CSF. Tushinski et al. [1982] measured the rate at which macrophages remove M-CSF at various different concentrations, which gives estimates of c_{max} and c_{half}.

However, macrophages demonstrate significant heterogeneity in the numbers of sur-

face molecules they express [Laskin et al., 2001]. As demonstrated above, the rate at which cells consume growth factor is directly proportional to the receptor synthesis rate, so variation in receptor expression should be directly correlated with variation in the maximum consumption rate c_{max}. The simulations represent cell heterogeneity by giving each cell a different value of c_{max}, using a log-normal distribution as was used in Burke et al. [1997] for T cells.

4.2.2 Proliferative Response

Following other modelers [Zandstra et al., 2000, Burke et al., 1997] and evidence in the experimental literature [Chen et al., 1987, Smith, 1989], I assume that some threshold amount of bound growth factor is required for a cell to pass the restriction point. Equation (3.9) represents the rate at which growth factor is bound. Each simulated cell has an internal variable S which tracks the cumulative signal received. If S reaches a positive threshold value s_r, the cell passes the restriction point and divides a fixed amount of time t_c later.

S does not represent any real molecular species inside cells; it is instead an abstract measure of the progress a cell has made towards the restriction point. In real cells, progress towards the restriction point is the result of competition between production and degradation of intracellular molecules that regulate the cell cycle. I am assuming that the net result of these competing processes is proportional to the number of receptor-ligand binding events. Because Tushinski et al. [1982] report some proliferation even at low growth factor concentrations, I assume that this net effect is always nonnegative. This model does not account for cell behavior in the complete absence of growth factor; cells become quiescent when growth factor is removed, and require a lag period of several hours after re-introduction of growth factor to reenter the cell cycle [Tushinski and Stanley, 1985]. This would require a decrease in S during the starvation period. However, it is not clear that this implies the need for decay in S in the presence of growth factor. For simplicity,

and because all of these simulations use nonzero growth factor concentrations, I omit a mechanism for decreasing S.

To summarize:

$$\Delta S = c(L)\Delta t \tag{4.1}$$

$$S > s_r : \text{cell will divide after time } t_c \tag{4.2}$$

4.2.3 Cell Survival

In the absence of growth factor, macrophage populations in vitro exhibit exponential decay [Tushinski et al., 1982] at a rate d_{max}. However, the rate at which the population decays decreases as the growth factor concentration is increased. I assume that resting cells have some probability of dying that depends on the current growth factor concentration, or more properly, on the cell's perception of the growth factor concentration. Based on an analysis of the data in Tushinski et al. [1982], I use the following form for a cell's probability of dying in a small time Δt:

$$p(d) = \frac{d_{max} d_{half}}{c(L) + d_{half}} \Delta t \tag{4.3}$$

which drops off rapidly at first and then gradually approaches 0; the probability is half its maximal value when $c(L) = d_{half}$. I assume that the death rate for cells past the restriction point is negligible.

At the population level, the internalization and destruction of growth factor by macrophages could be important, as it indicates that regulation of cell populations might be at least partly controlled by competition for growth factor. Consumption of ligand completes a negative feedback loop in which increasing numbers of cells decrease the ligand concentration, which then causes a reduction in cell numbers.

4.2.4 Model Summary and Calibration

I used CyCells with the model described above to reproduce the results reported in Table 1 of Tushinski et al. [1982]. In this experiment, 300,000 bone-marrow-derived macrophages were kept in culture with varying amounts of M-CSF for three days, with the culture medium replaced each day. At the end of that time Tushinski *et al.* measured the total cell population and percentage of cells in S phase. The cells had been cultured for several days in M-CSF before the beginning of the experiment; a control experiment showed that one-third of the initial cell population was in S phase at the beginning of the experiment.

To simulate this experiment, I define two cell types to represent resting and cycling cells. This is a modeling convenience; both 'types' represent macrophages, and individual cells may change type during the simulation. All cells consume growth factor as described in section 4.2.1. Resting cells use the amount of growth factor bound to increment their internal S value as described in section 4.2.2. Cells with an S value greater than or equal to s_r becoming cycling cells. These cells track how long they have been in the cell cycle, and divide—producing two resting cells—after time t_c. Resting cells die with a probability calculated as in equation 4.3; dividing cells do not.

The parameter values used for this experiment and throughout the rest of this chapter are shown in Table 4.1. The values for c_{max} and c_{half} come directly from Tushinski et al. [1982], translated into appropriate units for the CyCells model. The value for t_c is within a range given in Lauffenburger and Linderman [1993]. The maximum death rate d_{max} was estimated from cell culture data in Tushinski et al. [1982] in the absence of growth factor. All of these fairly straightforward parameter estimations were used to calculate appropriate values for s_r and d_{half}. s_r is roughly equal to the average time a cell takes to pass the restriction point times the growth factor consumption rate. The former can be determined from the cell cycle time t_c and the ratio between cycling and resting cells. This ratio and the consumption rate can be estimated from the data in Tushinski et al. [1982].

	Meaning	Mean value
c_{max}	maximum consumption rate	36 molecules/s
c_{half}	concentration for half-maximal consumption	1.3×10^{-10} M
s_r	restriction point threshold	700,000
t_c	cell cycle time	12 hours
d_{max}	maximum death rate	1×10^{-5} /s
d_{half}	consumption rate for half-maximal death	.37 molecules/s

Table 4.1: Parameters affecting macrophage proliferation and survival. Note that individual cells each have different values of c_{max}, s_r and t_c; the value shown is the population mean.

At a growth factor concentration of 2.2 pM, Tushinski et al. [1982] saw little change in the total cell number, indicating that the average number of resting cells entering the cell cycle must be balanced by the average number dying. This gives an estimate for the death rate at this growth factor concentration, which is used with d_{max} to calculate d_{half}.

I initialized the simulations with 100,000 cycling cells and 200,000 resting cells. Different simulations used different initial growth factor concentrations, in accordance with [Tushinski et al., 1982], and the growth factor concentration was reset to the initial value at the beginning of each simulated day. Tushinski et al. [1982] measured the final population size after three days in terms of the amount of DNA in each culture dish. I translated this amount to a number of cells using their assumptions about the amount of DNA per cell, which varies with the number of cycling cells and therefore the amount of growth factor present. These estimates, therefore, are rather coarse, making a more detailed parameter fit problematic. The simulations showed rough agreement with the final population sizes from [Tushinski et al., 1982], as shown in Table 4.2.

However, the simulations show significant variation in the percentage of cycling cells, as shown in Figure 4.2. Tushinski et al. [1982] report only the initial and final percentages of S-phase cells. Simulations record more detailed dynamics than can be observed in culture experiments. First, since roughly a third of the cell population is already committed to divide at the start of the experiment, there is always an initial increase in the cell pop-

Growth Factor Concentration	Experimental final cell number	Simulation final cell number
0	25000	34042 (178)
8.8 pM	78000	194056 (506)
22 pM	270000	313341 (366)
110 pM	1000000	845488 (890)
440 pM	2000000	2077536 (1255)

Table 4.2: Comparison between simulations and Tushinski's experiments. See text for description of experiment. Middle column shows cell numbers estimated from amount of DNA reported in Tushinski et al. [1982]. Final column shows mean (standard deviation) cell numbers from 5 simulations for each growth factor concentration. Simulation parameter values shown in Table 4.1.

ulation regardless of ligand concentration. This initial burst is amplified in the runs with higher ligand concentration as more cells enter the cell cycle, and is followed by a period when large numbers of cells divide and few are left in the cell cycle. Second, there is significant ligand depletion for most of the experiments in between the daily replenishments. Since Tushinski et al. [1982] measured M-CSF removal, this is not really surprising, but I found that it causes a temporary decline in cell counts at the end of each day in otherwise-growing cell populations. These two effects produce oscillations in the ratio of cycling to resting cells. It would be interesting to see whether this kind of oscillation could be seen in culture if measurements were made more frequently.

4.2.5 Related Models

There are numerous models of cell division which do not depend on extracellular signals, although the idea of dividing the cell cycle into variable- and fixed-length periods has been around for some time. Smith and Martin [1973] proposed that the switch from the variable-length 'A-state' to the fixed-length 'B-state'—comparable to passing the restriction point as described in section 4.2—is random. Many more recent models ([e.g., Tyrcha, 2001]) treat the probability as dependent on cell age or cell mass; Tyrcha points out that 'mass' may represent cumulative mitogen signalling. In other cases, there is no

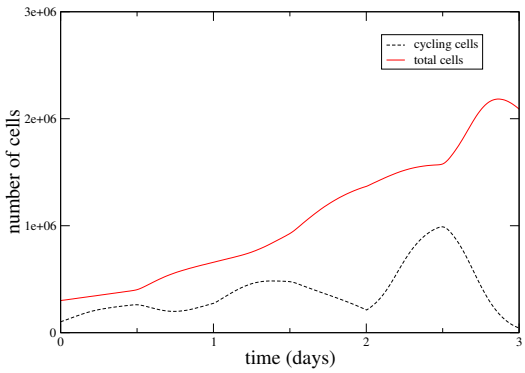

Figure 4.2: Simulation of Tushinski's experiment. Total cell population and number of cycling cells at high growth factor concentration (set to 4.4×10^{-10} M at the start of each day). Simulation shown is representative of five runs. Parameter values shown in Table 4.1.

distinction between the different parts of the cell cycle, but the population growth rate depends on the growth factor concentration [Lauffenburger and Linderman, 1993]. These models represent cells growing in high concentrations of growth factor, so ligand depletion is often ignored.

A model described in Morel et al. [1996] and Burke et al. [1997] of T cell growth in response to IL-2 and IL-4 has some similarities to the models in this chapter. They use a distribution of receptor synthesis values to capture heterogeneity in the cellular responses to ligand. They also divide the cell cycle into variable and fixed portions, where the former depends on cells accumulating a certain number of binding events. However, their focus is on synergy between two growth factors in conditions of fairly high growth factor concentration, and they do not include cell death.

4.3 Proliferation-Driven Homeostasis

I take the model developed in the section 4.2.4 as a plausible model of macrophage proliferation and survival in response to M-CSF and now turn to the consequences for mac-

rophage homeostasis in vivo. In this section, the population is replenished exclusively through local proliferation; the next section adds influx of monocytes from the bloodstream.

4.3.1 Differential Equation Model

Before presenting the individual-based model and simulation results, it is helpful to start with a mathematical description of the population as a whole. I have two subpopulations of macrophages: resting cells, represented by their concentration A, and those that have passed the restriction point, represented by their concentration B. They change according to:

$$\frac{dA}{dt} = 2rB - k(L)A - l(L)A \tag{4.4}$$

$$\frac{dB}{dt} = -rB + k(L)A \tag{4.5}$$

where r is the fixed rate at which proliferating cells divide, k is the rate at which resting cells pass the restriction point, and l is the loss rate. In addition to the variable death rate used in the last section, the loss term includes efflux.

I assume that growth factor is produced at rate p (where p is in molecules/s). Growth factor is lost at a fixed rate n in addition to removal by macrophages. M-CSF is particularly resistant to degradation by proteases [Stanley and Metcalf, 1971], but molecules can be lost to the surrounding environment. The change in ligand concentration is

$$\frac{dL}{dt} = \frac{p}{VN_{Av}} - \frac{c(L)}{N_{Av}}(A+B) - nL \tag{4.6}$$

(N_{Av} is Avogadro's number.) Note that although cells that have passed the restriction point no longer require growth factor, I assume that they would continue to bind and internalize growth factor.

From equations (4.4) and (4.5), a steady-state system requires $k = l$. Since both of these depend on L, this determines the steady-state ligand concentration. Then, from (4.6), the steady-state cell density is determined by the fact that growth factor production must balance consumption and loss. In other words, the cell proliferation and survival parameters alone determine the steady-state ligand concentration, and then the growth factor production and loss rates determine the population that can be supported.

In order to have a certain fraction f of the cells dividing at any given time, as observed in vivo, there is another constraint on k. With $B = f(A+B)$, equation (4.5) implies $k = rf/(1-f)$. Because of the steady-state requirement just mentioned, the loss rate l would need to have the same value. Since $r \sim 1/t_c$, k and l should be on the order of 2%/day in order to have approximately 3% of the cells in S phase.

However, k is not a parameter of the individual-based model; although the loss rate l has a direct relation to individual cells' probabilities of dying and migrating out of the compartment, k is somewhat more complicated. The probability that an individual cell will pass the restriction point depends on its rate of binding growth factor ($c(L)$ from section 4.2) and on the threshold point s_r. It also depends on the loss rate, because cells must survive long enough to reach the restriction point. Some of these parameters in turn depend on the growth factor concentration, which may vary over the lifetime of the cell. Finally, there is no straightforward way to relate this individual cell probability to the instantaneous population rate k.

4.3.2 Simulations

To implement this model in CyCells, I start with the model used in section 4.2 but add constitutive production of growth factor, growth factor decay, and probability of macrophage loss due to efflux. For the moment I assume that growth factor is produced by a different cell type; I will address autocrine regulation in section 4.5. The simulated compartment

represents a volume of 0.001 ml, which should hold approximately 1000 macrophages at normal lung densities based on estimates in [Fisher et al., 1988].

Estimates for loss rates of alveolar macrophages vary widely. Fritsch and Masse [1992] reported death rates of 5–6%/day and efflux rates of 2–3%/day in rats. Other researchers do not distinguish between death and efflux, but report loss rates ranging from 1 to 18%/day [Blusse van Oud Alblas et al., 1983, Coggle and Tarling, 1984, Shellito et al., 1987] I ran simulations with efflux rates of 0, 5, and 10 %/day.

I first initialized the ligand concentration to 2×10^{-11} M, approximately the concentration at which cell counts changed least in Tushinski et al. [1982]. Since there are no good estimates for growth factor production rates, I arbitrarily chose a growth factor loss rate of 0.006/min, which is within the range of cytokine half-times given in Fishman and Perelson [1999], and then estimated the production rate which should maintain the cell population at the chosen concentration. As mentioned earlier, the primary effect of these two parameters is on the steady-state cell density.

This simulation experiment was not entirely successful, as shown in Figure 4.3 for the no-efflux case. Table 4.3 shows the final ligand concentrations and cell numbers for all simulations. Although the system does reach a steady state, cell densities are much higher and ligand concentrations much lower than expected. By contrast, although the cell density did not change significantly for the same concentration in Tushinski's experiments, the simulation of the same experiment showed that the system was not really at steady state. Also, because ligand depletion effects were significant, the average ligand concentration actually would have been lower than 2×10^{-11} M.

Because of the feedback between growth factor concentration and cell population, the system settles at a ligand concentration at which entry into the cell cycle balances cell loss. When the growth factor production rate is more appropriate for this concentration, the number of cells becomes closer to the desired value of 1000, as shown in Table 4.4.

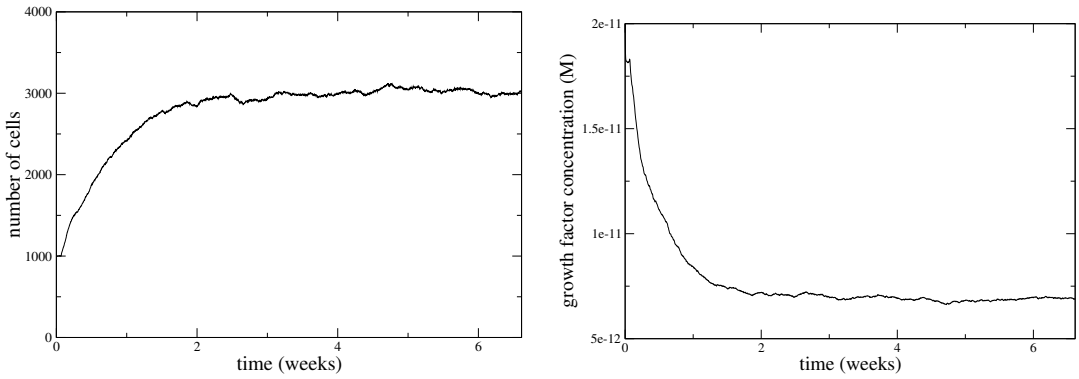

Figure 4.3: Initial simulation of proliferation-dependent homeostasis. Cell population (left) and ligand concentration (right) are shown for the single simulation done with these parameter values. Growth factor loss rate n: 0.006/min; production rate p: 6000 molecules/s; no efflux. All other parameters as shown in Table 4.1.

Note that the steady-state ligand concentrations corresponding to different efflux rates are the same as seen in Table 4.3; changing the growth factor production rate does not affect the steady-state concentration, as expected. I started these simulations with 1000 cells; it still took several days to reach the steady-state shown in Table 4.4.

The fraction of the cell population that is dividing is about twice that observed in vivo. Lowering this fraction would require changing the steady-state point of the system by

Efflux rate	Concentration	# cells	% cycling cells
0%/day	6.9×10^{-12} (1.1×10^{-13})	3022 (38)	7.2% (0.4%)
5%/day	8.3×10^{-12} (1.4×10^{-13})	2489 (25)	8.6% (0.5%)
10%/day	1.0×10^{-11} (9.6×10^{-14})	2021 (16)	10% (0.4%)

Table 4.3: Results of initial proliferation-driven homeostasis simulation. Concentration and cell values are given as mean (standard deviation) calculated from samples taken over the steady-state portion of each simulation. For these parameter values, only one simulation was done for each parameter set. Growth factor loss rate n: 0.006/min; production rate p: 6000 molecules/s; all other parameters as in Table 4.1.

Efflux rate	Concentration	# cells	% cycling cells
0%/day	6.9×10^{-12} (1.5×10^{-13})	857 (20)	7.6% (0.9%)
5%/day	8.3×10^{-12} (2.3×10^{-13})	683 (20)	8.9% (1.0%)
10%/day	1.0×10^{-11} (2.7×10^{-13})	527 (16)	10% (1.5%)

Table 4.4: Results of corrected proliferation-driven homeostasis simulation. Steady-state concentration and cell values are given as simulation mean (standard deviation). Five simulations were done for each parameter set. Growth factor loss rate n: 0.006/min; production rate p: 2000 molecules/s; all other parameters as in table 4.1.

changing model parameters affecting cell survival and proliferation. As noted above, the loss rate would also have to be very low; the total loss rates in these runs are about 15–20%/day. A lower ligand concentration would decrease the rate at which cells commit, but would also drastically raise the death rate, so the system cannot stabilize at such a concentration.

There are a number of possible reasons for the discrepancy. It is possible that a better model of cell death would account for both the culture data and the data from alveolar macrophages in vivo. On the other hand, there may be significant differences between bone-marrow-derived macrophages and alveolar macrophages that the model does not address at all. Also, the model only accounts for the effects of a single growth factor on the macrophage population; it is likely that other mechanisms would lower the loss rate and the fraction of cycling cells in vivo. Another alternative is to offset loss rates with influx from circulation, as in the next model variation.

4.4 Influx-Driven Homeostasis

This section looks at a system driven primarily by influx of cells from circulation. There is still local division in this system, as observed in vivo, but only newly arrived cells divide.

4.4.1 Differential Equation Model

This version still has resting and dividing macrophages (A and B, respectively), but adds monocytes (C) entering from the circulation at rate i. When the monocytes pass the restriction point, they become dividing cells, which produce resting effectors when they divide:

$$\frac{dA}{dt} = 2rB - l(L)A \tag{4.7}$$

$$\frac{dB}{dt} = k(L)C - rB \tag{4.8}$$

$$\frac{dC}{dt} = i - k(L)C - l(L)C \tag{4.9}$$

Note that, unlike the other terms, the influx rate does not depend on the local cell population. The number of cells migrating into the alveoli depends on the circulating precursor population; I assume here that this population is large enough to ignore possible effects of depletion. Migration of cells across the epithelial barrier into the alveolar compartment is a complex process in vivo, but also a relatively quick one. While division can take on the order of hours, migration generally occurs within a few minutes. I assume that influx is a random process occurring at a fixed rate.

All three cell types consume ligand:

$$\frac{dL}{dt} = \frac{p}{VN_{Av}} - \frac{c(L)}{N_{Av}}(A+B+C) - nL \tag{4.10}$$

In this system, there is always a steady state, although the parameters will determine whether it is biologically feasible. In particular, k and l are no longer required to be equal.

Efflux rate	Concentration	# cells	% cycling cells
0%/day	5.5×10^{-12} (1.2×10^{-13})	986 (26)	2.4% (0.4%)
5%/day	6.5×10^{-12} (1.3×10^{-13})	838 (26)	2.7% (0.4%)
10%/day	7.6×10^{-12} (2.1×10^{-13})	706 (20)	3.1% (0.7%)

Table 4.5: Results of influx-driven homeostasis simulation. Steady-state concentration and cell values are given as simulation mean (standard deviation). Five simulations were done for each parameter set. Growth factor loss rate n: 0.006/min; production rate p: 2000 molecules/s; influx rate: 1.4 cells/ml/s; all other parameters as in Table 4.1.

4.4.2 Simulations

The simulation model includes one cell type for each of the equations above. The only new parameter value is the influx rate i; estimates of monocyte migration into the lungs [Blusse van Oud Alblas et al., 1983] give a value of 1.4 cells/ml/s.

Results are shown in Table 4.5. In these runs, the percentage of cycling cells is closer to that observed in vivo. One reason for this may be that the continual influx of new cells reduces the need for local proliferation to balance loss.

The steady-state ligand concentrations are fairly low, leading to higher death rates; even without efflux, the loss rate is around 18%/day. Death rates were unusually high in the proliferation-driven model as well, which may be an artifact of the macrophage model. However, comparing the two homeostasis models still shows higher loss rates in the influx model than the proliferation model. It seems reasonable that a constant influx of new cells would be balanced by higher loss rates; this system has greater cell turnover.

4.5 Autocrine Regulation

Equations (4.6) and (4.10) represent a paracrine control system; growth factor is produced by a cell type other than the one it affects. But mature macrophages are capable of pro-

ducing M-CSF [Becker et al., 1989] and possibly regulating themselves. To explore the possible effects of autocrine regulation, I ran some simulations in which all of the cells produce their own growth factor. The secretion rate was chosen so that a population of 1000 cells would produce the same amount of growth factor used in the earlier simulations. Since the goal is only a general assessment of autocrine effects, I did not vary the secretion rate based on cell maturity.

In the proliferation-driven system, autocrine growth factor production made the steady state unstable; simulations with cell counts below the steady-state point died out, while those with cell counts above the steady-state grew without bound. In contrast, simulations with monocyte influx were still stable, but the final cell counts were slightly lower in the high-efflux runs.

In the paracrine system, cells reduced ligand concentration through consumption. In the autocrine system, the net effect is to increase ligand concentration. The negative feedback described in section 4.2.3 has been changed to a positive feedback. In the proliferation-driven system, this works to drive the system away from the ligand concentration at which $k = l$. However, the influx-driven system is stable even without this negative feedback; autocrine rather than paracrine production may change the location of the steady state, but not its stability.

4.6 Summary

The previous sections showed that homeostasis may be achieved with either an influx-driven or a proliferation-driven system. It is very likely that both mechanisms are used in vivo, with each dominating under different circumstances. However, the influx-driven system is inherently more stable, and accounts for the observed ability of macrophages to produce their own growth factor. More detailed information on death rates in normal cell

cultures or the kinetics of death in individual cells would help refine the basic model of cell behavior. The homeostasis model predicts a correlation between monocyte influx and higher macrophage loss rates; it might be possible to confirm this correlation either directly or by testing for expression of adhesion molecules involved in monocyte trafficking.

Cell consumption of growth factor was significant, and the resulting negative feedback was essential for stability of the population replenished only through local proliferation. Whether or not ligand depletion is relevant for a particular molecular mediator depends on the binding properties of that ligand and its receptor, but it is likely that other molecular signals are affected by cell density. Autocrine regulation is another mechanism for which the effects depend on the context of the entire system. Purely autocrine regulation is potentially destabilizing but can work in combination with other regulatory mechanisms.

For the homeostasis models, the only significant source of spatial heterogeneity is the number and location of cells secreting growth factor. In the autocrine system, or a paracrine system in which many cells contribute to the growth factor concentration, the results of spatially explicit simulations are similar to those presented for a homogeneous molecular concentration. Results are significantly different if growth factor is supplied by a small number of sparsely distributed tissue cells, in which case the rate of molecular diffusion and manner of cell movement are also important. However, given the large ratio of tissue cells to alveolar macrophages, the latter situation is not likely to be relevant.

Spatial effects are important in infection, however, and these will be addressed in the next chapter. Chapter 5 also addresses the interactions between homeostatic signals and inflammatory signals.

Chapter 5

Macrophage–Pathogen Interactions

Macrophages are often the first immune system cells to encounter foreign particles and microbes inhaled into the lungs. Many foreign objects are eliminated by resident macrophages; others stimulate an inflammatory response that recruits more phagocytes to the infected area. Some pathogens are readily cleared; others establish a persistent infection. Several significant diseases are caused by pathogens that have adapted to survive within macrophages. In all of these scenarios, the eventual outcome of the infection can be strongly influenced by the initial interactions between macrophages and pathogens.

This chapter looks at some simple models of macrophage-bacterial interactions incorporating spatial effects. I give a brief description of factors affecting macrophage-pathogen encounter probabilities in section 5.1. I then introduce the simulated tissue structures that will be used throughout the rest of the dissertation in section 5.2. Section 5.3.2 explores a number of factors affecting initial growth of intracellular bacteria. Section 5.4 compares my results to an existing model of early intracellular infection and section 5.5 summarizes the findings of this chapter.

5.1 Macrophage-Pathogen Encounter

Infection dynamics are driven by encounters between immune system cells and pathogens. Immune system models often use the law of mass action, which says that the rate of productive encounters between two species is proportional to the product of their concentrations [Ling and Segel, 1988]. This is an appropriate simplification for well-mixed systems, in which reactants move randomly and neither concentration is sufficiently high to cause interference effects. However, these assumptions are often violated in areas of local infection. Macrophages respond chemotactically to a large variety of molecular signals, so their movement is not completely random. Also, due to inflammation, local cell densities can be very high, further constraining the ways in which cells can move and affecting encounter probabilities. This section describes the effect of macrophage movement and chemotaxis on encounters in an unstructured space; later sections address complications due to tissue structure or large cell densities.

The probability of macrophage-pathogen encounter depends on a number of factors including relative cell velocities, cell densities, and contact distance (the maximum distance at which a macrophage can detect a pathogen). Chemotaxis alone depends on the number and spatial distribution of chemokine sources, the diffusion and decay rates of the chemokine, and the responsiveness of cells to that chemokine. Fisher and Lauffenburger [1987] came up with an expression for population encounter rates based on probabilities that a cell would move towards or away from the nearest target. They do not explicitly include chemokine gradients or concentrations. Their formula accounts for effects of chemotaxis, contact distance, and cell densities, but is rather complicated. Any such expression naturally depends on assumptions about cell behavior, but those assumptions are not clear from looking at the derived expression. In contrast, CyCells simulations do not require specification of an encounter probability; it is a natural consequence of specifying cell movement parameters that are more directly related to observable phenomena.

Parameter	Meaning	Value	Source
s	macrophage speed	2 μm/min	Lauffenburger and Linderman [1993]
p	macrophage persistence time	30 min	Lauffenburger and Linderman [1993]
R_M	macrophage radius	5 μm	estimate
R_P	pathogen radius	1 μm	estimate
h	phagocytic distance	10 μm	estimate
L_{min}	minimum chemokine concentration	1 pM	Thomson [1998]

Table 5.1: Parameters for macrophage movement and phagocytosis. Macrophages and pathogens represented as spheres with the specified radii for collision resolution purposes. However, since real cells are not spheres and macrophages can extend pseudopods to sense their surroundings, I assume that macrophages can detect pathogens within 10 μm. For chemotactic movement, the chemokine concentration must be greater than L_{min}. Chemokine sensitivities vary, but the value listed is close to 1 molecule per cell volume and therefore represents a reasonable lower bound below which gradients will not be detectable.

Consider a model in which encounter between macrophage and pathogen is the limiting factor in clearance of the pathogen. To isolate the effects of cell movement on encounter rates, I use a fixed number of macrophages and do not include pathogen replication or movement. Macrophages move about the space and eliminate pathogens whenever they get close enough. Macrophage movement may be random or chemotactic. General cell movement and phagocytosis in CyCells were explained in sections 3.3.1 and 3.4.2; the parameters affecting macrophage-pathogen encounters are shown in Table 5.1. Assume that each pathogen secretes a diffusible molecule that may be chemoattractant for macrophages; many pathogens either produce such substances or induce their production in nearby cells. Chemotactic movement is simulated by moving macrophages in the direction of the chemoattractant gradient if the signal is strong enough.

Figure 5.1 shows that when cell movement is random, simulated pathogen clearance follows the exponential decay predicted by the mass action description. Chemotaxis can greatly decrease the pathogen clearance time by increasing encounter rates. However, the degree to which chemotaxis differs from random movement varies with a number of factors. In Figure 5.1, early pathogen clearance does not get as much benefit from chemotaxis

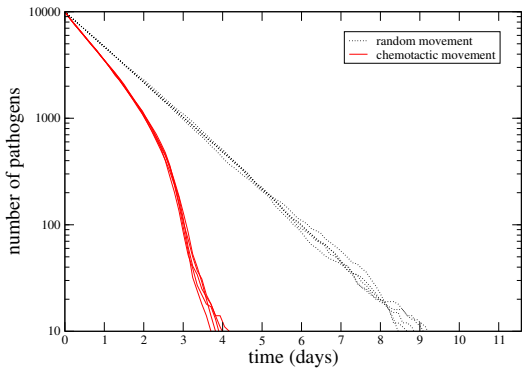

Figure 5.1: Effect of chemotaxis on pathogen clearance. 1000 macrophages either move randomly (dotted lines) or follow a chemokine (solid lines) produced by the pathogen. Macrophages eliminate pathogens within the contact distance shown in Table 5.1. For these simulations, chemokine was produced at 1 molecule/pathogen/s, and had a half-life of about an hour and a diffusion coefficient of 10^{-8} cm^2/s. Molecular concentration grid size was 50 μm. Five simulations each for random and chemotactic movement are shown.

due to the large initial pathogen density. Late pathogen clearance declines again because the chemokine signal gets weaker as pathogens are removed; in this particular example, individual pathogens do not produce enough chemokine for more distant macrophages to detect. Maintenance of detectable chemokine gradients and concentrations depends on chemokine production, decay, and diffusion rates.

5.2 Tissue Structure

Tissue spatial structure can also constrain the way that cells move, and it has an effect on cell migration from circulation. Many details of tissue structure are beyond the scope of this work, but I have experimented with two layouts for the space in which simulated infections take place. Both continue to use a 1 mm^3 (1 μl) volume as in chapter 4.

The first layout, shown in Figure 5.2 , was intended to resemble the general structure of alveoli in the lungs. The regular grid of simulated cells represents alveolar walls. As

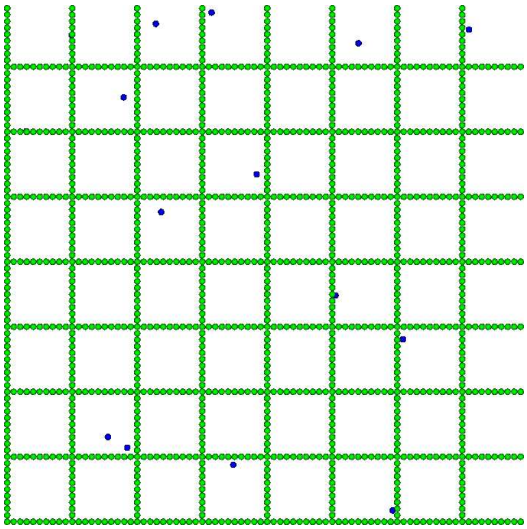

Figure 5.2: Simulated alveolar structure. Each edge of the simulated space is 1 mm. Cells making up the grid represent cells of the alveolar walls; the other cells represent macrophages normally present on the alveolar epithelium. This screenshot shows a thin slice through the 3D volume, so only a fraction of the cells are visible.

shown in Figure 4.1, alveolar walls actually contain epithelial cells, interstitial tissue, and capillaries, so these simulated cells do not have a one-to-one correspondence with real cells. The primary purpose of these simulated tissue cells was to act as gateways, as described in section 3.1.2, determining where and when new monocytes enter the simulated alveolar compartment.

However, this is a rather crude representation of the structure in which macrophages actually move, and imposes more constraints on macrophage movement than necessary. The structure shown in Figure 5.2 requires significant computation for collision resolution between macrophages and tissue cells that is somewhat unrealistic. The actual alveolar tissue is not as rigid, and macrophages can move between alveoli and through alveolar walls. Also, infection and inflammation take place both with the alveolar space and within the interstitium—the latter would be inside the simulated tissue cells—which may swell. All of these factors make a realistic representation of the alveolar space very difficult.

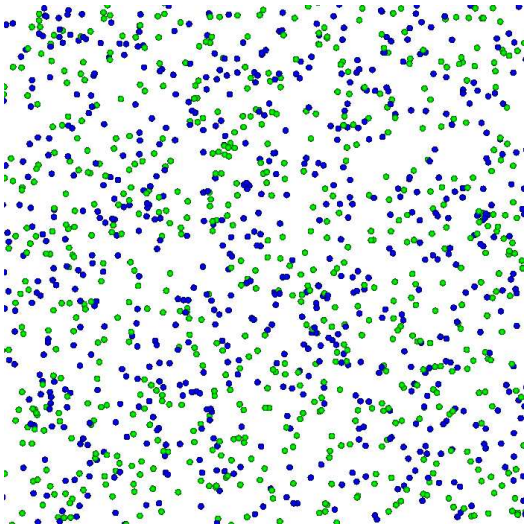

Figure 5.3: Simulation structure with randomly distributed gateways. Each edge of the simulated space is 1 mm. Green cells are gateways; dark blue cells are macrophages. This screenshot shows the entire 3D volume projected onto the paper.

The spatial effects of most interest are those that develop during the course of infection as cells aggregate in response to some stimulus. These effects can still be captured with the relatively unstructured space shown in Figure 5.3. 1000 gateway cells are randomly distributed throughout the volume, allowing influx rates to vary according to local cytokine concentrations. No distinction is made in this version between interstitial and alveolar spaces.

5.3 Intracellular Bacteria

Although macrophages can eliminate many kinds of pathogens, several kinds of *facultative intracellular bacteria* have adapted to survive inside macrophages. These include the pathogens responsible for tuberculosis, leprosy, typhoid fever, and Legionnaire's disease, with the first of these being closest to an idealized intracellular bacterium [Kaufmann,

1999]. These bacteria can survive extracellularly, but prefer to live and replicate within macrophages. Kaufmann [1999] describes the immune response to these pathogens in detail; a brief sketch of early tuberculosis infection as described by Dannenberg and Rook [1994] will suffice here.

Infection begins when macrophages phagocytose bacteria, but cannot destroy them. Bacteria replicate inside the macrophages. When the infected cells die, they release their bacilli, which may then be phagocytosed by other macrophages. This is aided by the recruitment of other macrophages to the area by an inflammatory response initiated by the original infected cells. Control of these pathogens generally requires T cell help, but there is a delay before significant numbers of T cells are available. During this delay, bacteria replicate exponentially.

Although the initial macrophage response is generally unable to kill many of these bacteria, it may still have a significant effect on the eventual outcome of the infection. Even a small reduction in the initial pathogen burden translates to a large decrease in the expanded population that the later response will have to handle. Similar advantages may result from limiting the bacterial growth rate. This section defines a model that is used to illustrate possible effects of macrophage recruitment, phagocytosis, and antimicrobial activity on initial intracellular bacterial growth.

5.3.1 Model Description

This model is designed to capture some of the general characteristics of a hypothetical intracellular bacterial infection, considering only the interactions between macrophages and bacteria. These interactions are driven by macrophage-bacterial encounters, which in term depend on macrophage recruitment to the site of infection. Macrophages vary in their abilities to phagocytose and destroy bacteria; this heterogeneity is incorporated into the model. Macrophage and bacterial behaviors are illustrated in Figure 5.4 and described

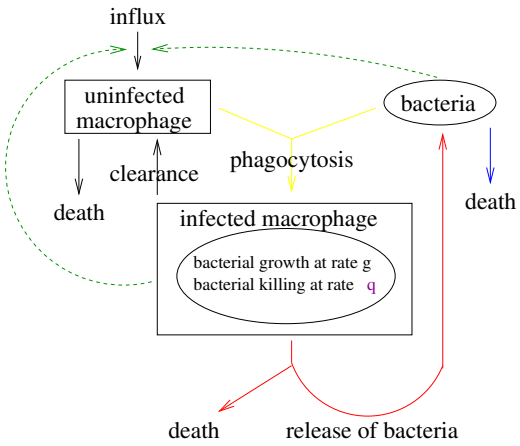

Figure 5.4: Schematic of intracellular infection model showing interactions between macrophages and bacteria. Note that both uninfected and infected macrophages phagocytose bacteria. The bacterial growth rate g is constant; q varies from cell to cell.

in more detail in the following sections. Parameter values are summarized in Table 5.2.

Macrophage Dynamics

Most of these simulations used a fixed macrophage influx rate i and a fixed loss rate l_M which together maintain a homeostatic macrophage population in the absence of infection. In these simulations, no distinction is made between monocytes and macrophages. However, one set of experiments below considers the interactions between the infection model and the homeostatic mechanisms of Chapter 4.

As explained in section 3.4, macrophages have an attribute representing their phagocytic ability, expressed as a value between 0 and 1. A separate global model parameter ϕ defines a threshold on this phagocytic ability that must be met for phagocytosis to take place. The fraction of the macrophage population that can phagocytose bacteria is $1-\phi$; if $\phi = 0$, all macrophages can phagocytose bacteria. Increasing values of ϕ represent increasing difficulty of phagocytosing the pathogen or decreasing phagocytic competence of

the macrophage population.

When an uninfected macrophage phagocytoses a bacterium, it becomes infected. Infected macrophages may also continue to phagocytose bacteria. Infected macrophages die at the same fixed rate l_M as uninfected macrophages, but may also die from excessive bacterial load. If the number of intracellular bacilli exceeds a threshold value N, the cell dies. Infected cells release the bacilli they contain when they die (which can be less than N if the cell dies normally).

Bacterial Dynamics

Bacteria replicate intracellularly, but may also be killed by the host cell. The rate at which bacteria divide intracellularly depends on genetic factors of both the bacteria and the host cells, and the degree to which the host cell has been activated to kill intracellular bacteria. Within each infected cell, I assume that there is some probability $g\Delta t$ with which intracellular bacteria divide. The value of g is fixed for each simulation, representing some particular combination of host and pathogen genetic factors. There is a separate probability $q\Delta t$ with which macrophages may kill intracellular bacteria; $q = 0$ for unactivated cells. Macrophages vary in their activation status and ability to express antimicrobial products, so each macrophage was given a value of q chosen from a uniform distribution between 0 and some q_{max}.

The fate of extracellular bacteria has a significant effect on overall dynamics, depending on whether they exhibit net growth, net death, or a net steady state. Although some intracellular bacteria may replicate extracellularly under the appropriate conditions—making the infection much harder to control—net extracellular growth will not be considered here. Simulations below explore two options: 1) extracellular bacteria die with probability $l_B\Delta t$, and 2) the extracellular loss rate is negligible. The latter case represents bacteria that can persist in the body in a dormant state.

Inflammation

Bacteria often induce an inflammatory response, which increases the local number of immune system cells. It is generally assumed that the increased influx is proportional to the local bacterial load. However, since neither macrophages nor the endothelial cells that allow migration of new monocytes from circulation can directly determine the bacterial load, this information must be communicated by cytokines and other molecular signals. There are numerous cytokines that affect recruitment of immune system cells from circulation and their movement within tissues. However, I assume here that these functions can all be represented by a single abstract pro-inflammatory molecule X. Inflammatory recruitment i_X occurs as a saturating function of the local X concentration L_X:

$$i_X = \frac{i_{max} L_X}{i_{half} + L_X} \tag{5.1}$$

where i_{max} is the maximum influx rate and i_{half} is the X concentration at which the actual rate is half-maximal. The saturating form reflects the assumption that there is some physical limit on the number of cells that can migrate at once, due either to availability of the cells in circulation or to limits on their passage through the endothelium and epithelium.

I assume that both extracellular bacteria and infected macrophages produce X at a fixed rate p_X and that it decays at a fixed rate n_X. The choice of which values to use in these simulations is somewhat arbitrary; the parameters of real interest are those determining how the concentration affects recruitment of phagocytes. The primary tuning parameter here will be the half-saturation constant i_{half} which determines how steeply influx changes in response to X concentration. I assume that the maximum influx rate is an order of magnitude higher than the homeostatic influx rate used in the previous chapter. This is probably an underestimate, but is enough of an increase to illustrate inflammation dynamics.

Parameter	Meaning	Value Range	Source
i	homeostatic influx rate	1.4 cells/ml/s	Blusse van Oud Alblas et al. [1983]
l_M	macrophage death rate	.12/d	chosen to balance i
ϕ	phagocytic threshold	0–1	varied
l_B	extracellular bacterial death rate	1/d or 0	varied
g	intracellular bacterial growth rate	1.4/d	estimate
q_{max}	max intracellular bacterial kill rate	0–4g/d	varied
N	macrophage capacity for bacteria	5 or 50	varied
i_{max}	maximum inflammatory influx rate	10 cells/ml/s	estimate
i_{half}	half-saturation, X on influx rate	1pM–10nM	varied
p_X	X secretion rate	100 molecules/cell/s	estimate
n_X	X decay rate	0.07/min	Fishman and Perelson [1999]
D	X diffusion rate	10^{-8} cm^2/s	estimate

Table 5.2: Parameters for intracellular bacteria model. Estimated values are chosen to be biologically plausible, but are not based on any specific organism. Varied parameters are discussed in more detail in the relevant sections of the text.

Initialization

Simulations were initialized with 1000 macrophages and 100 bacteria, using the tissue structure shown in Figure 5.3. Simulations used a time step of 20 seconds and a grid size of 50 μm for molecular concentrations. I ran five simulations for each parameter set. In general, there was significantly less variation between runs with the same parameter values than between parameter sets.

Simulations ran for approximately 3 simulated weeks (two million seconds). In many infections, T cells and other immune system cells would be involved before the end of this period, but these other cell types are not included in these simulations. The longer period allows for comparison between the macrophage-only responses in this chapter and those involving T cells in the next chapter.

5.3.2 Simulation Results

Simulations are used to explore the relationships between individual model components—phagocytosis, influx, and cell and bacterial death—and their effect on the developing in-

fection. There is little quantitative data available on localized inflammatory responses, so it is difficult to compare the simulations to experimental results. The simulations explore qualitative effects of various model parameters on the local bacterial and macrophage populations. Each of the subsections below varies one parameter value while holding the others constant in order to observe the general trends in infection dynamics.

Infection pathology is not directly represented here, but could be associated with increasing bacterial load, increasing macrophage density, or both. Increasing bacterial load represents spread of the infection; extracellular bacteria and/or infected cells may produce substances that damage local tissues. Excessive macrophage densities may also disrupt local tissue function, and in some cases can cause more damage than the pathogen itself.

Many of the simulations focus on the case where macrophages are unable to kill the bacteria. In general, faster growth of the bacterial population drives both increased bacterial load and increased macrophage population. Increasing numbers of bacteria and infected cells secrete more inflammatory signals, recruiting more macrophages to the area. But there are a number of factors that influence the rate of growth; these are addressed in the following sections. The final section considers the possibility that macrophages can kill intracellular bacteria, but vary in their ability to do so.

Interaction between homeostatic and inflammatory cytokines

One question to address is how this inflammatory response interacts with the homeostatic mechanisms described in the last chapter; in particular, how the effects of growth factor interact with the effects of the inflammatory signal. Figure 5.5 shows bacterial load and total macrophage numbers for some representative runs using different homeostatic mechanisms. Two sets of simulations were based on the influx-driven homeostasis model of section 4.4, one with autocrine growth factor secretion and the other with paracrine growth factor production. A third set did not include growth factor, but used a fixed macrophage

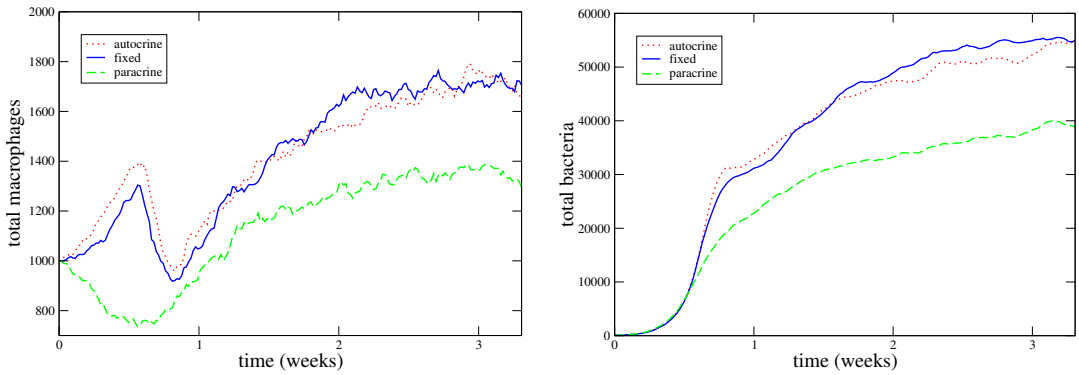

Figure 5.5: Effect of homeostasis mechanism on inflammation. Total macrophage numbers (left; includes infected and uninfected cells) and total bacteria numbers (right; includes intracellular and extracellular bacilli) over time for different homeostatic schemes. autocrine: macrophage survival is controlled by growth factor that they produce themselves; fixed: macrophage death rate is fixed at 1/d; paracrine: macrophage survival is controlled by growth factor secreted by other cells. Parameter values: $\phi = 0$, $q_{max} = 0$, $N = 50$, $i_{half} = 100$pM; remaining values as in Table 5.2. Each line shows a single run representative of 5 simulations.

death rate paired with the same influx rate used in the other simulations. Inflammation parameters i_{max} and i_{half} were kept the same in all simulations.

Figure 5.5 shows limited macrophage increase and bacterial growth for the model using paracrine growth factor production. The growth factor supply is fixed in this case, so the macrophage population is restricted in a density-dependent fashion by competition for growth factor. As influx increases initially, growth factor decreases and the death rate increases. As influx continues to increase, it eventually allows the total macrophage population to rise, but with more cell turnover. The total increase is less than that seen in the other simulations. This has the effect of also limiting the bacterial population because there are fewer macrophages available to phagocytose bacteria and permit their growth.

For the same set of influx parameters, autocrine production of growth factor allows a much larger increase in both macrophage and bacteria numbers, as shown in Figure 5.5.

Growth factor production increases with increasing macrophage populations, so that cells do not die from lack of growth factor. In fact, the increased growth factor also causes slight increase in local proliferation. This corresponds to observations of positive feedback loops in real immune responses in which multiple mechanisms act to increase the number of responding cells, although the actual mechanisms are more complex than those used here. There is evidence both that growth factor production is increased during inflammation [Seelentag et al., 1987, Roth et al., 1997] and that inflammatory signals can stimulate survival and proliferation [Xaus et al., 2001].

Real infections include both regulatory mechanisms, those to increase the population of responding cells, and those to increase the death rate of those cells so that they do not persist too long [Ma et al., 2003]. How these stimulatory and inhibitory signals are reconciled is not really understood. For simplicity, the rest of the models use the fixed death rate, which produces dynamics intermediate to the two growth factor-dependent models.

Macrophage influx

Because bacteria in this model only grow inside macrophages, the increase in bacterial load is closely tied to macrophage influx rates. Macrophage influx in turn is tied to the bacterial growth, since increasing numbers of bacteria and infected cells increase the X concentration and therefore the influx rate. However, since the influx rate saturates, there is a maximum size that the macrophage population can reach.

Figure 5.6 shows how the initial macrophage and bacteria population dynamics are affected by macrophage influx. Simulations were done for several values of i_{half}; lower values of i_{half} cause more rapid influx in response to a particular concentration of X than do higher values of i_{half}. For very high values of i_{half} there is little or no inflammatory influx. Decreasing values of i_{half} lead to increasing macrophage recruitment and associated

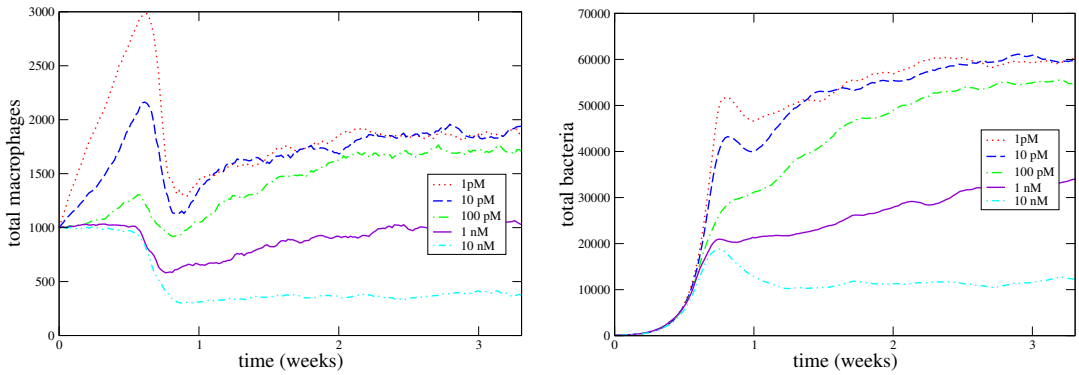

Figure 5.6: Effect of influx rate on infection dynamics. Total macrophage numbers (left; includes infected and uninfected cells) and total bacteria numbers (right; includes intracellular and extracellular bacilli) over time for several values of i_{half} (shown in legend). Other parameter values: $\phi = 0$, $l_B = 1/d$, $q_{max} = 0$, $N = 50$; remaining values as in Table 5.2. Each line shows a single run representative of 5 simulations.

bacterial growth. For all of these simulations, the bacteria soon outnumber the macrophages. As most of the macrophages become infected, the overall macrophage death rate increases as more infected macrophages die from excessive bacterial load. This causes a decline in macrophage numbers after reaching a peak.

Phagocytosis

When macrophages are unable to kill their intracellular bacteria, increased population phagocytosis rates may also exacerbate infection, as shown in Figure 5.7. In this series of simulations, the phagocytic threshold ϕ was varied to change the percentage of the macrophage population capable of phagocytosing bacteria. If a small fraction of macrophages phagocytose bacteria, there is limited opportunity for bacterial growth. As this fraction increases, bacterial growth increases. Increased bacterial growth can be associated with both increased macrophage influx and increased macrophage death; the latter effect dominates in Figure 5.7.

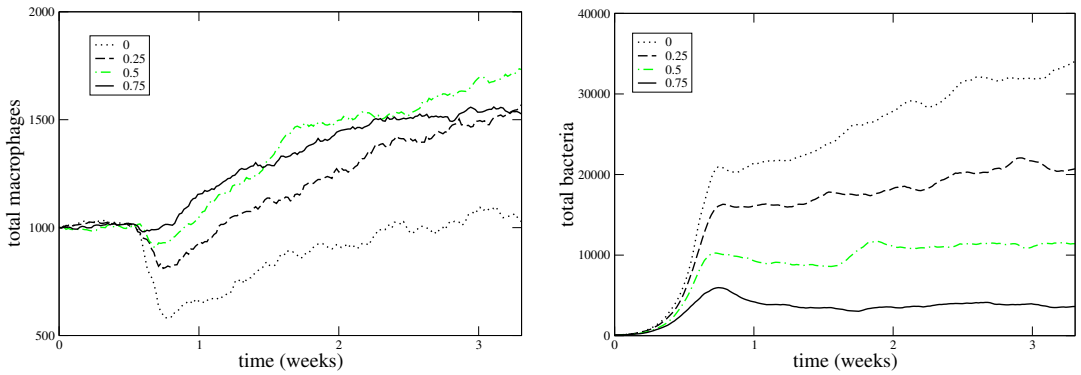

Figure 5.7: Effect of phagocytic competence on infection dynamics. Total macrophage numbers (left; includes infected and uninfected cells) and total bacteria numbers (right; includes intracellular and extracellular bacilli) over time for several values of ϕ (shown in legend). Other parameter values: $l_B = 1/d$, $q_{max} = 0$; $N = 50$, $i_{half} = 1$nM, remaining values as in Table 5.2. Each line shows a single run representative of 5 simulations.

Infected Cell Death

The simulations described so far used $N = 50$, which comes from an estimate of the macrophage capacity for the bacteria that causes tuberculosis [Wigginton and Kirschner, 2001]. A smaller value of N could represent the ability of infected cells to commit suicide or be killed by other cells to limit intracellular pathogen growth. Figure 5.8 shows representative simulations for $N = 50$ and $N = 5$. Although the trends in macrophage numbers are similar for these two simulations, bacterial growth continues longer and reaches much higher levels in the former case. This illustrates the advantage in limiting the time that bacteria remain inside their host cells. Removing pathogens from these refuges limits their opportunities to continue replicating, if only temporarily.

Bacterial Persistence

When there is significant extracellular bacterial death, eventual clearance or a chronic steady state is theoretically possible because intracellular growth may be balanced by ex-

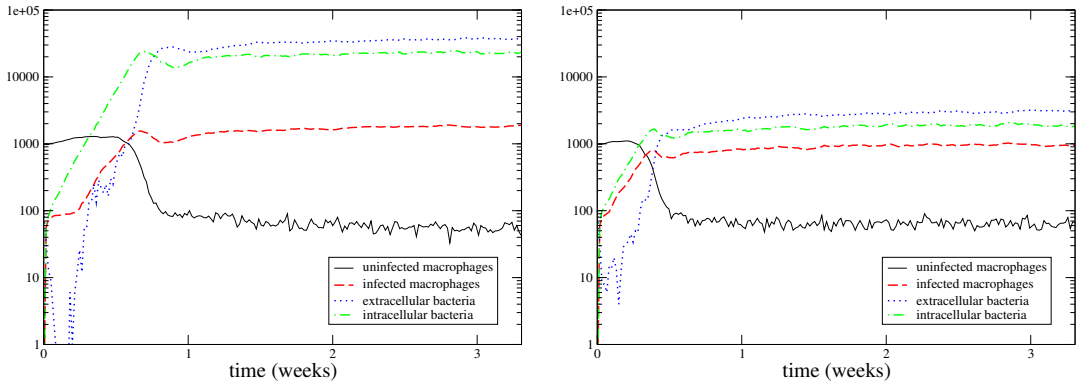

Figure 5.8: Effect of macrophage capacity for bacteria on infection dynamics. Macrophage and bacteria time courses for two values of the intracellular bacterial burden that causes infected cell death; $N = 50$ (left) and $N = 5$ (right). Other parameter values: $\phi = 0$, $l_B = 1/d$, $q_{max} = 0$, $i_{half} = 10$pM; remaining values as in Table 5.2. Each figure shows time courses for a single run representative of 5 simulations.

tracellular death. When the extracellular death rate is 0 (or sufficiently small), the steady state is no longer possible without killing intracellular bacteria. Although the intracellular bacterial population is limited by the availability of macrophages, extracellular bacteria continue to accumulate as infected cells die. This is illustrated in Figure 5.9. However, the rate of accumulation is still slowed by decreased influx, decreased phagocytosis, or decreased bacterial capacity of macrophages as described in the previous sections.

Antimicrobial activity

Up to this point, macrophages in all simulations were unable to kill intracellular bacteria ($q = 0$). This section explores the possibility that macrophages have varying abilities to kill bacteria. This could be due to innate antimicrobial activity or nonspecific activation due to random encounters with stimulatory factors; mechanisms are not considered here. The point is to evaluate the general effect on the overall infection dynamics.

A number of authors have pointed out that there is considerable heterogeneity among

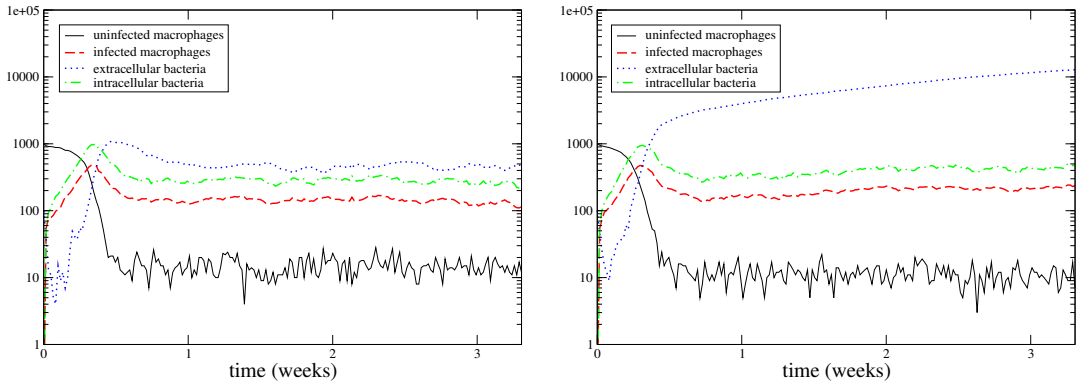

Figure 5.9: Effect of extracellular bacterial death on infection dynamics. Macrophage and bacteria time courses when extracellular bacteria do (left) or do not (right) die. Parameter values: $\phi = 0$, $q_{max} = 0$, $N = 5$, $i_{half} = 10$nM; remaining values as in Table 5.2. Each figure shows time courses for a single run representative of 5 simulations.

macrophages [Naito et al., 1996, Laskin et al., 2001, Hume et al., 2002, Ravasi et al., 2002], but there are no good quantitative measures of what this might mean in terms of pathogen control. I tested uniform q value distributions of varying widths, using three values of the maximum killing rate q_{max}: 1) q_{max} equal to the bacterial growth rate g, 2) $q_{max} = 2g$, and 3) $q_{max} = 4g$. These give cases where the average macrophage 1) still permits net intracellular pathogen growth, 2) maintains bacteriostasis, or 3) kills bacteria faster than they can grow. Note that if all macrophages are given a value of $q > g$, bacteria can be cleared fairly rapidly, but each of these distributions includes some macrophages that are unable to clear their bacterial burden.

In all cases, higher values of q_{max} reduced bacterial numbers, as expected. In some cases, bacteria could be eliminated completely. However, even when most of the macrophages can kill bacteria and bacteria also die extracellularly, bacteria may continue to grow, as shown in Figure 5.10. A key factor in these cases is the large value of N; bacterial growth in the relatively small number of incompetent macrophages can exceed bacterial death everywhere else. Influx and phagocytosis also play a role; initial bacterial growth

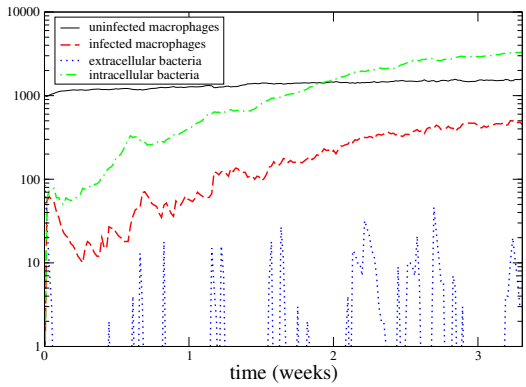

Figure 5.10: Continued bacterial growth with significant antimicrobial activity. Macrophage and bacteria time courses are shown for a single run representative of 30 simulations. Parameter values: $\phi = 0$, $l_B = 1/d$, $q_{max} = 4g$, $N = 50$, $i_{half} = 10$pM; remaining values as in Table 5.2.

is reduced with decreasing phagocytosis and influx rate (increasing ϕ and i_{half}) as well as decreasing N.

On the other hand, even when extracellular bacterial death is negligible, bacteria can be controlled or even eliminated by a heterogeneous macrophage population. Clearance requires small values of N. For large N, increased bacterial killing can still control otherwise unbounded bacterial growth, as shown in Figure 5.11. In addition to reducing the overall bacterial load, antimicrobial activity changes the nature of the infection. When all or most macrophages are unable to kill bacteria, bacterial growth was limited only by the availability of macrophages to infect. There were more extracellular bacteria than macrophages could phagocytose. In the simulations with increased antimicrobial activity, there are relatively few extracellular bacteria and many more uninfected cells, indicating that macrophages are exerting some control over bacterial growth. This is illustrated in the screenshots in Figure 5.12.

These effects depend on the particular distribution of antimicrobial abilities among macrophages. What matters most is the percentage of macrophages that allow contin-

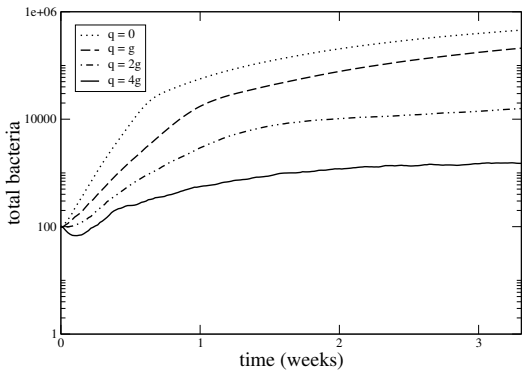

Figure 5.11: Partial control of pathogen burden. Total bacterial load over time for simulations in which macrophages have varying abilities to kill bacteria. Each curve shows an average time course over five simulations. Parameter values: $\phi = 0$, $l_B = 0$, $q_{max} = 4g$, $N = 50$, $i_{half} = 1$nM; remaining values as in Table 5.2.

ued pathogen growth (those with low q values). To understand the dynamics of these intracellular pathogens, a better quantitative understanding of macrophage antimicrobial capabilities is necessary. This includes identifying not only the average effect on bacterial growth, but the possible range of expression of antimicrobial function.

5.4 Related Work

Gammack et al. [2004] published a model of the macrophage response to infection with the pathogen that causes tuberculosis. They used a one-dimensional system of partial differential equations to relate the spread of infection to phagocytosis, macrophage activation, and bacterial growth rates. In their model, bacteria replicated extracellularly as well as intracellularly, leading to the finding that the infection could spread even with negligible phagocytosis. On the other hand, macrophage activation in their model resulted in immediate killing of all bacteria within the host cell. Under these conditions, increased phagocytosis tended to decrease the magnitude of the infection, and they found minimal

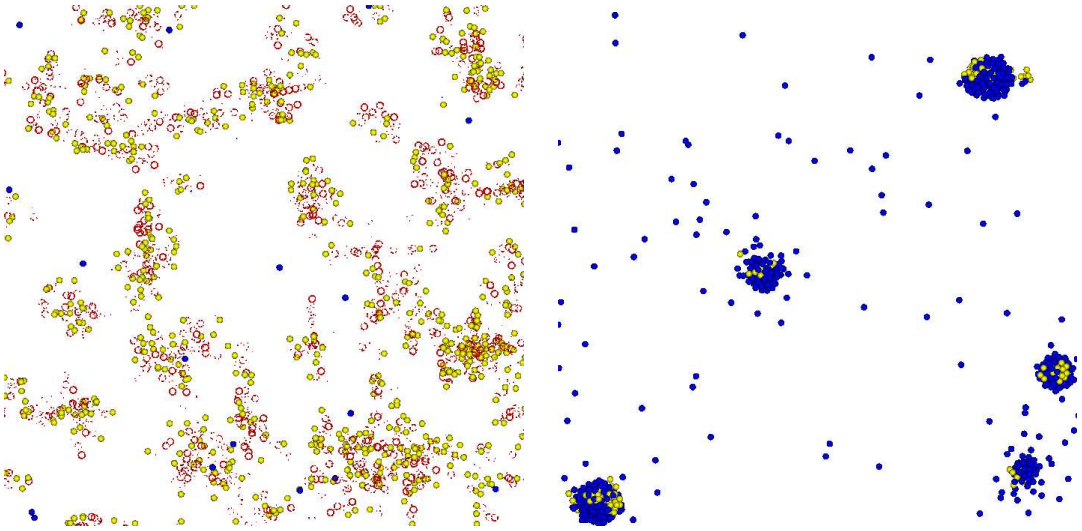

Figure 5.12: Final screenshots from simulations with and without antimicrobial activity. The figure on the left was produced by a simulation in which extracellular bacteria died ($l_B = 1/d$) but macrophages did not kill intracellular bacteria ($q_{max} = 0$); the figure on the right was produced by a simulation in which bacteria were killed intracellularly ($q_{max} = 4g$) but did not die extracellularly ($l_B = 0$). Other parameter values: $\phi = 0$, $N = 50$, $i_{half} =$ 1nM; remaining values as in Table 5.2. Tissue cells were removed from the figures to make it easier to distinguish the remaining cell types. Large dark blue cells are uninfected macrophages, large yellow cells are infected macrophages, and the very small red cells and arcs are extracellular bacteria.

effects in varying the influx rate. However, Kaufmann [2001] notes that intracellular clearance is generally not an all-or-nothing event; hence the representation used in my model. This also allows for the observed heterogeneity in macrophages, which is not incorporated in differential equation models. The last point is particularly important as it may allow persistent infection.

5.5 Summary

This chapter described some abstract models of initial macrophage interactions with bacteria. Section 5.1 illustrated the advantages of using a spatial, individual-based model for representing the likelihood of initial macrophage-bacteria encounters. The remaining simulations explored the ways in which the early macrophage response may affect initial intracellular bacterial growth.

In many cases, limiting influx or phagocytosis slowed bacterial spread. Simulations exploring the effect of influx on the spread of infection did so by varying the sensitivity to the inflammatory signal X, but influx could also be reduced by limiting the production of inflammatory cytokines. Alveolar macrophages are reported to inhibit inflammatory responses in the lungs [Lipscomb et al., 1995]. This inhibitory phenotype may be a trait acquired through evolution, reflecting more difficulties with excessive inflammatory responses than with inadequate inflammatory responses. Similarly, phagocytosis studies in vitro show that typically only 20–30% of macrophages are able to phagocytose the mycobacterium that causes tuberculosis [Silver et al., 1998], despite the fact that macrophages are usually assumed to be extremely phagocytic. The simulations showed that this lack of phagocytic competence may actually be beneficial with a pathogen that the macrophages are unable—at least initially—to control.

Another factor affecting bacterial load in this model was the size of the bacterial burden causing infected cell death (N). This is a somewhat artificial parameter; it is not clear that the number of intracellular pathogens should be linked to death of the host cell in this way. A better choice might have been simply to vary the infected cell death rate. However, the threshold on intracellular pathogen load particularly targets *unactivated* infected cells; macrophages that are able to kill intracellular bacteria are much less likely to reach this threshold. There is speculation in the tuberculosis literature that T cell killing of infected cells, as well as activation, may be important for control of the pathogen [Kaufmann,

2002]. The simulations support the idea that killing of unactivated infected cells could indeed help lower the bacterial burden. The effect is even greater if there is a chance that the bacteria will be rephagocytosed by a more activated macrophage. However, the effectiveness of this mechanism may depend on the ability to distinguish activated from unactivated macrophages.

Without any antimicrobial activity, the above mechanisms—reducing influx, phagocytosis, and maximum intracellular pathogen load—can limit bacterial growth, but do not really constitute control of the pathogen. Bacteria still overwhelm the macrophages and the infection site is characterized by large numbers of extracellular bacteria. In contrast, antimicrobial activity not only reduced the total bacterial load, but also contained the infection. Simulations in which there was at least some bacterial killing showed significantly reduced numbers of extracellular bacteria. This could greatly reduce the chances of bacteria spreading through airways or blood to establish infection in other areas of the body.

The apparent steady states achieved in some of these simulations are misleading. This model incorporates only a limited portion of the immune response; the nature of that response will change over time as other cell types are recruited to the site of infection. Also, even in infections with a stable bacterial load, disease may be progressing. The immune response itself may be responsible for pathology; activated macrophages are known to cause tissue damage Kaufmann [1999]. On the other hand, the model also ignores many of the potential advantages of inflammation. In addition to eliminating those pathogens that can be destroyed, recruited cells carry out many other necessary functions, such as tissue repair. An immune response involves many potentially conflicting functions that continue to adapt to the current conditions as the infection develops [Segel and Bar-Or, 1999].

Immune regulation must somehow balance the positive and negative aspects of each immune function. In reality, none of the rates used in this model are fixed. Expression of phagocytic receptors, production of inflammatory signals, macrophage activation, etc. can

all be up- or down- regulated. In addition, regulatory mechanisms interact with each other. As a simple example, section 5.3.2 showed two different effects of homeostatic regulation on a developing inflammatory response. The next chapter looks at more complex regulatory interactions. It addresses a specific intracellular infection, and builds on the abstract model by including the role of T cells and regulatory cytokines.

Chapter 6

Pulmonary Tuberculosis

The previous chapter looked at effects of spatial and cellular heterogeneity on macrophage–pathogen interactions. However, each macrophage's ability to phagocytose and kill bacteria was assumed to be fixed. In reality, macrophage functions can be up- or down-regulated over time. These phenotypic changes are the result of changes in gene expression, which is an inherently stochastic process [Hume, 2000]. However, the probabilities with which each macrophage will become activated or deactivated, for example, are influenced by the local cytokine concentrations and interactions with neighboring cells.

The actions of regulatory cytokines during infection are extremely complex, and the pattern of cytokine secretion varies in response to different pathogens. In order to make use of experimental data on cytokine production and the resulting effects on particular cell types, it is helpful to focus on a specific infection, rather than the abstract models used in the previous chapter. This chapter explores the early stages of infection with *Mycobacterium tuberculosis* or *Mtb*, an intracellular pathogen that causes tuberculosis.

The tuberculosis (TB) model builds on the simple intracellular pathogen model by adding both contact-dependent and cytokine-dependent interactions between macrophages and T cells. It combines a large number of experimental observations about individual

components of the response in an attempt to clarify their significance in an integrated system. Section 6.1 reviews some of the relevant biology; section 6.2 explains how that information is represented in the model. Simulation results are discussed in section 6.3 and compared to related models in section 6.4. Section 6.5 discusses the contributions of this model and possibilities for future work.

6.1 Tuberculosis Infection

Tuberculosis causes approximately two million deaths each year, making it a serious health problem. In addition, approximately one third of the world population is infected with the pathogen that causes this disease, *Mycobacterium tuberculosis* (*Mtb*) [Corbett et al., 2003]. In most cases, the immune response controls the infection, but does not eliminate it, and a latent chronic infection results [Stewart et al., 2003]. 10–20% of individuals infected only with *Mtb* later develop clinical disease; the percentage is higher for cases of coinfection with HIV [Corbett et al., 2003]. In a recent review, Stewart et al. [2003] identified two key questions about the immune response to *Mtb*:

> First, having controlled the infection, why does the immune response stop short of eliminating the remaining bacteria? Second, having coped with persistent infection over a prolonged period, what triggers the breakdown to active progressive disease?

This chapter focuses on the first question and the initial response to *Mtb*.

Experiments in mice and other animals show a common trend after aerosol infection with *Mtb*; bacteria replicate in the lungs for approximately 3 weeks, then the bacterial load stabilizes [North and Jung, 2004]. Duration of the growth phase and peak bacterial load may vary with the *Mtb* strain and initial dose size; Rhoades et al. [1997] show bacterial

loads of 100–2000 times the initial dose approximately 3 weeks after infection. Stabilization of the bacterial load is thought to coincide with the expression of T cell immunity in the lungs [North and Jung, 2004]. T cells are also thought to be important in control of human tuberculosis because depletion of T cells (as seen in AIDS, for example) is associated with enhanced disease [Kaufmann, 2001]. However, the exact mechanisms of pathogen control are not completely understood.

Bacterial control is thought to depend on the formation and maintenance of *granulomas* in the lungs. These are roughly spherical lesions in which bacilli are contained by immune system cells. Although there may be multiple infected sites, lesions develop independently of each other [Dannenberg and Rook, 1994]. Granulomas are very complex structures that develop over time, but they begin as localized aggregations of macrophages in which bacteria replicate, as described in the last chapter. This initial growth is thought to be slowed or halted by T cell activation of macrophages. In response, *Mtb* may also downregulate their own growth in order to persist in a state that is less detectable by the immune system [Wayne and Sohaskey, 2001, Shi et al., 2003]. Although the total bacterial load is fairly stable after this point, lesions in mice show continued pathological progression [Rhoades et al., 1997].

6.1.1 T Cells and Macrophage Activation

Under the appropriate conditions, macrophages can be activated to increase their ability to kill recently ingested pathogens; chronically infected macrophages lose their ability to become activated [Janeway et al., 1999]. Without continued stimulation, activated macrophages may become deactivated. In vitro, murine macrophages can be activated to kill *Mtb* by addition of the appropriate cytokines, but human macrophages seem to also require the presence of T cells [Bonecini-Almeida et al., 1998]. Brookes et al. [2003] suggest that contact between T cells and macrophages is required for full macrophage activation.

Some contact is certainly required in vivo, because recruited T cells do not produce their cytokines until they recognize antigen presented by macrophages in the infected tissue [Janeway et al., 1999].

Before T cells can be recruited to the lungs, sufficient T cells must be sensitized in the lymphoid organs to initiate expansion of the *Mtb*-specific T cell pool, as described in chapter 2. The model below does not include these effects, focusing only on events within the infected tissues. However, the time required to generate this T cell population and initiate trafficking to the lungs is incorporated. In mice, *Mtb*-specific T cells are first detected in the lungs about 2 weeks after infection [Chackerian et al., 2002].

6.1.2 Cytokines in Tuberculosis Infection

Numerous cytokines produced both by macrophages and by T cells can promote or inhibit macrophage activation. A few of the cytokines thought to be most important in control of intracellular infections in general and tuberculosis in particular are tumor necrosis factor-α (TNF), interleukin-10 (IL-10), and interferon-γ (IFN-γ or just IFN). Protective roles for IFN and TNF have been demonstrated in *Mtb* infection; the role of IL-10, which downregulates many immune system functions, is more controversial [Kaufmann, 1999].

Phagocytosis of many pathogens, including *Mtb*, induces macrophages to produce TNF [Kaufmann, 1999]. Macrophage production of TNF begins soon after infection, but is transient [Thomson, 1994]. T cells may also be induced to produce TNF; the amount of TNF produced by T cells is generally much greater than that from macrophages [Barnes et al., 1993, Engele et al., 2002]. TNF is a pleiotropic cytokine; it has been observed to have many different effects on a variety of cell types, some of which are contradictory, and many of which are not completely understood. One of the better-known effects, however, is to induce production of chemokines and expression of adhesion molecules on endothelial cells to facilitate migration of immune system cells from circula-

tion into infected tissues [Thomson, 1994]. In other words, TNF is responsible for many of the effects attributed to the abstract inflammatory signal X in the simple model of Chapter 5. TNF also synergizes with IFN to activate macrophages, although it is apparently incapable of activating macrophages alone [Flesch and Kaufmann, 1990].

IL-10 is an anti-inflammatory cytokine produced by both macrophages and T cells in response to inflammatory signals. It inhibits macrophage activation and production of cytokines. IL-10 is thought to be important in keeping immune responses in check, but may also permit pathogen growth when responses are damped excessively [Moore et al., 2001].

IFN is produced primarily by T cells and appears to be the most important cytokine for macrophage activation [Ma et al., 2003].

6.2 TB Model

The TB model is illustrated schematically in Figure 6.1. As in the model of section 5.3.1, uninfected macrophages become infected by phagocytosing bacteria, and infected cells return to the uninfected state if they manage to kill their intracellular pathogens. However, there are numerous additions representing activation and inducible secretion of cytokines. Detailed descriptions of the transitions shown in Figure 6.1 are given below; the parameters are summarized in Table 6.1.

6.2.1 Macrophage and T Cell Dynamics

Macrophages are replenished both through homeostatic and inflammatory influx as in section 5.3.1. However, in this model, inflammation depends on TNF rather than X:

$$i_{C_{TNF}} = \frac{i_{max} C_{TNF}}{i_{half} + C_{TNF}} \tag{6.1}$$

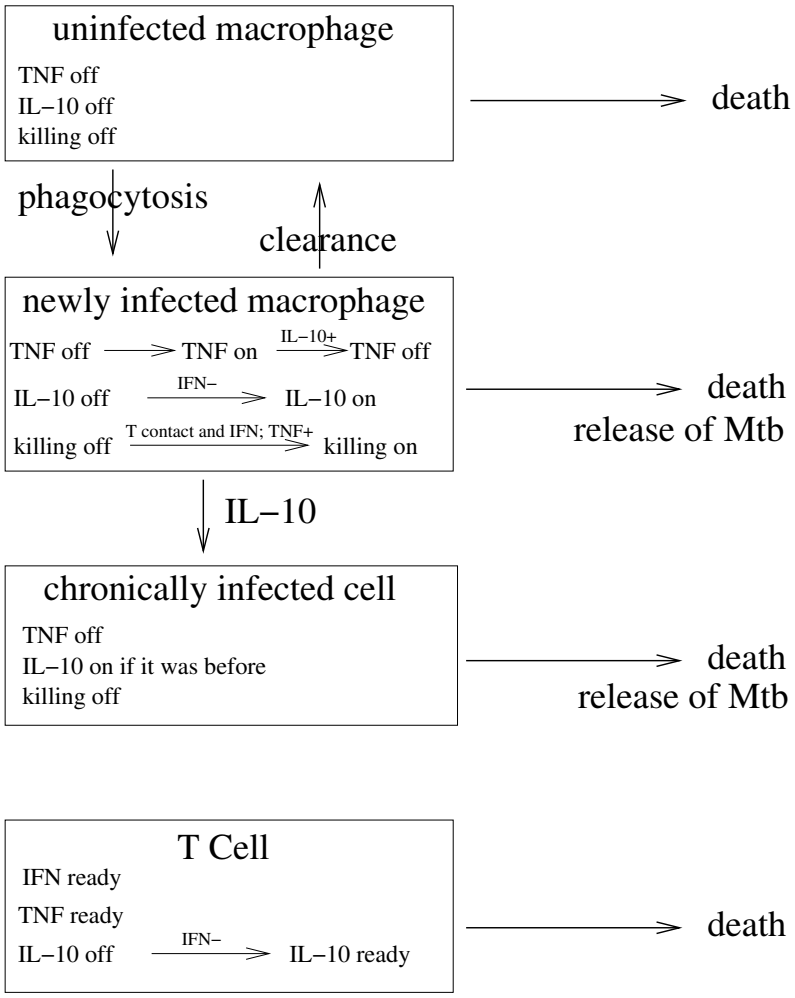

Figure 6.1: Schematic of TB model showing macrophage and T cell behaviors. Most cytokine production is inducible rather than constitutive; this is indicated by the transitions from "off" to "on" or "ready". T cell secretion is marked as "ready" rather than on because T cells only secrete these cytokines when in contact with a newly infected macrophage. Only newly infected macrophages can become activated; this is indicated by the transition turning on (bacterial) killing. T cell contact and detectable IFN are required for macrophage activation. IL-10+ indicates that presence of IL-10 increases the transition probability; IFN- indicates a negative effect of IFN on the transition probability.

T cells migrate in response to TNF in the same way, but there is a delay before T cell influx begins, to represent the time required to mount a T cell response. The model does not take

into account possible depletion of cells in circulation; this effect should not be significant for the short-term responses considered here.

T cells and macrophages have fixed death rates l_T and l_M, respectively. In addition, infected macrophages may die due to excessive bacterial load N as in Chapter 5.

T cells are smaller than macrophages; the simulation uses a radius of 3 μm. I was unable to find data on lymphocyte movement, so T cells are assumed to move the same way that macrophages do, using the speed and persistence times shown in Table 5.1. Macrophages and T cells can interact when they are 10 μm apart.

6.2.2 *Mtb* Dynamics

There is no provision for extracellular *Mtb* growth or death in this model. Dannenberg and Rook [1994] claim that extracellular growth is not significant in the early stages of infection. There is also evidence that *Mtb* persist within tissues for years without replicating [Manabe and Bishai, 2000, Wayne and Sohaskey, 2001], indicating negligible extracellular death.

The intracellular growth rate is taken to be fixed in this model; the possible *Mtb* switch into a nonreplicating state [Shi et al., 2003] is assumed to occur after the time period covered by these simulations. Other factors affecting intracellular dynamics are discussed in the next section.

6.2.3 Macrophage Activation

As in the simpler model in Chapter 5, intracellular bacterial replication occurs with a probability $g\Delta t$ and death of intracellular bacteria occurs with a probability $q\Delta t$ for each bacillus. For unactivated macrophages, $q = 0$. Macrophage activation is represented by

changing the value of q to q_{max} (referred to in the diagram as turning killing on) with some probability $a\Delta t$. Kaufmann [2001] notes that even highly activated macrophages may fail to fully eradicate their intracellular pathogens. In the model, the likelihood of this happening depends on the relative values of g and q. If a cell does manage to kill all of its intracellular bacilli, it reverts to the uninfected state.

Activation requires contact between the infected cell and a T cell, and a nonzero IFN concentration. It is also probabilistic, with the chances of activation increasing with increasing concentrations of IFN and TNF. This activation probability is assumed to be of the form:

$$a\Delta t = a_{max}\frac{C_{IFN}(1+a_{TNF}C_{TNF})}{C_{IFN}(1+a_{TNF}C_{TNF})+m_{IFN}}\Delta t \tag{6.2}$$

where C_{IFN} and C_{TNF} are the concentrations of IFN and TNF, respectively. a_{max} is the maximum rate at which cells become activated. The estimate for a_{max} of 1/d comes from the observation that it takes roughly a day to start production of reactive nitrogen intermediates (RNI) thought to be important in control of *Mtb* [Schroder et al., 2004]. m_{IFN} represents the concentration of IFN at which the activation rate is half of its maximum value. a_{TNF} represents the effect of TNF on macrophage activation; TNF alone is insufficient to activate macrophages, but increasing concentrations of TNF together with nonzero IFN concentrations increase the activation rate.

The probability $u\Delta t$ that a newly infected cell becomes chronically infected (and therefore unable to produce TNF or kill bacteria) increases with increasing concentrations of IL-10:

$$u = u_{max}\frac{C_{IL-10}}{C_{IL-10}+m_{IL-10}} \tag{6.3}$$

where C_{IL-10} is the concentration of IL-10, u_{max} is the maximum transition rate, and m_{IL-10} is the IL-10 concentration at which the rate is half-maximal.

6.2.4 Cytokine Production

Differences in cytokine concentrations in culture reflect differences in the number of cytokine-producing cells, rather than in production rates for each cell. Cytokine production depends on transcriptional regulation within individual cells; Hume [2000] suggests that it is more appropriate to think of this regulation in terms of probabilities of transcription rather than rates. Accordingly, inducible cytokine production in the simulated cells is modeled by giving them some probability of starting or stopping cytokine secretion.

Macrophage Cytokine Secretion

Mtb may induce newly infected macrophages to produce TNF and/or IL-10. There are separate probabilities controlling whether or not each cell will start production of each cytokine. The probability of starting TNF secretion is fixed, given by $v_{on}\Delta t$. The rate listed in Table 6.1 has the average infected cell starting to produce TNF about a day after infection. The probability $w\Delta t$ of starting IL-10 secretion depends on IFN:

$$w = w_{max}\frac{m_{IFN}}{C_{IFN} + m_{IFN}} \tag{6.4}$$

In this case, the maximal rate w_{max} occurs when there is no IFN; increasing concentrations of IFN decrease the probability that a cell will start secreting IL-10. m_{IFN} represents the IFN concentration at which the rate is half-maximal; the same value was used here as in equation 6.2.

Once secretion has been 'turned on,' a cell continues to secrete at a fixed rate until secretion is turned off. The rates are p_{MTNF} and p_{MIL-10} for TNF and IL-10, respectively. Macrophage IL-10 production is only turned off if the macrophage becomes uninfected. TNF production is turned off when a cell becomes chronically infected, and may be turned off earlier with a probability $v\Delta t$ that increases with IL-10:

$$v = v_{off}\frac{C_{IL-10}}{C_{IL-10} + m_{IL-10}} \tag{6.5}$$

v_{off} is the maximal turn off rate; m_{IL-10} in this equation is the same as that in 6.3.

Parameters for macrophage cytokine secretion were chosen so that the resulting concentrations were in rough agreement with those observed in culture experiments [Engele et al., 2002].

T Cell Cytokine Secretion

T cell cytokine production requires contact between the T cell and a newly infected macrophage; chronically infected cells lose their ability to stimulate T cell cytokine production. All T cells are assumed to be capable of producing IFN and TNF when they enter the infected tissue, but the ability to produce IL-10 is delayed as reported in Yssel et al. [1992]. 'Turning on' T cell IL-10 production is modeled the same way macrophage IL-10 production is:

$$w = w_{max} \frac{m_{IFN}}{C_{IFN} + m_{IFN}} \tag{6.6}$$

Cytokine secretion rates are fixed, as for macrophages; the rates are p_{TTNF}, p_{TIL-10} and p_{TIFN} for TNF, IL-10 and IFN, respectively.

T cell secretion parameters were chosen so that the resulting concentrations were in rough agreement with those observed in experiments [Barnes et al., 1993, Tsukaguchi et al., 1999].

6.2.5 Cytokine Decay and Diffusion

All cytokines are assumed to decay and diffuse at fixed rates. The rates used are the same for all cytokines, which have roughly similar molecular weights. As noted in section 5.3.2, cell removal of cytokines through binding and internalization may have cell density-dependent effects on cytokine concentrations and therefore on cell behavior and

Parameter	Meaning	Value	Source
ϕ	phagocytic threshold	0.7	Engele et al. [2002]
g	intracellular *Mtb* growth rate	0.5/d	Silver et al. [1998], MacMicking et al. [2003]
q_{max}	max intracellular *Mtb* kill rate	varied	Bonecini-Almeida et al. [1998]
N	maximum #bacilli/macrophage	50	Wigginton and Kirschner [2001]
a_{max}	maximum macrophage activation rate	1/d	Schroder et al. [2004]
a_{TNF}	effect of TNF on activation rate	10^{10}	estimate
u_{max}	maximum rate of chronic infection	.1/d	estimate
v_{on}	infected cell TNF 'turn on' rate	1/d	Engele et al. [2002]
v_{off}	maximum infected cell TNF 'turn off' rate	1/d	Engele et al. [2002]
w_{max}	maximum IL-10 'turn on' rate	2/d	Engele et al. [2002]
m_{IL-10}	half-sat constant, IL-10	25 pM	Wigginton and Kirschner [2001]
m_{IFN}	half-sat constant, IFN	100 pM	estimate
p_{MTNF}	macrophage TNF secretion rate	600 molecules/cell/s	Engele et al. [2002]
p_{MIL-10}	macrophage IL-10 secretion rate	60 molecules/cell/s	Fulton et al. [1998], Engele et al. [2002]
p_{TIFN}	T cell IFN secretion rate	200 molecules/cell/s	Barnes et al. [1993], Tsukaguchi et al. [1999]
p_{TTNF}	T cell TNF secretion rate	2000 molecules/cell/s	Barnes et al. [1993], Tsukaguchi et al. [1999]
p_{TIL-10}	T cell IL-10 secretion rate	1 molecule/cell/s	Barnes et al. [1993], Tsukaguchi et al. [1999]
i	homeostatic influx rate	1.4 cells/ml/s	Blusse van Oud Alblas et al. [1983]
i_{max}	maximum recruitment rate	100 cells/ml/s	Serbina and Flynn [1999]
i_{half}	half-saturation, TNF on influx rate	10pM	estimate
l_M	macrophage death rate	.12/d	chosen to balance i
l_T	T cell death rate	.23/d	Reinhardt et al. [2001]
h_T	Macrophage-T cell contact distance	10 μm	estimate
n	cytokine decay rate	0.07/min	Fishman and Perelson [1999]
D	cytokine diffusion rate	10^{-8} cm^2/s	Young et al. [1980]

Table 6.1: Base parameters for TB model. Individual parameters are varied for some simulations as indicated in the following sections. Unless otherwise noted, i_{max} and i_{half} apply to both macrophages and T cells, but i affects only macrophage influx. Note that many of these parameter values are not explicitly given in the cited references, but estimates are based on data available in those references.

population dynamics. However, there is insufficient information on binding and internalization rates of the cytokines used in this model to include this effect. Implications of this limitation will be discussed below.

6.2.6 Initialization

Each simulation represents the development of a single nascent granuloma, and is therefore initialized with a single *Mtb*-infected macrophage in the center of the 1 mm^3 simulated compartment shown in Figure 5.3. 1000 uninfected macrophages are also present initially, but no T cells. Simulations used a time step of 20 seconds and a molecular grid size of 50

μm. I ran 30 simulations for each parameter set.

6.3 Simulation Results

The model additions for cytokine production and regulatory effects are based largely on in vitro studies of cell cultures. These include some rather complicated feedback interactions, but the model is still vastly simpler than the real system. In general, the effect of these feedback loops is to regulate cell recruitment and macrophage activation, varying parameters that were fixed in Chapter 5. This includes indirect effects, as some of the cytokines regulate cytokine production. The simulations are used to determine how well these feedback interactions, operating between individual neighboring cells, can capture key aspects of the infection dynamics in tissue.

Most model parameters were chosen to try to match data from human cells, partly because most culture studies of alveolar macrophage responses to *Mtb* are done with human cells. However, early infection dynamics in humans are not observable, so simulation results are compared to observations in mice for lack of a better alternative. The first sets of simulations described below illustrate the behavior of the model with the parameter values shown in Table 6.1, which are used to illustrate general characteristics of simulation dynamics and lesion structure. Section 6.3.2 simulates earlier availability of T cells that may result from vaccination. Subsequent experiments in sections 6.3.3 through 6.3.5 look at the effect of varying cytokine production and sensitivity parameters in a way that reflects known variations in humans or in mice.

6.3.1 Results with Base Parameter Set

There is considerable variation in simulation results for a single parameter set, as illustrated for *Mtb* and macrophage counts in Figure 6.2. Such variation is likely to happen

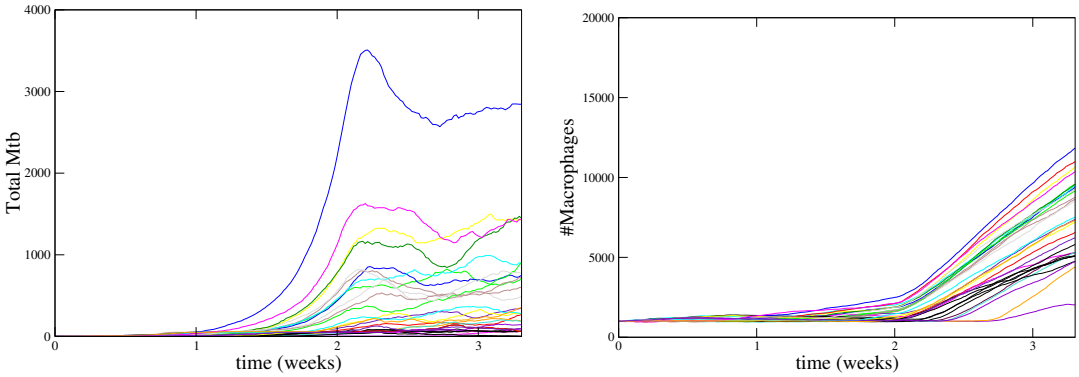

Figure 6.2: Outcome variability for TB model with base parameter set. Total numbers of *Mtb* (left) and macrophages (right) over time for 30 simulations of the base parameter set. $q_{max} = 2$/d; other parameter values as shown in Table 6.1. T cell influx began 2 weeks after the start of infection.

within an infected animal or person as well; each curve in the figure might represent the fate of a single bacillus landing in a different location within the lung. Lesions with different characteristics have been observed in different locations within the same animal [Rhoades et al., 1997, Davis et al., 2002]. There is always some chance that *Mtb* at some location will be eliminated; this happens in 1 of the 30 simulations for this parameter set. On the other hand, bacterial growth in other locations can be very high.

In these simulations, T cell influx begins two weeks after infection to agree with observations in mice [Chackerian et al., 2002]. Figure 6.2 shows that macrophage recruitment is greatly enhanced after the arrival of T cells; T cells secrete larger amounts of TNF. Early recruitment is limited by smaller numbers of infected cells as well as their lower TNF secretion rate. In most of these simulations, *Mtb* grow within the initial infected cell for over a week before that cell dies. The TNF produced by a single infected cell stimulates only a weak inflammatory response. Also, IL-10 can inhibit TNF production, further reducing early inflammation.

The total bacterial burden in mouse lungs is the result of growth within many inde-

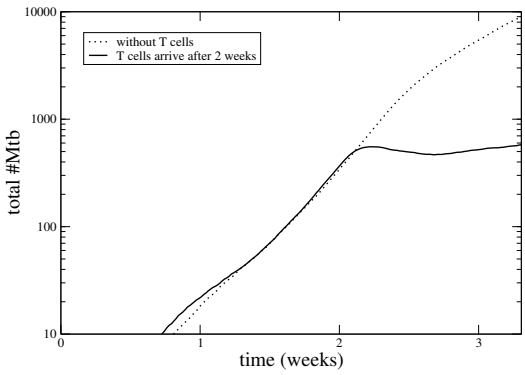

Figure 6.3: Average simulated *Mtb* growth with base parameter set. $q_{max} = 2$/d; other parameter values as shown in Table 6.1. Each line shows a time course averaged over 30 simulations.

pendent lesions. In order to compare simulation results to those from experiments, I use the average simulated *Mtb* growth. This is shown in Figure 6.3 for the simulations plotted in Figure 6.2. For comparison, Figure 6.3 also shows results from a set of simulations in which there are no T cells. The general trend matches that seen in experiments; initial exponential growth arrested shortly after the arrival of T cells. Cytokine concentrations are also within reasonable ranges (not shown).

The shape of the initial growth curve may vary due to factors discussed in Chapter 5: macrophage influx rates, phagocytosis rates, and infected cell death rates, in addition to bacterial growth rates. The macrophage population may also have some innate ability to kill *Mtb*, although this was not included in these simulations. Experimental evidence indicates that this ability is negligible in the majority of the recruited cells, although Dannenberg and Collins [2001] believe that the resident macrophages infected first are more likely to be activated.

Once T cells arrive, they begin activating macrophages, which begin to kill some of the *Mtb*. Some intracellular growth may continue in macrophages before they become activated. Also, not all macrophages become activated or remain activated even when a large

number of T cells are present. Stochasticity and variations in each macrophage's local environment are factors in macrophage activation and deactivation. The result is heterogeneity in macrophage antimicrobial activity, similar to that seen at the end of Chapter 5, although in this case antimicrobial capabilities change over time and are influenced by external stimuli. The *Mtb* curve after the arrival of T cells is the net result of growth in unactivated macrophages and killing by activated macrophages. If the rate of killing by activated macrophages (q_{max}) is not sufficiently high, the *Mtb* population may continue to rise, although at a reduced rate compared to the initial growth phase.

Lesion Structure

The fastest-growing lesion gives some indication of the worst-case outcome for the parameter values used. A graphical illustration of the center of the lesion at the end of the worst-case simulation from Figure 6.2 is shown in Figure 6.4. This shows an aggregation of uninfected and infected macrophages and T cells. T cells tend to cluster, presumably in areas of high TNF concentration. These clusters include many newly infected cells, which can produce TNF and induce T cell production of TNF. T cells may also linger in areas where infected cells have died but the TNF concentration is still high. Those T cells not in contact with a newly infected macrophage do not produce cytokines. Infected cells on the fringes of these clusters may receive inadequate T cell and cytokine stimulation, particularly once they stop secreting TNF. These are the cells most likely to become chronically infected and allow continued bacterial growth.

There are no extracellular *Mtb* in Figure 6.4, and the infection is contained. In contrast, simulations without T cells produced lesions like that shown in Figure 6.5, in which there are larger numbers of infected cells and significant numbers of extracellular *Mtb*. There are also still large numbers of uninfected cells in the latter simulation because in this model, a large percentage of the macrophages are unable to phagocytose *Mtb*. This is based on in vitro data [Engele et al., 2002]; it may be that phagocytosis is upregulated during infection

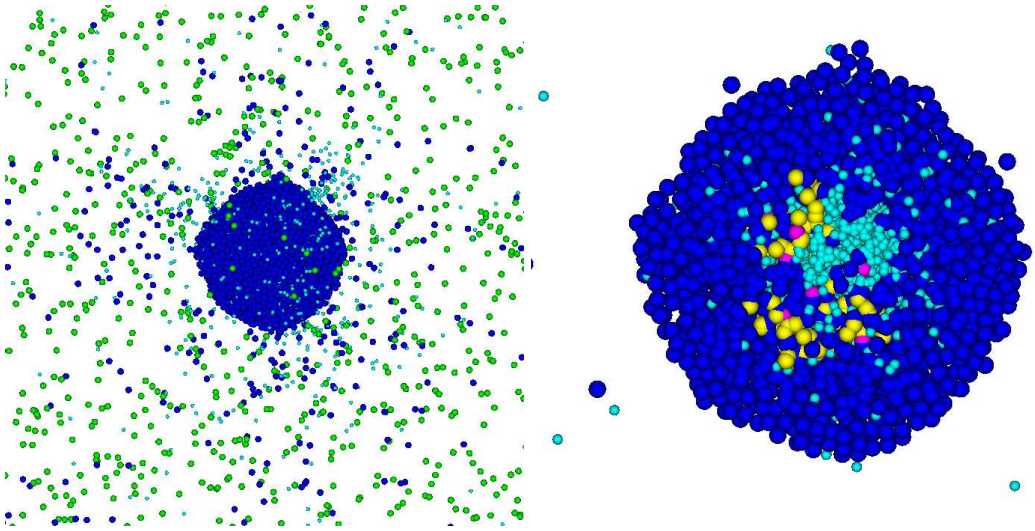

Figure 6.4: Simulated lesion with base parameter set. Left: screenshot of the entire simulated volume. Right: thin slice through the center of the lesion. The green tissue cells were removed from the figure on the right to make it easier to distinguish the remaining cell types. Large dark blue cells are uninfected macrophages, large yellow cells are newly infected macrophages, large magenta cells are chronically infected macrophages, and smaller cyan cells are T cells. There are no extracellular *Mtb* in this image. $q_{max} = 2$/d; other parameter values as shown in Table 6.1.

in vivo.

Figure 6.4 shows a tight cluster of T cells in the center of the simulated lesion. Rhoades et al. [1997] describe T cells in early lesions as being clustered around blood vessels or around activated macrophages, but apparently this does not result in a large clump of T cells like that seen in Figure 6.4. Since macrophage activation and T cell cytokine production depend on contact between macrophages and T cells, this difference could affect simulation results. The tight cluster in the simulation is due in part to the lack of real tissue structure, which allows cells to pack densely and also allows the lesion to grow around simulated blood vessels (gateway cells). The total number of T cells may also be greater than it should be, due to excessive influx or insufficient T cell death rates. This possibility might also explain why there is very little delay between the initial arrival

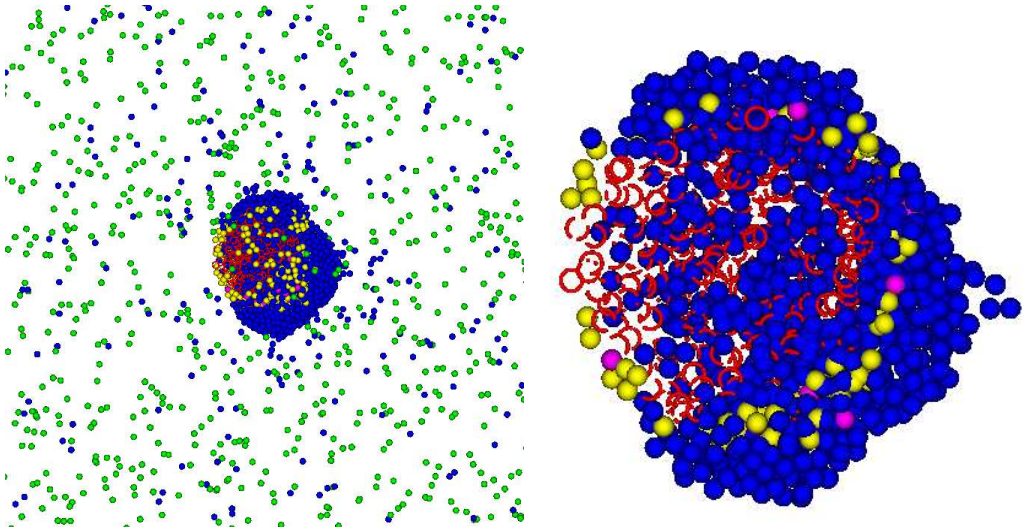

Figure 6.5: Simulated lesion without T cells. Left: screenshot of the entire simulated volume. Right: thin slice through the center of the lesion. The green tissue cells were removed from the figure on the right to make it easier to distinguish the remaining cell types. Large dark blue cells are uninfected macrophages, large yellow cells are newly infected macrophages, large magenta cells are chronically infected macrophages, and the very small cells and arcs are extracellular *Mtb*. Parameter values shown in Table 6.1.

of T cells and the decline in the *Mtb* population shown in Figure 6.3; experiments in mice show a later peak in the bacterial load. However, there are no estimates of the numbers of different cell types in individual lesions for comparison to the simulated lesion cell composition.

6.3.2 Timing of T Cell Influx

The time required for expansion of an antigen-specific population of T cells is thought to be less than a week [Janeway et al., 1999]. However, antigen must reach the lymphoid organs in large enough quantities before this expansion can begin. It is thought that slow bacterial dissemination in tuberculosis infection is responsible for the delay in appearance of *Mtb*-specific T cells [Chackerian et al., 2002]. The slow progression early in the simulations—

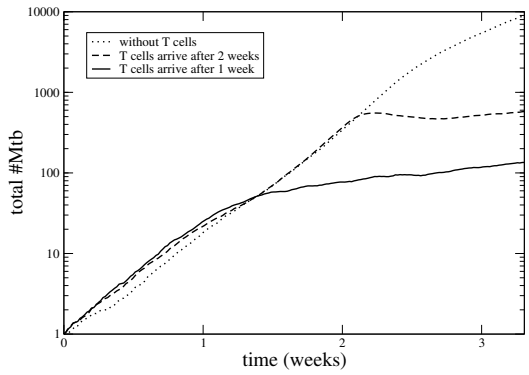

Figure 6.6: Effect of earlier T cell influx on simulated *Mtb* growth. $q_{max} = 2$/d; other parameter values as shown in Table 6.1. Each line shows a time course averaged over 30 simulations.

due both to slow bacterial growth and slow recruitment of immune system cells—support the notion that transport of antigen to lymphoid organs would also be slow.

The goal of tuberculosis vaccination is to increase the population of *Mtb*-specific T cells that will be available early in infection in the hopes of preventing disease. However, experiments in mice show that although vaccination reduces the bacterial load, it does not clear the infection [North and Jung, 2004]. This is exactly the scenario shown in simulations in which T cell influx begins one week after infection. Figure 6.6 shows simulated *Mtb* growth curves for T cell delays of 1 and 2 weeks; again, runs with no T cells are shown for comparison. Earlier T cell arrival allows earlier inhibition of *Mtb* growth and a significant reduction in the bacterial load. However, there is still significant growth within unactivated macrophages in both sets of simulations. Only 2 of 30 simulations with a 1-week delay in T cell influx cleared their pathogens

This suggests that factors other than the availability of T cells limit the immune system's ability to control this pathogen. The following sections evaluate the contribution of each of the cytokines included in the model.

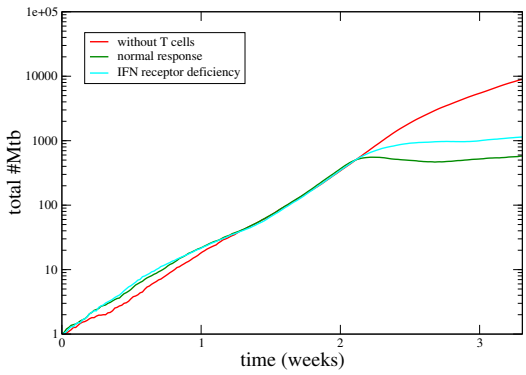

Figure 6.7: Average simulated *Mtb* growth with IFN receptor deficiency (solid line); results from Figure 6.3 included for comparison (dotted and dashed lines). For solid line, $m_{IFN} = 2$ pg/ml; other parameter values as shown in Table 6.1 Each line shows a time course averaged over 30 simulations.

6.3.3 IFN Receptor Deficiency

A genetic susceptibility to mycobacterial infection has been linked to absence of the primary receptor for IFN, IFN-γR1 [Newport et al., 1996]. Experiments with IFN-γR1-deficient mice deficient show that loss of this receptor impairs the ability to control *Mtb* growth [MacMicking et al., 2003]. This deficiency is represented in the model by raising the value of m_{IFN} to 2 pg/ml, which makes macrophages much less sensitive to IFN. This affects both macrophage activation and IFN inhibition of IL-10 production.

The average *Mtb* growth in these simulations is compared to the previous simulations in Figure 6.7. Although the bacterial load is increased compared to the simulation of a normal response, there is still more control of the pathogen than seen in experiments with mice [MacMicking et al., 2003]. It is not clear whether this is due to a problem with the expression used for IFN sensitivity, or an actual difference between human and mouse parameter values.

Nevertheless, the difference in bacterial load between the models of normal response

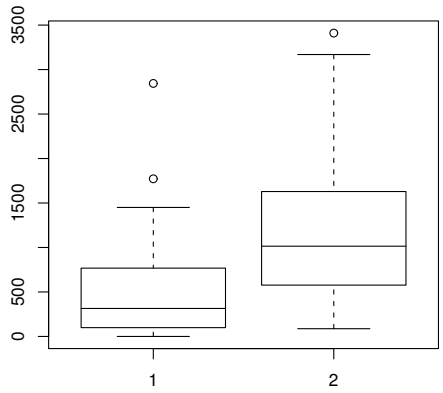

Figure 6.8: Effect of IFN receptor deficiency. Distributions of *Mtb* numbers after 23 days for base parameter set (1) and IFN receptor deficiency (2). The box-and-whisker plot shows median (line through the box), first and third quartiles (ends of the box), minimum and maximum values (lines at the ends of the 'whiskers') and outliers (marked by circles) for each set of simulations. (The maximum value does not include outliers).

and IFN receptor deficiency is significant. Figure 6.8 compares the distributions of the two sets of simulation results. Although there is some overlap, the IFN receptor deficiency model has many simulations for which *Mtb* loads are much higher. A two-sample t-test of the means of these distributions indicates that the difference is significant (P=0.005). If disease is associated with *Mtb* burdens above some threshold level, the results would agree with observations that the chances of developing active disease are increased in the IFN receptor deficiency model.

6.3.4 IL-10 Knockout

As mentioned in section 6.1.1, the role of IL-10 in tuberculosis is not fully understood. To determine its effect in the model, I did a set of simulations in which IL-10 production was

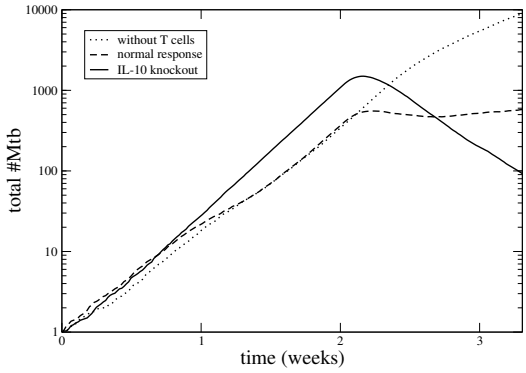

Figure 6.9: Average simulated *Mtb* growth with IL-10 knockout (solid line); results from Figure 6.3 included for comparison (dotted and dashed lines). For solid line, $p_{MIL10} = p_{TIL10} = 0$; other parameter values as shown in Table 6.1 Each line shows a time course averaged over 30 simulations.

eliminated. The resulting time course, shown in Figure 6.9 shows a very different trend than in the previous models.

In the model, IL-10 inhibits both inflammation and macrophage activation. Its removal initially allows more macrophage recruitment and therefore more *Mtb* growth. After the arrival of T cells, however, it allows increased bacterial killing in a number of ways. Absence of IL-10 allows increased production of IFN, strengthening the activation signal that macrophages receive. It allows macrophages to become or remain activated for longer periods of time. It also allows infected macrophages to continue secreting TNF, increasing the chances that T cells will find them by chemotaxis.

Some or all of these effects are probably overstated in the model. Although researchers hoped that inhibition of IL-10 would lead to increased antimicrobial activity like that shown in Figure 6.9, studies of *Mtb* infection in IL-10 knockout mice show little change from infection in normal mice. The results are contradictory; one study shows an early transient reduction in bacterial loads [Roach et al., 2001], another shows evidence of increased IFN production, but no difference in *Mtb* loads [Jung et al., 2003]. Neither shows

an increase in initial bacterial growth or inflammation. Differences between simulation and experimental results may be due to the effects of cytokines not included in the model of section 6.2, some of which may compensate for IL-10 in vivo.

6.3.5 Increased TNF Production

Genetic variation in TNF genes is associated with increased levels of TNF and may be associated with increased susceptibility to a number of diseases including some involving macrophage pathogens [Hill, 1998]. The cause of increased pathology in these diseases is not really understood, and there do not appear to be any documented associations between increased TNF levels and tuberculosis outcome. However, since TNF is an important cytokine in tuberculosis, I ran some simulations with the TNF secretion rates p_{MTNF} and p_{TTNF} increased 5-fold.

Unlike the previous variants, this change does not significantly affect the simulated *Mtb* growth curve, as shown in Figure 6.10. Increased TNF concentrations lead to increased cell recruitment, more infected cells and small increases in the other cytokines produced; apparently all of the increases compliment each other to result in little net change to the bacterial dynamics.

Figure 6.11 shows that although the bacterial load is similar ($P > 0.5$), the size of the lesion, as determined by the total number of macrophages, is significantly larger ($P = 2.5 \times 10^{-7}$). Increased lesion size may indicate increased pathology. On the other hand, Chackerian et al. [2002] noticed that mice able to survive *Mtb* infection longer had faster initial lesion growth than more susceptible mice. As in the simulations, bacterial load for the first few weeks was the same in both strains. Chackerian et al. [2002] hypothesized that faster initial growth enhanced development of the T cell response, with beneficial effects later in the infection. This is just one example of ways in which individual aspects of the immune response may be either detrimental or beneficial, or perhaps both.

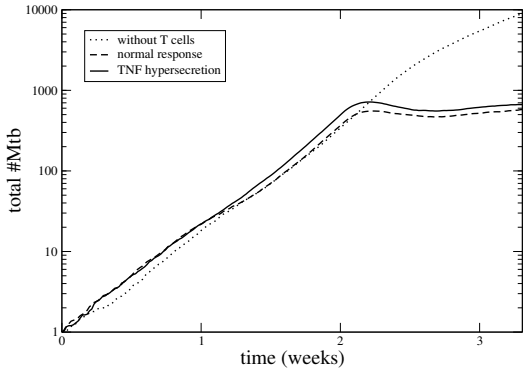

Figure 6.10: Average simulated *Mtb* growth with increased TNF secretion (solid line); results from Figure 6.3 included for comparison (dotted and dashed lines). For solid line, $p_{MTNF} = 3000$, $p_{TTNF} = 10000$; other parameter values as shown in Table 6.1 Each line shows a time course averaged over 30 simulations.

6.4 Related Work

Antia et al. [1996] used a very simple differential equation model to show that some sort of dormant stage could allow long-term bacterial persistence at low densities. Their model takes a systemic view of the infection, in which the difference between pathogen clearance and persistence depends on the amplitude of oscillations in the total bacterial load; these sorts of oscillations are not seen in tuberculosis infection. This view also makes it difficult to evaluate the separate effects of immune cell recruitment and local, variable expression of effector functions.

Kirschner's group modeled cytokine regulation in pulmonary tuberculosis using differential equations [Wigginton and Kirschner, 2001, Marino and Kirschner, 2004]. Their models include the induction of multiple T cell subsets with different effector functions and their potential roles in chronic infection, with little mention of the early response. As a result, they focus on a slightly different set of cytokines than I do. These differences make it difficult to compare their models and mine directly, but also highlight the fact that there are many aspects of this disease that still require further study.

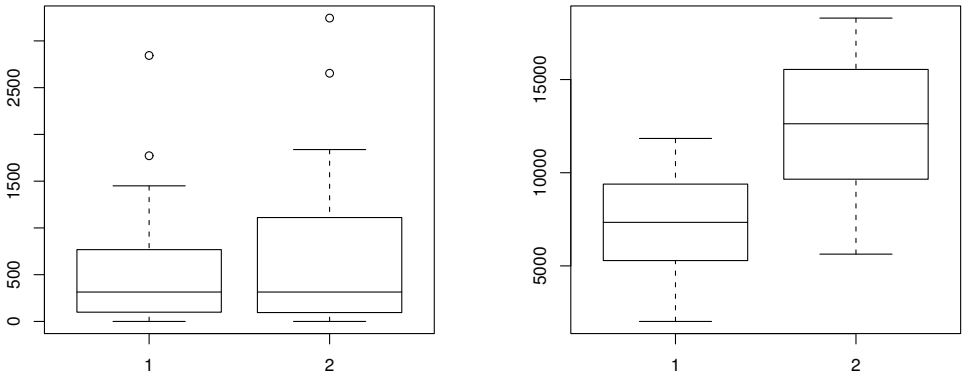

Figure 6.11: Effect of increased TNF production. Distributions of *Mtb* load (left) and total number of macrophages (right) after 23 days for base parameter set (1) and TNF hypersecretion (2).

6.5 Summary

The TB model described here represents an attempt to merge a conceptual model of the key factors in tuberculosis infection with semi-quantitative data from in vitro experiments to reproduce results from several different animal studies. This is a very difficult undertaking which thus far has met partial success. Simulation results represent qualitative agreement with some experimental results, indicating the potential usefulness of the model. Discrepancies with other results identify areas in which the conceptual model, its implementation, or numerical values require refinement.

Simulations successfully reproduce the ability of the immune response to reduce initial bacterial growth and contain the infection. They also illustrate several factors that may allow some *Mtb* to evade destruction:

- spatial isolation may prevent some macrophages from receiving sufficient T cell

and/or cytokine stimulation;

- cytokine regulation of macrophage activation may not allow cells to become or remain activated long enough to clear their intracellular bacterial load;
- inherent deficiencies in macrophage antimicrobial capabilities, as demonstrated in Chapter 5 may also be important.

Another possibility, that changes in *Mtb* gene expression account for both evasion of antimicrobial mechanisms and reduced bacterial growth, was not addressed here. These changes seem to be triggered by the immune response [North and Jung, 2004], so I am assuming that there is a period when the pathogen may be vulnerable before these evasion strategies take full effect.

It is particularly interesting that earlier T cell influx, representing either quicker initiation of an adaptive response or vaccination, does not change the qualitative infection dynamics. Earlier involvement of T cells arrests bacterial growth at a lower population size, but does not significantly increase the likelihood of clearing the pathogen. Although T cells increase macrophage activation, they also increase macrophage recruitment, which may contribute to spread of the infection. In the simulations, increased numbers of T cells tend to clump and therefore do not improve the chances of activating isolated macrophages. It is important to note that even if spatial distributions of cells in the simulations do not reflect those in vivo, the qualitative effect of some macrophages remaining unactivated due to spatial isolation is still plausible. On the other hand, spatial effects are not the only factor preventing macrophage activation in the simulations. Adjusting the cytokine network by removing IL-10 allows enhanced macrophage activation despite the spatial distribution. Again, while this particular effect is not demonstrated in animal models, the possibility that the cytokine network could be manipulated to increase macrophage activation still exists. Effective tuberculosis prevention and treatment strategies may need to concentrate not only on increasing the total number of *Mtb*-specific T cells, but also

on improving their colocalization with infected macrophages and/or shifting the cytokine balance to adjust relative contributions of recruitment and activation.

A number of cytokines are known or believed to have an effect on macrophage activation. The effect of IFN is best understood, and the model presented in this chapter partially captures the enhanced susceptibility to *Mtb* caused by reduced IFN signalling. I also explored some less well understood cytokine effects on infection dynamics, using examples of known variations in cytokine genes as a basis for choosing parameters to change. The simulations suggest that suppression of IL-10 could have a significant effect on the ability to control *Mtb*, but do not show any correlation between TNF production and *Mtb* growth. Comparisons between these simulations and experimental results highlight areas where the conceptual model or its implementation in simulation is lacking.

The discrepancy in the effect of removing IL-10 between simulation and experiments reflects an inadequacy of the conceptual model. IL-10 is known to inhibit both inflammation and macrophage activation, and the possibility that this may significantly affect infection dynamics does not contradict expectations. In other words, the simulation results are in agreement with the current understanding of at least some of IL-10's roles. However, given that they contradict experimental results, there must be some other regulatory interactions that the model does not include. It is not clear whether some known mechanism described in the biological literature might correct this particular discrepancy, or whether the biology itself is unknown.

In contrast, implementation of the model is probably responsible for the partial failure to adequately characterize the effects of IFN receptor deficiency in simulation. Certainly the understanding is that eliminating or severely reducing the IFN signal should make it nearly impossible for macrophages to kill *Mtb*. There are a number of possible reasons why some bacterial killing still takes place in the simulations; more work will be necessary to investigate these possibilities and to identify an appropriate solution. One possibility is that representing the probability of macrophage activation as a saturating function of

the IFN concentration does not adequately capture cell sensitivities to external stimuli. Although it prevents excessive responses to large signals, it still allows responses to very small signals. Even when the value of this function is very low, the cumulative probability becomes significant over time. It may be necessary to incorporate a threshold preventing activation unless the perceived cytokine signal is above some lower bound.

It is also possible that local cytokine concentrations are allowed to get too high, making it difficult to determine where this lower bound should be. Cytokine concentrations in the simulations continue to increase as long as the number of cells producing them increases. Local concentrations are somewhat constrained by limits on how densely cells can pack, but this is a rather artificial limit, as repulsion between cells is the only factor counteracting chemotaxis to control the local cell density. Increases in cytokine concentrations should also be limited by regulatory mechanisms—either through cell consumption, as described in chapter 4, or through feedback regulation on cytokine production, or both. Both effects could make cytokine concentrations depend nonlinearly on the local cell density. However, although these effects are likely to be important, there is little quantitative data available to characterize them in a model. Simulating cytokine consumption is also difficult, particularly in a spatial simulation. Extra care must be taken to make sure that spatial resolution of molecular concentrations and time step sizes are compatible. It can also require more complicated methods for interpolating between the molecular grid and cell positions; there is an additional danger of artificially reducing concentrations below zero when attempting to distribute the effects of cytokine removal over multiple grid points.

More quantitative data would also aid model refinement. Numbers and spatial distributions of the various cell types in lesions appear to be important, but are not well characterized in vivo. Locating small lesions within the first few weeks of infection is difficult, but a better understanding of the changes in cell composition over time would allow more direct comparison between simulation results and animal models. This includes a better understanding of how cells move within three-dimensional tissues. Chapter 5 sim-

ulations indicate that it may also be important to quantitatively characterize heterogeneity in macrophage antimicrobial abilities.

In addition to addressing specific discrepancies between experiments and simulation, there are many components of the immune response to *Mtb* that are worth investigating in more detail; I list just a few here. Simulations in Chapter 5 illustrated the potential importance of killing infected macrophages that cannot be activated. There is evidence that T cells can kill infected cells as well as activating them [Tsukaguchi et al., 1995, Tan et al., 1997] and that cytokines including TNF and IL-10 may affect death of infected cells [Oddo et al., 1998, Rojas et al., 1999, Keane et al., 2000]. The cytokine network is much more complex than that represented here, especially in regulating cell migration. TNF and other cytokines initiate cytokine and chemokine signaling cascades involving local tissue cells as well as immune system cells. These can both amplify the initial inflammatory trigger and induce production of anti-inflammatory cytokines. Modeling may help clarify the contributions of these and other mechanisms.

There is a great deal of interest in developing better vaccines and exploring potential cytokine therapies for tuberculosis, but development is hindered by the enormous complexity of the immune response to this pathogen. Simulations such as these can be used to aid understanding of this complexity and to explore potential interactions not observable in experiments. The local effects of cytokines and cellular interactions early in infection are particularly important, and also very difficult to characterize in vivo. The model described in this chapter is still in the development phase, but demonstrates the potential advantages of combining simulation with experiments. Further model refinement and validation, aided by better quantitative biological data, will make these simulations more useful.

Chapter 7

Conclusion

I developed a hybrid spatial simulator for modeling intercellular interactions and used it to evaluate several models of peripheral immune system dynamics. There are a number of features specifically motivated by the desire to make biologically relevant models of intracellular infections. These include dynamics on different scales; CyCells can handle intracellular pathogen dynamics, contact-mediated cell-cell interactions, and cell interactions with the molecular environment. There is significant flexibility in the way models can be defined, supporting the ability to do iterative model development and to compare alternative model structures. I took advantage of this flexibility to explore several aspects of intercellular interactions. This work makes some contributions towards understanding regulation of peripheral immune system cells and also highlights several issues about modeling these systems.

Chapter 4 addressed regulation of macrophage homeostasis by secreted growth factor. It showed that cell consumption as well as production of cytokines can be an important aspect of regulation. Simulations of in vitro macrophage cultures predict that consumption of growth factor and periodic replenishment could induce oscillations in the numbers of cycling and resting cells. Simulations of in vivo regulation of homeostasis showed that

a system in which cells are replenished by influx from circulation is more stable than one dependent on only local proliferation. Both mechanisms are probably used, but the observed amount of local division seems remarkably constant; situations inducing greater death or efflux of macrophages are probably correlated with a balancing increase in influx from circulation.

Chapter 5 primarily explored the initial inflammatory response to a macrophage pathogen. The homeostatic regulatory mechanisms of Chapter 4 interacted with the inflammatory response in different ways, with paracrine control of the macrophage population limiting inflammation while autocrine control boosted it. Because these pathogens turn the immune response to their own advantage, bacterial growth could be limited somewhat by damping various parts of the response, including recruitment of cells from circulation or phagocytosis. More significant growth inhibition could be achieved by killing infected cells. True control or clearance, however, could only be achieved by activating macrophages to kill intracellular pathogens. Inability of some macrophages do to this could allow a persistent infection, with a degree of control established by more competent macrophages.

Chapter 6 added T cell and cytokine regulation of macrophage activation to study the early stages of tuberculosis infection. It illustrates how spatial effects and cytokine regulation might combine to prevent some macrophages from being activated, allowing bacteria to escape destruction. This can continue to happen even in a model of vaccination which shortens the delay before initiation of the T cell response. Simulation variants exploring the roles of different cytokines show qualitative agreement with current understanding of those roles, but show some discrepancies with experimental results. Clarification is particularly required for the role of IL-10 and other cytokines that may share overlapping functions. There are many possibilities for future work with the TB model, some of which are outlined in section 6.5.

The models in each chapter build on at least some portion of the previous models. They

also illustrate different styles of modeling. In Chapters 4 and 6, I put significant effort into obtaining quantitative data for the modelled system and validating the simulations to the extent that I was able. In contrast, Chapter 5 is a less constrained exploration of a broader range of parameter values, some of which may not be biologically plausible. The former approach grounds the model in experimental data in an effort to describe what the immune system actually does; the latter allows exploration of what it could or should do. Both approaches have their merits. In Chapter 4, sufficient data were available to make quantitative comparisons between simulations and experiments. In Chapter 6, although a similar quantitative approach was taken, the complexity of the system and gaps in our knowledge enabled only qualitative evaluations. More abstract 'what-if' models like those in Chapter 5 can help identify potentially interesting areas in which to focus model exploration.

Validation of biological models is severely hampered by the lack of quantitative data, particularly for parameter estimation. Voit [2000] notes: "One could even claim that parameter estimation is currently the limiting step in biomathematical modeling." One option for determining free parameters is to test a range of possible values to see which combination best fits the system-level data. This approach is not feasible for the models presented here because of the large number of parameters relative to the amount of available quantitative data; this ratio makes the chance of overfitting the limited data fairly high. Rather than trying to fit the models at the system level, I tried to choose both model structure and parameter values based on knowledge of individual components (e.g molecular dynamics, cytokine secretion, etc.). This approach also has problems, in that isolation of components may change the way they behave, but it does reduce the scale of the parameter estimation problem. Inability of the composite model to produce the desired or expected behavior may indicate areas needing correction or refinement. However, even when such a model produces the desired system-level behavior, it's not clear that the model structure or parameter values are optimal in any sense. In particular, there is little guarantee that they will generalize to capture untested behaviors. Sensitivity analysis studies using different parameter values could determine how robust the results are and which parameters have the

largest effect on model dynamics. As for the initial parameter estimates, better quantitative data would help establish reasonable ranges of each parameter value to explore.

In order to model these particular systems, I incorporated a number of mechanistic elements I thought likely to be important for modeling localized infections into CyCells. The term 'mechanistic' is somewhat misleading, because any level of modeling hides some details about how the modelled system actually works. I use the term here to refer to capturing aspects of what individual cells actually do, as opposed to relying solely on average population rates. This includes accounting for the delays involved in cell division and tracking individual intracellular bacteria within macrophages, for example. This level of detail may not be necessary in all cases. However, it is not always clear beforehand which details are most important. Frequently, simplifying assumptions are made with no attempt to determine the effect on the system dynamics. CyCells makes it possible to investigate the consequences of many such assumptions.

Even when the specifics of individual cell behavior are shown to be important, the effort to model the system at this level of detail is hampered by the lack of quantitative data describing these processes in real cells. Chapter 5 illustrated the importance of quantitatively characterizing expression of macrophage antimicrobial mechanisms. In the case of intracellular cell responses to receptor-ligand binding, even the qualitative behavior is only poorly understood. However, the necessary data are starting to become available through increasing use of flow cytometry and other methods for studying individual cells. As the data become available, models can gradually be refined. Conversely, modeling may illustrate which kinds of data are most likely to be important.

There are a number of areas in which the simulator implementation could be improved. I put more effort into making the simulator flexible than into making it efficient. Accurate simulations currently depend on the use of small time steps; it may be possible to improve run times by using elements of discrete event simulations and implicit numerical methods. On the other hand, interactions between cells and molecules cause a number of numerical

evaluation difficulties when both are moving. To simplify these, the effects of cell density on molecular diffusion were ignored. The consequences of this simplification need to be evaluated. Implementing accurate molecular dynamics in a multicellular simulation is problematic. Cell-mediated removal of molecules from the extracellular environment adds another complication not addressed in many models, and requires careful evaluation of interpolation functions and their dependencies on time step and grid sizes. Due to lack of data, this aspect of cell–molecule interactions was not really addressed in this work, but it should be important in future models. Simulation of cell movement could also be improved. There are some stochastic aspects to chemotaxis that were not included in the CyCells implementation. Also, adding cell-cell adhesion could be important for modeling localized multicellular structures such as granulomas. Finally, there are a number of engineering issues involved in turning code used for research into a robust, user-friendly tool.

Despite these limitations, CyCells provides a useful alternative to existing modeling approaches. Much is made of the fact that agent-based simulations are computationally intensive, but this does not mean they are intractable. Even a fairly complicated simulation is generally less time-consuming than experiments with animal models. They also do not have to be unmathematical, as I believe the examples in this dissertation show. An individual-based view can also be more intuitive than a population-based model, especially for models that capture phenomena on multiple scales. For example, it is more straightforward to specify separately how bacteria grow inside cells, the various ways a cell might die, and what happens to bacteria when their host cell dies than it is to come up with an expression for the average rate at which bacteria are released from a heterogeneous population of infected cells. Encounters between cells are also difficult to describe accurately in the average, general case, whereas they are a natural consequence of movement and collision rules in CyCells. Models are specified in terms of more primitive, less abstract properties of the real system. As models get more complicated, the ability to relate the model assumptions to observed phenomena in the modelled system becomes increas-

ingly important. This should also facilitate the progression from qualitative to increasingly quantitative models.

Individual-based and hybrid models can require significant programming effort. The generality of the sense-process-act framework for defining cell behaviors in CyCells enables it to be used for a wide variety of models. Some natural applications would include modeling other kinds of infections, cancer, and wound healing, but these are by no means the only possibilities.

Perhaps the most significant contribution of this work is the availability of the simulator code for future use and refinement. As mentioned in Chapter 2, similar multicellular simulators have been built before. There has been some duplication of effort in modeling intercellular interactions because each researcher built a new model or simulator and then did not make it available to anyone else. My hope is that this work will be a starting point for others, rather than an end.

Appendix A

Simulator Verification

Simulator verification, as opposed to model validation, is the attempt to show that the simulator code is correct. In general, simulator verification is done either with formal proofs or extensive testing. CyCells is too complex for formal proofs to be effective, so I used the latter approach. The testing process greatly reduces the chances that simulation results are affected by implementation errors, although it is impossible to eliminate the possibility of remaining errors in the code.

CyCells executes multiple models, and it is impossible to test its performance on every possible model. In addition, there are no existing results, either analytical or from other simulators, for comparison to many of the models it can simulate. Code verification therefore has to be performed on individual code components and simple models for which expected system behavior can be easily defined. I used a set of test drivers to test individual components of the simulator code each time the code was changed. These included tests of object interfaces and specific functions implementing diffusion, cell movement, and individual sense, process, and action functions described in Chapter 3.

In addition to testing individual components of the simulator, I also simulated some simple models for which analytical results are available for comparison. Many of these

show that CyCells gives the expected results in the cases of large, well-mixed populations. One example of a qualitative comparison was given in section 5.1, which illustrated that simulated population phagocytosis rates lead to exponential decay in the pathogen population in the case of random cell movement and intermediate cell densities, Some examples of quantitative tests are presented in the following sections.

A.1 Molecular Dynamics

The simplest tests are for molecular dynamics, since molecules are represented in their aggregate form in CyCells. In the absence of cell effects on molecular concentrations, the only changes are due to diffusion and decay. The average concentration C should decay according to:

$$C(t) = C_0 e^{-nt} \tag{A.1}$$

where t is time, C_0 is the initial concentration and n is the decay rate. Since the boundary conditions are periodic, diffusion should not affect the average concentration. These expectations are confirmed by the simulation results plotted in Figure A.1 together with the line representing equation A.1. Three values of the decay rate n were used that span the range reported for cytokines [Fishman and Perelson, 1994]. Simulations were done both with and without diffusion; only those with diffusion are plotted as the results from the two sets are nearly identical. The diffusion rate used was the maximum estimate from Francis and Palsson [1997]. Molecular dynamics are deterministic in CyCells, so a single simulation for each case is sufficient.

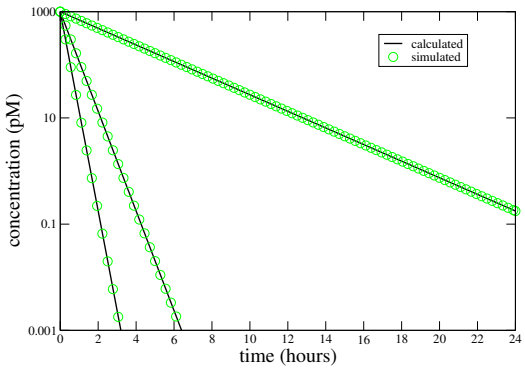

Figure A.1: Molecular decay. Simulation results (circles) and expected results from equation A.1 (line) are plotted for three values of the decay rate n: 0.0001/s, 0.0006/s and 0.0012/s. The diffusion rate in the simulations was 10^{-6} cm^2/s. Molecular grid size was 50 μm and the simulation time step was 20s (same values as used in Chapters 5 and 6).

A.2 Birth-Death Processes

The best example of a stochastic process for which analytic results are available is the birth-death process, which CyCells simulates for intracellular pathogen dynamics. In the models of Chapters 5 and 6, each infected cell has a relatively small number of pathogens subject to this birth-death process, leading to considerable variation in intracellular pathogen populations. However, simulations isolating just the birth-death process and using a large number of trials can confirm that the process produces the expected distribution of outcomes.

This distribution is characterized by equations describing the probability $p_N(t)$ that the population will reach a size N by time t, given the initial population size N_0 and the birth and death probabilities ($g\Delta t$ and $q\Delta t$, respectively). Different equations for $p_N(t)$ are appropriate for different combinations of g, q and N_0 [Bailey, 1964]. For $q = 0$ (pure birth process):

$$p_N(t) = \binom{N-1}{N_0-1} e^{-N_0 g t}(1-e^{-gt})^{N-N_0} \tag{A.2}$$

Another special case arises when $g = q$; for $N_0 = 1$:

$$p_0(t) = \frac{gt}{1+gt} \tag{A.3}$$

$$p_N(t) = \frac{(gt)^{N-1}}{(1+gt)^{N+1}} \quad N = 1,2,\ldots \tag{A.4}$$

Otherwise,

$$p_0(t) = \alpha^{N_0} \tag{A.5}$$

$$p_N(t) = \sum_{j=0}^{\min(N_0,N)} \binom{N_0}{j} \binom{N_0+N-j-1}{N_0-1} \alpha^{N_0-j} \beta^{N-j} (1-\alpha-\beta)^j \tag{A.6}$$

where

$$\alpha = \frac{q(e^{(g-q)t}-1)}{ge^{(g-q)t}-q} \tag{A.7}$$

$$\beta = \frac{g(e^{(g-q)t}-1)}{ge^{(g-q)t}-q} \tag{A.8}$$

If $N_0 = 1$, this simplifies to:

$$p_0(t) = \alpha \tag{A.9}$$

$$p_N(t) = (1-\alpha)(1-\beta)\beta^{N-1} \quad N = 1,2,\ldots \tag{A.10}$$

I used four different test cases for relevant birth and death rates in which the death rate was 1) zero, 2) equal to the birth rate, 3) nonzero but less than the birth rate, and 4) greater than the birth rate. Parameter values are shown in table A.1. For each case, I ran 10,000 trials starting with a single cell containing a single intracellular pathogen. I recorded the number of pathogens at time $t = 100,000$ s (a little over one day) for each run and calculated the proportion of trials producing each value of N for comparison to the calculated probabilities $p_N(t)$. Both the expected results and the simulation results are shown in Figure A.2.

Case	g	q	N_0
1	10^{-5}/s	0	1
2	10^{-5}/s	10^{-5}/s	1
3	2×10^{-5}/s	10^{-5}/s	1
4	2×10^{-5}/s	6×10^{-5}/s	10

Table A.1: Parameters for birth-death process tests.

These tests show that the simulator results are comparable to those for the analytic birth-death process. Other simulated stochastic processes use a similar approach in that the probability of an event or cell state change is assumed to be the product of a population rate (such as would be used in differential equations) and the time step.

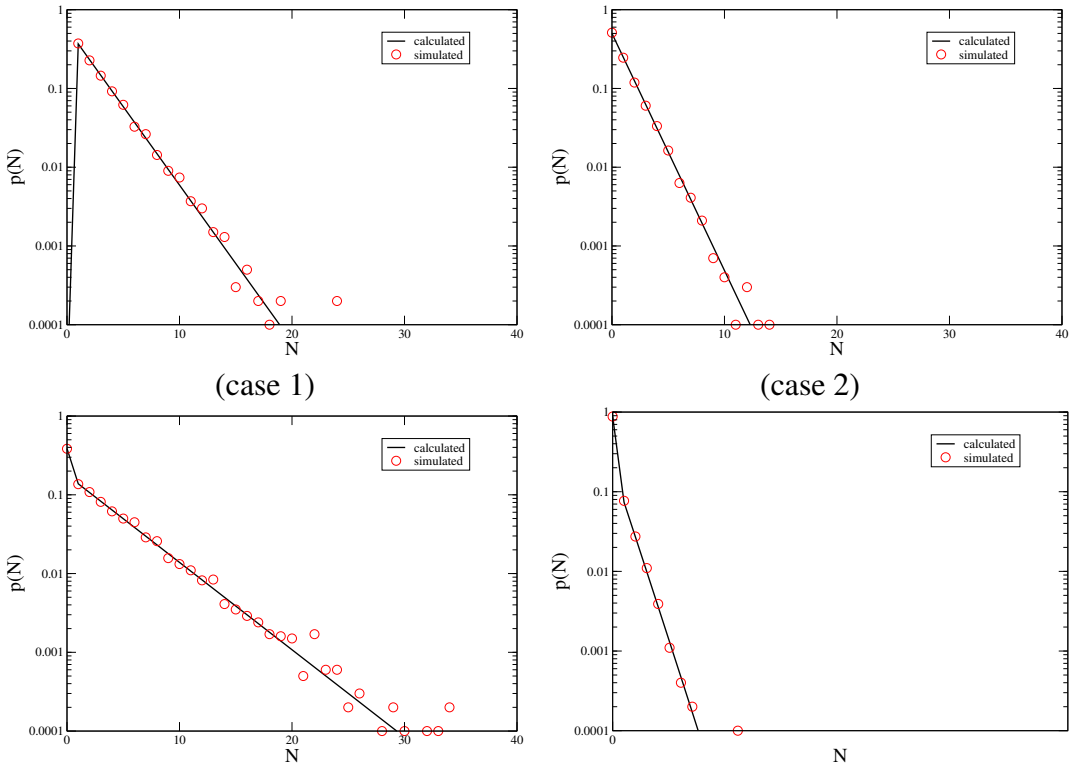

Figure A.2: Simulated Birth-Death Process. Simulation results (circles) and expected results (line) for the four cases described in Table A.1. The simulation time step was 20s.

References

A. Aderem. Phagocytosis and the inflammatory response. *J Infect Dis*, 187 Suppl 2: S340–5, Jun 15 2003.

K. S. Akagawa, K. Kamoshita, and T. Tokunaga. Effects of granulocyte-macrophage colony-stimulating factor and colony-stimulating factor-1 on the proliferation and differentiation of murine alveolar macrophages. *Journal of Immunology*, 141(10):3383–3390, November 1988.

M. Alber, A. Kiskowski, J. Glazier, and Y. Jiang. On cellular automaton approaches to modeling biological cells. In J. Rosenthal and D. Gilliam, editors, *Mathematical Systems Theory in Biology, Communication, and Finance, IMA Volume 132*, pages 1–40. Springer-Verlag, 2003.

R. Alur, C. Belta, V. Kumar, M. Mintz, G. Pappas, H. Rubin, and J. Schug. Modeling and analyzing biomolecular networks. *Computing in Science and Engineering*, 4, Jan-Feb 2002.

R. Antia and J. C. Koella. A model of non-specific immunity. *Journal of Theoretical Biology*, 168(2):141–150, May 1994.

R. Antia, J. C. Koella, and V. Perrot. Models of the within-host dynamics of persistent mycobacterial infections. *Proc R Soc Lond B Biol Sci*, 263(1368):257–63, Mar 22 1996.

A. L. Asachenkov, G. I. Marchuk, R. R. Mohler, and S. M. Zuev. Immunology and disease control: a systems approach. *IEEE Transactions on Biomedical Engineering*, 41(10), October 1994.

N. T. J. Bailey. *The elements of stochastic processes*. John Wiley & Sons, Inc., New York, 1964.

C. T. Baker, G. A. Bocharov, C. A. Paul, and F. A. Rihan. Modelling and analysis of time-lags in some basic patterns of cell proliferation. *J Math Biol*, 37(4):341–71, Oct 1998.

P. F. Barnes, J. S. Abrams, S. Lu, P. A. Sieling, T. H. Rea, and R. L. Modlin. Patterns of cytokine production by mycobacterium-reactive human T-cell clones. *Infect Immun*, 61 (1):197–203, Jan 1993.

S. Becker, R. B. Devlin, and J. S. Haskill. Differentiatial production of tumor necrosis factor, macrophage colony stimulating factor, and interleukin 1 by human alveolar macrophages. *Journal of Leukocyte Biology*, 45(4):353–361, 1989.

C. Bergmann, J. L. van Hemmen, and L. A. Segel. How instruction and feedback can select the appropriate T helper response. *Bull Math Biol*, 64(3):425–46, May 2002.

A. Blusse van Oud Alblas, H. Mattie, and R. van Furth. A quantitative evaluation of pulmonary macrophage kinetics. *Cell and Tissue Kinetics*, 16(3):211–9, May 1983.

A. Blusse van Oud Alblas and R. van Furth. Origin, kinetics and characteristics of pulmonary macrophages in the normal steady state. *Journal of Experimental Medicine*, 149:1504–1518, 1979.

G. A. Bocharov and A. A. Romanyukha. Mathematical model of antiviral immune response. III. Influenza A virus infection. *J Theor Biol*, 167(4):323–60, Apr 21 1994.

M. G. Bonecini-Almeida, S. Chitale, I. Boutsikakis, J. Geng, H. Doo, S. He, and J. L. Ho. Induction of in vitro human macrophage anti-Mycobacterium tuberculosis activity: requirement for IFN-γ and primed lymphocytes. *J Immunol*, 160(9):4490–9, May 1 1998.

D. H. Bowden. The alveolar macrophage. *Environmental Health Perspectives*, 55:327–341, 1984.

R. H. Brookes, A. A. Pathan, H. McShane, M. Hensmann, D. A. Price, and A. V. Hill. $CD8^+$ T cell-mediated suppression of intracellular Mycobacterium tuberculosis growth in activated human macrophages. *Eur J Immunol*, 33(12):3293–302, Dec 2003.

G. Bruns, P. Mössinger, D. Polani, R. Schmitt, R. Spalt, T. Uthmann, and S. Weber. Xraptor. http://www.informatik.uni-mainz.de/∼polani/XRaptor/XRaptor.html.

M. A. Burke, B. F. Morel, T. B. Oriss, J. Bray, S. A. McCarthy, and P. A. Morel. Modeling the proliferative response of T cells to IL-2 and IL-4. *Cellular Immunology*, 178(1): 42–52, 1997.

R. Callard, A. J. George, and J. Stark. Cytokines, chaos, and complexity. *Immunity*, 11 (5):507–13, Nov. 1999.

A. A. Chackerian, J. M. Alt, T. V. Perera, C. C. Dascher, and S. M. Behar. Dissemination of Mycobacterium tuberculosis is influenced by host factors and precedes the initiation of T-cell immunity. *Infect Immun*, 70(8):4501–9, Aug 2002.

D. L. Chao, M. P. Davenport, S. Forrest, and A. S. Perelson. A stochastic model of cytotoxic T cell responses. *J Theor Biol*, 228(2):227–240, 2004.

Charon. http://www.cis.upenn.edu/mobies/charon/index.html.

B. D. Chen, T. Chou, and C. R. Clark. Delineation of receptor-mediated colony-stimulating factor (CSF-1) utilization and cell production by precursors of mononuclear

phagocytic series at various stages of differentiation. *British Journal of Haematology*, 67(4):381–386, 1987.

B. D. Chen, C. Kuhn, 3rd, and H. S. Lin. Receptor-mediated binding and internalization of colony-stimulating factor (CSF-1) by mouse peritoneal exudate macrophages. *Journal of Cell Science*, 70:147–66, Aug 1984.

B. D. Chen, M. Mueller, and T. H. Chou. Role of granulocyte/macrophage colony-stimulating factor in the regulation of murine alveolar macrophage proliferation and differentiation. *Journal of Immunology*, 141(1):139–144, July 1988.

J. E. Coggle and J. D. Tarling. The proliferation kinetics of pulmonary alveolar macrophages. *Journal of Leukocyte Biology*, 35(3):317–327, March 1984.

E. L. Corbett, C. J. Watt, N. Walker, D. Maher, B. G. Williams, M. C. Raviglione, and C. Dye. The growing burden of tuberculosis: global trends and interactions with the HIV epidemic. *Arch Intern Med*, 163(9):1009–21, May 12 2003.

D. Corry, P. Kulkarni, and M. F. Lipscomb. The migration of bronchoalveolar macrophages into hilar lymph nodes. *American Journal of Pathology*, 115(3):321–328, June 1984.

J. C. Dallon. Numerical aspects of discrete and continuum hybrid models in cell biology. *Applied Numerical Mathematics*, 32(2):137–159, February 2000.

A. M. Dannenberg, Jr. and F. M. Collins. Progressive pulmonary tuberculosis is not due to increasing numbers of viable bacilli in rabbits, mice and guinea pigs, but is due to a continuous host response to mycobacterial products. *Tuberculosis (Edinb)*, 81(3): 229–42, 2001.

A. M. Dannenberg, Jr. and G. A. W. Rook. Pathogenesis of pulmonary tuberculosis: an interplay of tissue-damaging and macrophage-activating immune responses—dual

mechanisms that control bacillary multiplication. In B. R. Bloom, editor, *Tuberculosis: pathogenesis, protection, and control*. ASM Press, Washington D.C, 1994.

J. M. Davis, H. Clay, J. L. Lewis, N. Ghori, P. Herbomel, and L. Ramakrishnan. Real-time visualization of mycobacterium-macrophage interactions leading to initiation of granuloma formation in zebrafish embryos. *Immunity*, 17(6):693–702, Dec 2002.

L. Edelstein-Keshet and A. Spiros. Exploring the formation of alzheimer's disease senile plaques in silico. *J Theor Biol*, 216(3):301–26, Jun 7 2002.

M. Engele, E. Stossel, K. Castiglione, N. Schwerdtner, M. Wagner, P. Bolcskei, M. Rollinghoff, and S. Stenger. Induction of TNF in human alveolar macrophages as a potential evasion mechanism of virulent Mycobacterium tuberculosis. *J Immunol*, 168(3):1328–37, Feb 1 2002.

E. S. Fisher and D. A. Lauffenburger. Mathematical analysis of cell-target encounter rates in two dimensions. the effect of chemotaxis. *Biophys J*, 51(5):705–16, May 1987.

E. S. Fisher and D. A. Lauffenburger. Analysis of the effects of immune cell motility and chemotaxis on target elimination dynamics. *Math Biosci*, 98(1):73–102, Feb 1990.

E. S. Fisher, D. A. Lauffenburger, and R. P. Daniele. The effect of alveolar macrophage chemotaxis on bacterial clearance from the lung surface. *American Review of Respiratory Disease*, 137:1129–1134, 1988.

M. A. Fishman and A. S. Perelson. Th1/Th2 cross regulation. *J Theor Biol*, 170(1):25–56, Sep 7 1994.

M. A. Fishman and A. S. Perelson. Th1/Th2 differentiation and cross regulation. *Bulletin of Mathematical Biology*, 61:403–436, 1999.

K. Fleischer and A. H. Barr. A simulation testbed for the study of multicellular development: The multiple mechanisms of morphogenesis. In C. G. Langton, editor, *Artificial Life III*. Addison Wesley Longman, Reading, 1994.

I. E. Flesch and S. H. Kaufmann. Activation of tuberculostatic macrophage functions by gamma interferon, interleukin-4, and tumor necrosis factor. *Infect Immun*, 58(8): 2675–7, Aug 1990.

K. Francis and B. O. Palsson. Effective intercellular communication distances are determined by the relative time constants for cyto/chemokine secretion and diffusion. *Proceedings of the National Academy of Sciences U S A*, 94(23):12258–62, Nov 11 1997.

P. Fritsch and R. Masse. Overview of pulmonary alveolar macrophage renewal in normal rats and during different pathological processes. *Environmental Health Perspectives*, 97:59–67, July 1992.

S. A. Fulton, J. V. Cross, Z. T. Toossi, and W. H. Boom. Regulation of interleukin-12 by interleukin-10, transforming growth factor-β, tumor necrosis factor-α, and interferon-γ in human monocytes infected with Mycobacterium tuberculosis H37Ra. *J Infect Dis*, 178(4):1105–14, Oct 1998.

D. Gammack, C. R. Doering, and D. E. Kirschner. Macrophage response to Mycobacterium tuberculosis infection. *J Math Biol*, 48(2):218–42, Feb 2004.

D. T. Gillespie. A general method for numerically simulating the stochastic time evolution of coupled chemical reactions. *Journal of Computational Physics*, 22:403–434, 1976.

S. Gordon. The role of the macrophage in immune regulation. *Res Immunol*, 149(7-8): 685–8, Sep-Oct 1998.

L. J. Guilbert and E. R. Stanley. The interaction of 125I-colony-stimulating factor-1 with bone marrow-derived macrophages. *The Journal of Biological Chemistry*, 261(9):4024–32, Mar 25 1986.

A. G. Harmsen, B. A. Muggenburg, M. B. Snipes, and D. E. Bice. The role of macrophages in particle translocation from lungs to lymph nodes. *Science*, 230:1277–1280, December 1985.

M. Head, N. Meryhew, and O. Runquist. Mechanism and computer simulation of immune complex formation, opsonization, and clearance. *J Lab Clin Med*, 128(1):61–74, Jul 1996.

T. K. Held, M. E. A. Mielke, M. Unger, M. Trautmann, and A. S. Cross. Kinetics and dose dependence of macrophage colony-stimulating factor-induced proliferation and activation of murine mononuclear phagocytes in situ: Differences between lungs, liver and spleen. *Journal of Interferon and Cytokine Research*, 16:159–168, February 1996.

A. V. Hill. The immunogenetics of human infectious diseases. *Annu Rev Immunol*, 16: 593–617, 1998.

D. A. Hume. Probability in transcriptional regulation and its implications for leukocyte differentiation and inducible gene expression. *Blood*, 96(7):2323–8, Oct 1 2000.

D. A. Hume, I. Ross, S. Himes, R. T. Sasmono, C. Wells, and T. Ravasi. The mononuclear phagocyte system revisited. *Journal of Leukocyte Biology*, 72:621–627, October 2002.

C. A. Janeway, P. Travers, M. Walport, and J. D. Capra. *Immunobiology: The immune system in health and disease*. Current Biology Publications, 1999.

M. K. Jenkins, A. Khoruts, E. Ingulli, D. L. Mueller, S. J. McSorley, R. L. Reinhardt, A. Itano, and K. A. Pape. In vivo activation of antigen-specific $CD4^+$ T cells. *Annu Rev Immunol*, 19:23–45, 2001.

Y. J. Jung, L. Ryan, R. LaCourse, and R. J. North. Increased interleukin-10 expression is not responsible for failure of T helper 1 immunity to resolve airborne Mycobacterium tuberculosis infection in mice. *Immunology*, 109(2):295–9, Jun 2003.

S. H. Kaufmann. How can immunology contribute to the control of tuberculosis? *Nat Rev Immunol*, 1(1):20–30, Oct 2001.

S. H. Kaufmann. Protection against tuberculosis: cytokines, T cells, and macrophages. *Ann Rheum Dis*, 61 Suppl 2:ii54–8, Nov 2002.

S. H. E. Kaufmann. Immunity to intracellular bacteria. In W. E. Paul, editor, *Fundamental Immunology*, chapter 40. Lippincott-Raven Publishers, Philadelphia, 1999.

J. Keane, H. G. Remold, and H. Kornfeld. Virulent Mycobacterium tuberculosis strains evade apoptosis of infected alveolar macrophages. *J Immunol*, 164(4):2016–20, Feb 15 2000.

A. Kelso. Th1 and Th2 subsets: paradigms lost. *Immunol Today*, 16(8):374–9, Aug 1995.

T. Kishimoto, T. Taga, and S. Akira. Cytokine signal transduction. *Cell*, 76(2):253–62, Jan 28 1994.

R. P. Lanza, R. Langer, and J. Vacanti, editors. *Principles of Tissue Engineering*. Academic Press, 2000.

D. L. Laskin, B. Weinberger, and J. D. Laskin. Functional heterogeneity in liver and lung macrophages. *Journal of Leukocyte Biology*, 70(2):163–70, Aug 2001.

D. Lauffenburger. Mathematical model for tissue inflammation: effects of spatial distribution, cell motility, and chemotaxis. In W. Jager, H. Rost, and P. Tautu, editors, *Biological growth and spread: mathematical theories and applications: proceedings of a conference held at Heidelberg July 16-21, 1979*, pages 397–409. Springer, 1980.

D. A. Lauffenburger and C. R. Kennedy. Analysis of a lumped model for tissue inflammation dynamics. *Mathematical Biosciences*, 53:189–221, 1981.

D. A. Lauffenburger and J. J. Linderman. *Receptors: Models for binding, trafficking, and signaling*. Oxford University Press, 1993.

N. A. Lee and J. J. Lee. The macroimportance of the pulmonary immune microenvironment. *Am J Respir Cell Mol Biol*, 21(3):298–302, Sep 1999.

Y. Lee, S. Kouvroukoglou, L. V. McIntire, and K. Zygourakis. A cellular automaton model for the proliferation of migrating contact-inhibited cells. *Biophys J*, 69(4):1284–98, Oct 1995.

H. Lin, B. L. Lokeshwar, and S. Hsu. Both granulocyte-macrophage CSF and macrophage CSF control the proliferation and survival of the same subset of alveolar macrophages. *The Journal of Immunology*, 142(2):515–519, January 1989.

C. C. Ling and L. A. Segel. *Mathematics Applied to Deterministic Problems in the Natural Sciences*. Society for Industrial and Applied Mathematics, Philadelphia, 1988.

M. F. Lipscomb, D. E. Bice, C. R. Lyons, M. R. Schuyler, and D. Wilkes. The regulation of pulmonary immunity. *Adv Immunol*, 59:369–455, 1995.

Y. Louzoun, S. Solomon, H. Atlan, and I. R. Cohen. Proliferation and competition in discrete biological systems. *Bull Math Biol*, 65(3):375–96, May 2003.

J. Ma, T. Chen, J. Mandelin, A. Ceponis, N. E. Miller, M. Hukkanen, G. F. Ma, and Y. T. Konttinen. Regulation of macrophage activation. *Cell Mol Life Sci*, 60(11):2334–46, Nov 2003.

J. D. MacMicking, G. A. Taylor, and J. D. McKinney. Immune control of tuberculosis by IFN-γ-inducible LRG-47. *Science*, 302(5645):654–9, Oct 24 2003.

Y. C. Manabe and W. R. Bishai. Latent Mycobacterium tuberculosis—persistence, patience, and winning by waiting. *Nat Med*, 6(12):1327–9, Dec 2000.

G. I. Marchuk. *Mathematical Modelling of Immune Response in Infectious Diseases*. Kluwer Academic Publishers, The Netherlands, 1997.

S. Marino and D. E. Kirschner. The human immune response to Mycobacterium tuberculosis in lung and lymph node. *J Theor Biol*, 227(4):463–86, Apr 21 2004.

R. Medzhitov and C. A. Janeway, Jr. Innate immunity: impact on the adaptive immune response. *Curr Opin Immunol*, 9(1):4–9, Feb 1997.

M. Meier-Schellersheim. *The immune system as a complex system: Description and simulation of the interactions of its constitutents*. PhD thesis, University of Hamburg, Hamburg, Germany, 2001.

D. Metcalf. Control of granulocytes and macrophages: molecular, cellular, and clincial aspects. *Science*, 254(5031):529–533, 1991.

K. W. Moore, R. de Waal Malefyt, R. L. Coffman, and A. O'Garra. Interleukin-10 and the interleukin-10 receptor. *Annu Rev Immunol*, 19:683–765, 2001.

S. Moqattash and J. D. Lutton. Leukemia cells and the cytokine network. *Proc Soc Exp Biol Med*, 219(1):8–27, Oct 1998.

B. F. Morel, M. A. Burke, J. Kalagnanam, S. A. McCarthy, D. J. Tweardy, and P. A. Morel. Making sense of the combined effect of interleukin-2 and interleukin-4 on lymphocytes using a mathematical model. *Bulletin of Mathematical Biology*, 58(3):569–594, 1996.

M. Naito, S. Umeda, T. Yamamoto, H. Moriyama, H. Umezu, G. Hasegawa, H. Usuda, L. D. Shultz, and K. Takahashi. Development, differentiation, and phenotypic heterogeneity of murine tissue macrophages. *J Leukoc Biol*, 59(2):133–8, Feb 1996.

G. J. Nau, J. F. Richmond, A. Schlesinger, E. G. Jennings, E. S. Lander, and R. A. Young. Human macrophage activation programs induced by bacterial pathogens. *Proc Natl Acad Sci U S A*, 99(3):1503–8, Feb 5 2002.

G. J. Nau, A. Schlesinger, J. F. Richmond, and R. A. Young. Cumulative toll-like receptor activation in human macrophages treated with whole bacteria. *J Immunol*, 170(10): 5203–9, May 15 2003.

M. J. Newport, C. M. Huxley, S. Huston, C. M. Hawrylowicz, B. A. Oostra, R. Williamson, and M. Levin. A mutation in the interferon-γ-receptor gene and susceptibility to mycobacterial infection. *N Engl J Med*, 335(26):1941–9, Dec 26 1996.

P. Nickerson, J. Steiger, X. X. Zheng, A. W. Steele, W. Steurer, P. Roy-Chaudhury, and T. B. Strom. Manipulation of cytokine networks in transplantation: false hope or realistic opportunity for tolerance. *Transplantation*, 63(4):489–94, Feb 27 1997.

R. J. North and Y. J. Jung. Immunity to tuberculosis. *Annu Rev Immunol*, 22:599–623, 2004.

M. A. Nowak and R. M. May. *Virus Dynamics*. Oxford University Press, 2000.

M. Oddo, T. Renno, A. Attinger, T. Bakker, H. R. MacDonald, and P. R. Meylan. Fas ligand-induced apoptosis of infected human macrophages reduces the viability of intracellular Mycobacterium tuberculosis. *J Immunol*, 160(11):5448–54, Jun 1 1998.

A. B. Pardee. G1 events and regulation of cell proliferation. *Science*, 246(4930):603–608, 1989.

J. L. Perez-Arellano, M. C. Alcazar-Montero, and A. Jimenez-Lopez. Alveolar macrophage: origin, kinetics and relationship with cells of the alveolo-interstitial region. *Allergologia et immunopathologia (International Journal for clinical and investigative allergology and clinical immunology)*, 18(3):175–183, 1990.

S. S. Pilyugin and R. Antia. Modeling immune responses with handling time. *Bull Math Biol*, 62(5):869–90, Sep 2000.

W. H. Press, S. A. Teukolsky, W. T. Vetterling, and B. P. Flannery. *Numerical Recipes in C: The art of scientific computining, second edition*. Cambridge University Press, 1998.

T. Ravasi, C. Wells, A. Forest, D. M. Underhill, B. J. Wainwright, A. Aderem, S. Grimmond, and D. A. Hume. Generation of diversity in the innate immune system: mac-

rophage heterogeneity arises from gene-autonomous transcriptional probability of individual inducible genes. *J Immunol*, 168(1):44–50, Jan 1 2002.

R. L. Reinhardt, A. Khoruts, R. Merica, T. Zell, and M. K. Jenkins. Visualizing the generation of memory $CD4^+$ T cells in the whole body. *Nature*, 410(6824):101–5, Mar 1 2001.

RePast. http://repast.sourceforge.net/.

E. R. Rhoades, A. A. Frank, and I. M. Orme. Progression of chronic pulmonary tuberculosis in mice aerogenically infected with virulent Mycobacterium tuberculosis. *Tuber Lung Dis*, 78(1):57–66, 1997.

D. R. Roach, E. Martin, A. G. Bean, D. M. Rennick, H. Briscoe, and W. J. Britton. Endogenous inhibition of antimycobacterial immunity by IL-10 varies between mycobacterial species. *Scand J Immunol*, 54(1-2):163–70, Jul-Aug 2001.

M. Rojas, M. Olivier, P. Gros, L. F. Barrera, and L. F. Garcia. TNF-α and IL-10 modulate the induction of apoptosis by virulent Mycobacterium tuberculosis in murine macrophages. *J Immunol*, 162(10):6122–31, May 15 1999.

P. Roth, A. Bartocci, and E. R. Stanley. Lipopolysaccharide induces synthesis of mouse colony-stimulating factor-1 in vivo. *J Immunol*, 158(8):3874–80, Apr 15 1997.

K. Schroder, P. J. Hertzog, T. Ravasi, and D. A. Hume. Interferon-γ: an overview of signals, mechanisms and functions. *J Leukoc Biol*, 75(2):163–89, Feb 2004.

W. K. Seelentag, J. J. Mermod, R. Montesano, and P. Vassalli. Additive effects of interleukin 1 and tumour necrosis factor-α on the accumulation of the three granulocyte and macrophage colony-stimulating factor mrnas in human endothelial cells. *EMBO J*, 6 (8):2261–5, Aug 1987.

L. A. Segel. Diffuse feedback from diffuse information in complex systems. *Complexity*, 5:39–46, 2000.

L. A. Segel. Controlling the immune system: diffuse feedback via a diffuse informational network. *Novartis Found Symp*, 239:31–40; discussion 40–51, 2001a.

L. A. Segel. Diffuse feedback from a diffuse informational network: in the immune system and other distributed autonomous systems. In L. Segel and I. Cohen, editors, *Design Principles for the Immune System and Other Distributed Autonomous Systems*, pages 203–226. Oxford University Press, 2001b.

L. A. Segel. How can perception of context improve the immune response? In L. Segel, editor, *Autoimmunity and Emerging Disease*, pages 169–191. Center for the Study of Emerging Disease, Jerusalem, 2001c.

L. A. Segel and R. L. Bar-Or. On the role of feedback in promoting conflicting goals of the adaptive immune system. *Journal of Immunology*, 163:1342–1349, 1999.

P. E. Seiden and F. Celada. A model for simulating cognate recognition and response in the immune system. *J Theor Biol*, 158(3):329–57, Oct 7 1992.

N. V. Serbina and J. L. Flynn. Early emergence of $CD8^+$ T cells primed for production of type 1 cytokines in the lungs of Mycobacterium tuberculosis-infected mice. *Infect Immun*, 67(8):3980–8, Aug 1999.

J. Shellito, C. Esparza, and C. Armstrong. Maintenance of the normal rat alveolar macrophage cell population. *American Review of Respiratory Disease*, 135(1):78–82, 1987.

L. Shi, Y. J. Jung, S. Tyagi, M. L. Gennaro, and R. J. North. Expression of Th1-mediated immunity in mouse lungs induces a Mycobacterium tuberculosis transcription pattern characteristic of nonreplicating persistence. *Proc Natl Acad Sci U S A*, 100(1):241–6, Jan 7 2003.

R. F. Silver, Q. Li, and J. J. Ellner. Expression of virulence of Mycobacterium tuberculosis within human monocytes: virulence correlates with intracellular growth and induction

of tumor necrosis factor α but not with evasion of lymphocyte-dependent monocyte effector functions. *Infect Immun*, 66(3):1190–9, Mar 1998.

D. Smith, S. Forrest, D. Ackley, and A.S.Perelson. Variable efficacy of repeated annual influenza vaccination. *Proceedings of the National Academy of Sciences*, 96:14001–14006, 1999.

J. A. Smith and L. Martin. Do cells cycle? *Proceedings of the National Academy of Sciences U S A*, 70(4):1263–7, Apr 1973.

K. A. Smith. The interleukin 2 receptor. *Annual Review of Cell Biology*, 5:397–342, 1989.

E. R. Stanley and D. Metcalf. Enzyme treatment of colony stimulating factor: evidence for a peptide component. *The Australian Journal of Experimental Biology and Medical Science*, 49(3):281–90, Jun 1971.

G. R. Stewart, B. D. Robertson, and D. B. Young. Tuberculosis: a problem with persistence. *Nat Rev Microbiol*, 1(2):97–105, Nov 2003.

M. C. Strain, D. D. Richman, J. K. Wong, and H. Levine. Spatiotemporal dynamics of HIV propagation. *J Theor Biol*, 218(1):85–96, Sep 7 2002.

Swarm. http://wiki.swarm.org/.

K. Takahashi, K. Kaizu, B. Hu, and M. Tomita. A multi-algorithm, multi-timescale method for cell simulation. *Bioinformatics*, 20(4):538–46, Mar 1 2004.

J. S. Tan, D. H. Canaday, W. H. Boom, K. N. Balaji, S. K. Schwander, and E. A. Rich. Human alveolar T lymphocyte responses to Mycobacterium tuberculosis antigens: role for $CD4^+$ and $CD8^+$ cytotoxic T cells and relative resistance of alveolar macrophages to lysis. *J Immunol*, 159(1):290–7, Jul 1 1997.

A. Thomson, editor. *The Cytokine Handbook, second edition*. Academic Press, 1994.

A. Thomson, editor. *The Cytokine Handbook, third edition*. Academic Press, 1998.

K. Tsukaguchi, K. N. Balaji, and W. H. Boom. $CD4^+$ $\alpha\beta$ T cell and $\gamma\delta$ T cell responses to Mycobacterium tuberculosis. similarities and differences in Ag recognition, cytotoxic effector function, and cytokine production. *J Immunol*, 154(4):1786–96, Feb 15 1995.

K. Tsukaguchi, B. de Lange, and W. H. Boom. Differential regulation of IFN-γ, TNF-α, and IL-10 production by $CD4^+$ $\alpha\beta TCR^+$ T cells and $V\delta2^+$ $\gamma\delta$ T cells in response to monocytes infected with Mycobacterium tuberculosis-H37Ra. *Cell Immunol*, 194(1): 12–20, May 25 1999.

R. J. Tushinski, I. T. Oliver, L. J. Guilbert, P. W. Tynan, J. R. Warner, and E. R. Stanley. Survival of mononuclear phagocytes depends on a lineage-specific growth factor that the differentiated cells selectively destroy. *Cell*, 28:71–81, 1982.

R. J. Tushinski and E. R. Stanley. The regulation of mononuclear phagocyte entry into S phase by the colony stimulating factor CSF-1. *Journal of Cellular Physiology*, 122: 221–228, 1985.

J. Tyrcha. Age-dependent cell cycle models. *Journal of Theoretical Biology*, 213(1): 89–101, Nov 7 2001.

D. M. Underhill and A. Ozinsky. Phagocytosis of microbes: complexity in action. *Annu Rev Immunol*, 20:825–52, 2002.

R. van Furth. Production and migration of monocytes and kinetics of macrophages. In R. van Furth, editor, *Mononuclear Phagocytes*, pages 3–12. Kluwer Academic Publishers, 1992.

A. Vawer and J. Rashbass. The biological toolbox: a computer program for simulating basic biological and pathological processes. *Comput Methods Programs Biomed*, 52 (3):203–11, Mar 1997.

E. O. Voit. *Computational Analysis of Biochemical Systems*. Cambridge University Press, 2000.

C. Warrender, S. Forrest, and L. Segel. Effective feedback in the immune system. In *Genetic and evolutionary computation conference workshop program*, pages 329–332. Morgan-Kaufmann, 2001.

L. G. Wayne and C. D. Sohaskey. Nonreplicating persistence of mycobacterium tuberculosis. *Annu Rev Microbiol*, 55:139–63, 2001.

A. Weiss and D. R. Littman. Signal transduction by lymphocyte antigen receptors. *Cell*, 76(2):263–74, Jan 28 1994.

J. E. Wigginton and D. Kirschner. A model to predict cell-mediated immune regulatory mechanisms during human infection with Mycobacterium tuberculosis. *J Immunol*, 166 (3):1951–67, Feb 1 2001.

G. T. Williams, C. A. Smith, E. Spooncer, T. M. Dexter, and D. R. Taylor. Haemopoietic colony stimulating factors promote cell survival by suppressing apoptosis. *Nature*, 343 (6253):76–79, 1990.

P. Woo. The cytokine network in juvenile chronic arthritis. *Rheum Dis Clin North Am*, 23 (3):491–8, Aug 1997.

J. Xaus, M. Comalada, A. F. Valledor, M. Cardo, C. Herrero, C. Soler, J. Lloberas, and A. Celada. Molecular mechanisms involved in macrophage survival, proliferation, activation or apoptosis. *Immunobiology*, 204(5):543–50, Dec 2001.

A. Yates, C. Bergmann, V. J. L. Hemmen, J. Stark, and R. Callard. Cytokine-modulated regulation of helper T cell populations. *J Theor Biol*, 206(4):539–60, Oct 21 2000.

M. E. Young, P. A. Carroad, and R. L. Bell. Estimation of diffusion coefficients of proteins. *Biotechnology and Bioengineering*, 22:947–955, 1980.

H. Yssel, R. de Waal Malefyt, M. G. Roncarolo, J. S. Abrams, R. Lahesmaa, H. Spits, and J. E. de Vries. Il-10 is produced by subsets of human $CD4^+$ T cell clones and peripheral blood T cells. *J Immunol*, 149(7):2378–84, Oct 1 1992.

P. W. Zandstra, D. A. Lauffenburger, and C. J. Eaves. A ligand-receptor signaling threshold model of stem cell differentiation control: a biologically conserved mechanism applicable to hematopoiesis. *Blood*, 96(4):1215–22, Aug 15 2000.